UNIVERSITY OF CALIFORNIA
SANTA CRUZ

THE MECHANISMS AND CONSEQUENCES OF LON PROTEOLYSIS IN *VIBRIO CHOLERAE*

A dissertation submitted in partial satisfaction of the
requirements for the degree of

DOCTOR OF PHILOSOPHY

in

MICROBIOLOGY AND ENVIRONMENTAL TOXICOLOGY

by

Avatar Joshi

December 2021

The Dissertation of Avatar Joshi
is approved:

Professor Fitnat H. Yildiz, Chair

Professor Peter Chien

Professor Karen M. Ottemann

Professor Victoria Auerbuch-Stone

Professor Manel Camps

Peter Biehl
Vice Provost and Dean of Graduate Studies

Table of Contents

List of Figures

List of Tables

Abstract

The Mechanisms and Consequences of Lon Proteolysis in *Vibrio cholerae*

by

Avatar Joshi

The discovery of ATP-dependent proteolysis began with Lon protease in the 1960s. Since that time, Lon (or LonA) has been identified as a key regulator of protein quality control and diverse cellular processes in archaea, bacteria, as well as in the mitochondria of eukaryotic cells. Despite nearly 60 years of research, the substrates of Lon and the mechanisms that dictate Lon proteolysis remain poorly understood. The work presented here focuses on understanding the mechanisms and consequences of Lon proteolysis in *V. cholerae*.

Vibrio cholerae is the Gram-negative facultative pathogen responsible for the diarrheal disease cholera. *V. cholerae* remains a threat to global public health. There are estimated to be 1.3–4.0 million cases of cholera and 21,000–143,000 deaths worldwide each year. Lon plays a critical role in regulating processes important for *V. cholerae*'s pathogenic cycle. For example, Lon regulates virulence factor production, type VI secretion system (T6SS)-dependent killing, biofilm formation, motility, c-di-GMP levels, cell division, and stress adaptation. Furthermore, *V. cholerae* mutants defective in Lon poorly colonize the host intestinal tract.

Previous work performed by the Yildiz lab identified Lon as a repressor of the T6SS, which was a novel function attributed to prokaryotic Lon. To better understand

how Lon might regulate the T6SS, I compiled the known functional and regulatory networks governing activation of the T6SS (Chapter 1). We then used whole proteome analysis to identify potential Lon targets that might explain Lon repression of the T6SS (Chapter 2). We identified TfoY as a Lon substrate and showed that Lon-dependent proteolysis of TfoY represses T6SS-dependent killing and motility. In addition, we used a combination of genetic and biochemical approaches to demonstrate that Lon binds to c-di-GMP and that c-di-GMP inhibits Lon-dependent proteolysis of TfoY.

Most analyses on Lon have focused on Lon-dependent regulation in planktonic grown cells. Thus, relatively little is known regarding how Lon regulates processes important for biofilm formation. We performed whole proteome and whole transcriptome analyses on WT and Δlon biofilms to identify potential Lon substrates and Lon-regulated pathways in biofilms (Chapter 3). Our analyses indicates that Lon isd important regulator of biofilm matrix production, virulence factor production, nucleotide pool homeostasis, iron homeostasis, and DNA repair pathways during the biofilm growth mode. The work outlined here provides valuable insights into how regulated proteolysis functions to control processes important for *V. cholerae* pathogenesis.

To my family, friends, and loved ones your support has meant everything.

Acknowledgments

I would like to thank my advisor, Fitnat Yildiz, who directed and supervised the research which forms the basis for this dissertation. She is a brilliant scientist whose feedback helped shape me as a scientist and as a person. Her involvement in these projects helped guide them into interesting and unique directions and, in doing so, created unique learning opportunities for me as well. I feel far more able to tackle scientific and personal challenges due to her training. Her work ethic and commitment to her students is truly inspirational. She has my eternal gratitude.

In addition, I would like to acknowledge each of my committee members for sharing their time and insights with me at various stages of my PhD. Karen Ottemann and Victoria Auerbauch-Stone were fantastic teachers. I learned much from them in our personal meetings, graduate classes, and from watching them teach undergraduate courses. They also provided insightful feedback on my dissertation research. In addition, Manel Camps provided thoughtful feedback both as a member of my dissertation committee and as the chair of my qualifying exam 1 committee. Finally, the importance of Peter Chien's guidance on work related to Lon protease cannot be overstated. His knowledge helped us overcome several significant obstacles and also helped guide us to ask interesting questions regarding Lon proteolysis in *Vibrio cholerae*. In addition, his students performed experiments that significantly elevated the research outlined in Chapters 2 and 3.

The text of this dissertation includes reprints of previously published material

with only minor updates and modifications from the original documents. These articles form the basis of the work presented in Chapters 1 and 2. The use of these documents in this dissertation is in compliance with the policy outlined by Cell's: Trends in Microbiology and PLOS Genetics. In addition, I have obtained permission from my co-authors to use this content as part of my dissertation.

The contents of Chapter 1 are from an article submitted to Cell's Trends in Microbiology and is titled, "The Rules of Engagement: The Type VI Secretion System in *Vibrio cholerae* PMCID: PMC5365375. I performed the majority of research and writing found in this review article. In addition, Benjamin Kostiuk, Andrew Rogers, and Jennifer Teschler contributed to the writing and editing of several sections. Finally, Fitnat Yildiz and Stefan Pukatzki shared their wealth of knowledge on *Vibrio cholerae* and the type VI secretion system with me and the other co-authors. Their feedback and editing helped shape the article into an insightful review that has been a benefit to the T6SS field.

The contents of Chapter 2 are from an article submitted to PLOS Genetics and is titled, "c-di-GMP inhibits LonA-dependent proteolysis of TfoY in *Vibrio cholerae*" PMCID: PMC7371385. I performed the majority of research and writing for this publication. In addition, I performed all *in vivo* experiments which formed the basis for this article. I would like to acknowledge the work of Samar Mahmoud and Justyne L. Ogdahl, who were responsible for the purification of *Vibrio cholerae* Lon protease. They also performed several important *in vitro* assays. Namely, the MANT-c-di-GMP binding assay, the FITC-casein proteolysis assay, and ATPase activity assay. Further-

more, they wrote the methods sections explaining how these assays were performed as well as the corresponding parts of the results sections. I would also like to acknowledge Soo-Kyoung Kim, who performed the Lon DRaCALA experiment and contributed to the writing of the corresponding methods section. Finally, I would like to thank Vincent Lee, Peter Chien, and Fitnat Yildiz for their contributions in overseeing this research as well as their editing and writing feedback.

I would like to give an additional acknowledgement to Justyne L. Ogdahl and Peter Chien for their contributions in performing the TMT-labeling and mass spectrometry for the proteomics experiment found in Chapter 3.

Chapter 1

Rules of Engagement: The Type VI Secretion System in *V. cholerae*

1.1 A Versatile Weapon for a Deadly Pathogen

The type VI secretion system (T6SS) is a contact-dependent contractile nanomachine used by bacteria to translocate a toxin coated, membrane puncturing device into neighboring cells [1, 2, 3]. Since its discovery, T6SS genes have been identified in over a quarter of sequenced Gram-negative bacteria and this highly abundant system has been shown to mediate antagonistic interactions against a wide variety of prokaryotic and eukaryotic organisms [1, 2, 4, 5, 6]. One of the first bacterium shown to possess the T6SS was *Vibrio cholerae* and thus, much of our understanding of T6SS structure, function, and regulation has been developed from continued study of the T6SS in this model pathogenic organism [1]. *V. cholerae* is a Gram-negative bacterium responsible

for the diarrheal disease cholera. There have been seven recorded cholera pandemics in the past 200 years, with the seventh still ongoing [7]. According to the World Health Organization, cholera infections continue to impact 1.4 to 4.3 million people globally and result in 21,000 to 143,000 deaths every year [8, 9]. While over 200 serogroups of *V. cholerae* have been characterized, pandemics have only been attributed to the O1 serogroup [7]. *V. cholerae* exists primarily in the aquatic environment, where it can be transmitted to a human host through the ingestion of contaminated food or water. *V. cholerae* has developed several mechanisms, including the T6SS, to compete with the diverse prokaryotic and eukaryotic organisms that it encounters in both the aquatic environment and human host. Emerging research on the activation of the T6SS suggests that it may contribute to the persistence and evolution of *V. cholerae* through direct antagonism of competing microbes [1, 10, 11]. Additionally, it is well established that the T6SS plays an important role in promoting *V. cholerae*'s fitness and pathogenicity in the host [6, 12, 13, 14, 15, 16, 17, 18, 19]. Current research suggests that *V. cholerae* uses the T6SS to kill off competing commensal microbes [16, 17, 18, 19, 20]. In addition, T6SS-mediated attacks on the host's microflora and intestinal tract may serve to modulate the host immune system, promoting virulence factor production and altering host intestinal mechanics in addition to host viability [16, 17, 18, 19].

Although significant discoveries have been made in the 15 years since the T6SS was initially discovered, there is still much to be uncovered about when and how the T6SS is deployed and the role it plays in environmental survival and infection. This review provides an update on the current knowledge of the structure, activity, and

function of the T6SS, as well as the signals and regulatory networks important for its activation in *V. cholerae*.

1.1.1 The Structure of the T6SS

The T6SS is a multicomponent toxin delivery apparatus that has structural and functional homology to the T4 bacteriophage tail spike [15,16]. Imaging studies suggest that translocation of T6SS effectors occurs through a contraction event that propels a membrane puncturing spike into neighbouring cells (Figure 1.1) [3, 21].

Assembly of the T6SS begins with the recruitment of baseplate proteins that anchor the outer sheath and the inner tube to the lipid membranes of the bacteria. The membrane complex is comprised of at least 8 different proteins, which provide structural stability and dock the remaining components [22]. After the membrane complex is assembled, the proteins that comprise the tip are recruited. The base of the tip is composed of a trimeric complex formed by valine-glycine repeat proteins (VgrG1-3), while the upper portion of the tip is composed of proteins containing repeating proline-alanine-alanine-arginine (PAAR) motifs [3, 23, 24]. Following tip assembly, an inner tube formed by hemolysin-coregulated protein (Hcp) hexamers encased within an outer tube composed of the VipA/VipB protein complex polymerizes onto the VgrG and PAAR-motif tip complex. The outer and inner tubes polymerize into the cytosolic space over the course of 30 seconds and can reach the membrane opposite the baseplate [21, 25, 26]. The T6SS can remain fully extended for several minutes until an unknown signal triggers rapid contraction of the outer sheath (5ms) and translocation of the inner

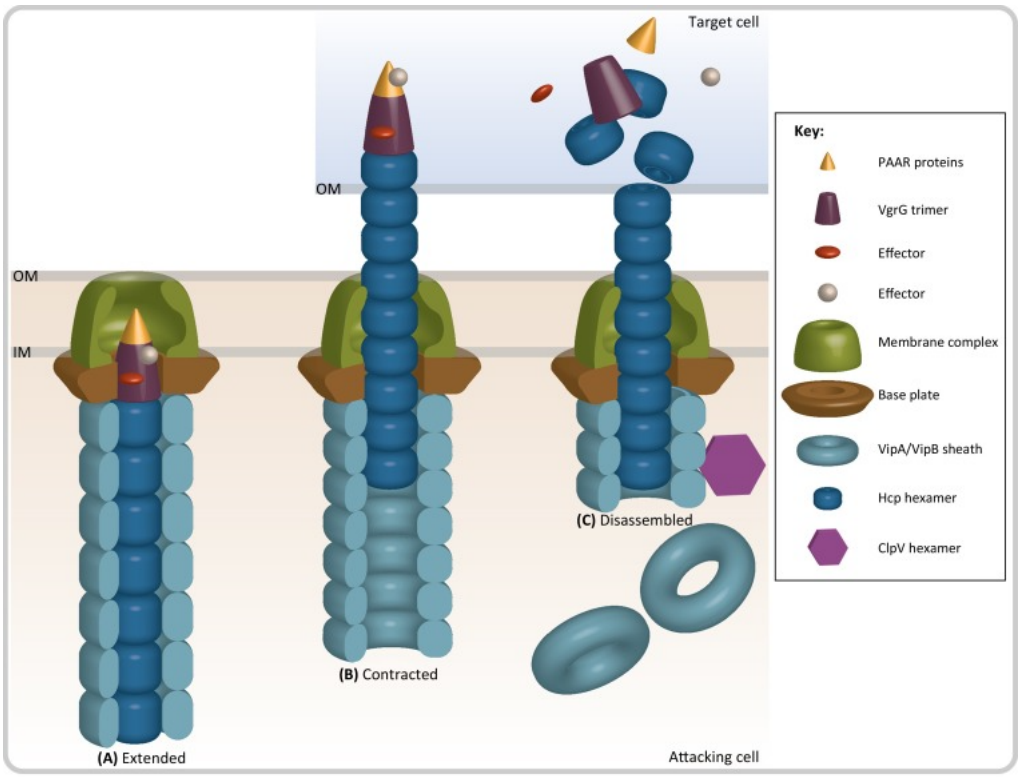

Figure 1.1: Contraction of the Type VI Secretion System (T6SS) Results in the Translocation of Effector Proteins. (A) The membrane complex is comprised of both a baseplate structure TssEFGK (HsiF and VasABE in *Vibrio cholerae*), as well as membrane anchoring components TssJLM (VasDFK in *V. cholerae*). The outer sheath (VipA/VipB) and inner tube (Hcp) proteins polymerize to form an extended tube that is assembled onto VgrG and PAAR-motif proteins at the cytoplasmic side of the membrane complex. Effector proteins are recruited to the PAAR or VgrG proteins. (B) After assembly, the T6SS complex remains stable until an unknown signal results in the contraction of the outer sheath and the propulsion of the inner tube into a neighboring cell. (C) Upon translocation of the inner tube, tip, and effector complex, the effector proteins can exhibit their toxic activity. Concurrently, the ATPase ClpV disassembles the outer sheath so that the components can be recycled.

tube into the extracellular space [21, 25]. In *Pseudomonas aeruginosa*, contraction of the outer sheath can occur in response to incoming T6SS attacks or other injuries to the outer membrane. However, the signals and mechanisms that govern contraction in *V. cholerae* remain elusive. After contraction and secretion occurs, the ClpV ATPase is recruited to disassemble and recycle the VipA/VipB tube components [21, 25, 27, 28].

Analysis performed in a variety of species suggests that effectors can associate with Hcp, PAAR-motif proteins, and VgrG [29, 30, 31, 32]. To date, all characterized *V. cholerae* T6SS effectors are either loaded onto the VgrG tip or are part of the tip proteins themselves. Both VgrG-1 and VgrG-3 harbor effector domains within their C-termini that either have actin cross-linking or peptidoglycan degrading abilities, respectively. Other effectors called 'cargo effectors', are loaded directly onto the tip of the T6SS. It was recently determined that loading of the cargo effector TseL is facilitated by the chimeric protein Tap-1 (also called Tec-1), which contains a VgrG-binding N-terminal domain and a TseL binding C-terminal domain [33, 34]. Finally, the so-called PAAR-motif proteins, which assemble into a cone-like structure at the tip of the T6SS and form a sharp point that facilitates membrane puncture, are hypothesized to harbour C- or N-terminal effector domains or to bind and load additional effectors [35]. Indeed, *V. cholerae* encodes a PAAR-motif protein that functions as an effector binding adaptor that loads the effector TseH [36]. It was also recently determined that T6SS effectors contribute to the proper assembly of the *V. cholerae* T6SS [37]. This effector onboard checking mechanism ensures that each T6SS attack has the capacity to deliver a toxic payload to neighboring cells.

1.1.2 Activity and Function of the T6SS

Pandemic strains of *V. cholerae* encode identical effectors suggesting these effectors contribute to *V. cholerae* pandemicity [10, 38]. Pandemic *V. cholerae* possess two T6SS effectors that target eukaryotic cells and utilizes these effectors as a means of escape from predatory amoeba in the environment. The VgrG-1 actin-crosslinking domain causes cytotoxic crosslinking in the predatory amoeba Dictyostelium discoideum and J774 macrophages (Figure 1.2B) [1]. Additionally, VgrG-1 has been associated with intestinal inflammation and diarrheal symptoms in the infant rabbit as well as efficient colonization of the infant mouse [6, 15].

Further, the actin-crosslinking domain of VgrG-1 has been shown to play a role in modulating host intestinal motility in the zebra fish model of infection, which leads to the expulsion of the host commensal *Aeromonass veronii* [17]. The cargo effector VasX targets both eukaryotic and prokaryotic cells by disrupting the cell membrane and has demonstrated activity against *D. discoideum* and *Escherichia coli* [39, 40]. Efficient colonization of the infant mouse and rabbit intestinal tract is also significantly influenced by the presence of the peptidoglycan degrading effector VgrG-3 [14]. The host intestinal tract is colonized with commensal bacteria that act as a barrier between *V. cholerae* and its preferred niche within the lumen of the small intestine. It has been shown that T6SS-active *V. cholerae* strains significantly alter the host microbiome [18, 17, 20]. Further, T6SS-dependent killing of host commensals in the infant mouse model alters the host immune response, ultimately promoting *V. cholerae* virulence

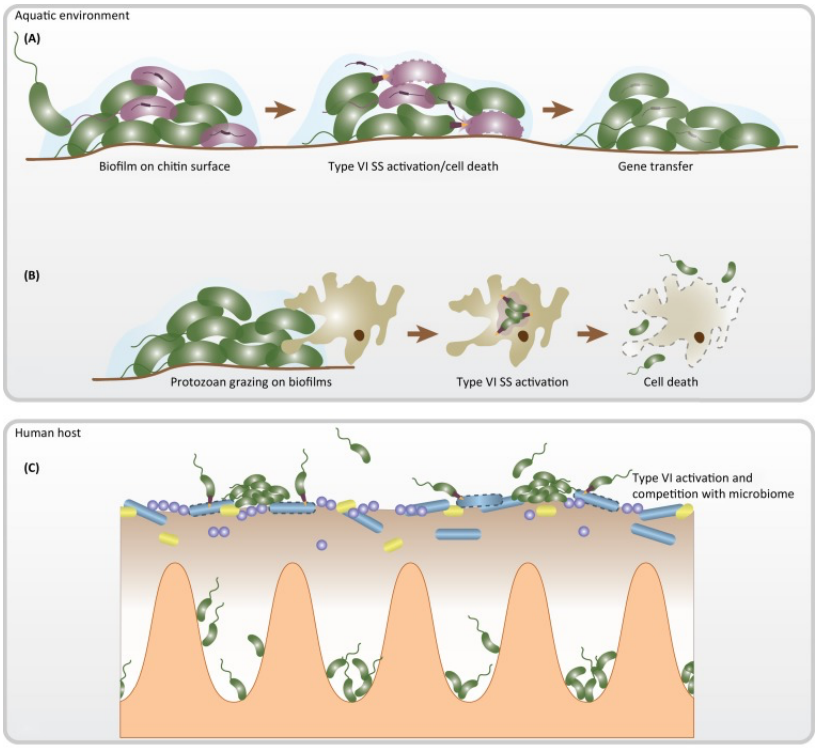

Figure 1.2: (A) In the aquatic environment *V. cholerae* often forms biofilms on chitin surfaces. Chitin oligomers serve as a signal for the coactivation of natural competency and the T6SS, which allows for the killing of competing microbes and the acquisition of released DNA (represented as linear fragments inside of intact cells and outside of compromised cells). (B) *V. cholerae* can also utilize the T6SS to escape from predatory protozoans. (C) During infection, the T6SS is believed facilitate *V. cholerae* colonization and virulence through the killing of host microbes. It may additionally target host macrophages or cause intestinal inflammation that can facilitate infection.

factor production and host fluid accumulation [17]. Finally, T6SS-dependent killing of commensal bacteria can reduce intestinal progenitor cell proliferation and epithelial renewal as well as reduce host viability in *Drosophila melanogaster* [19]. Together these studies demonstrate a role for the T6SS in promoting *V. cholerae*'s fitness in the host by attacking and killing the host's microbiota (Figure 1.2C) [18, 19].

The bactericidal activity of *V. cholerae*'s T6SS was not discovered until four years after the initial identification of the T6SS [41]. It is now thought that this activity plays a role in inter- and intra-species competition and clonal segregation [42]. When the *V. cholerae* T6SS targets another bacterial cell, two distinct outcomes can occur. If the neighbouring bacterium encodes the same immunity genes as the predator cell, the delivered effectors are deactivated, and the cell is protected. These two bacteria are said to be compatible. For VgrG-3, this effector-immunity interaction appears to occur at 1:2 ratios, as dimerization of the immunity protein is critical to its function. Alternatively, if the target bacterium does not encode the immunity genes it will be subject to cell lysis. Though the T6SS gene clusters are widely conserved among *V. cholerae* strains, the effectors and corresponding immunity proteins encoded in these clusters have been reported to be highly variable [10, 43]. This diversity in effector-immunity pairs contributes to intra- and inter-species competition in various environmental niches [38]. Although the factors and mechanisms that predict competition outcomes are still being explored, it is likely that the arsenal of effectors and immunity genes each bacteria possesses, each bacteria's ability to acquire new effector and immunity genes through horizontal gene transfer events, potential differences in growth rate, rate of fire of the

T6SS, and how the T6SS is regulated under specific conditions contribute to success during these antagonistic interactions [42, 44].

T6SS-mediated bacterial killing by pandemic *V. cholerae* is enacted by four effectors, including the lipase, TseL, and the pore forming colicin VasX, which both target the cell membrane, as well as two effectors that target peptidoglycan; the lysozyme VgrG-3 and the amidase TseH (Table 1.1) [23, 40]. Though these effectors have been shown to be active exclusively within the periplasm of the prey cell, a cytoplasmic-acting effector with proposed ribonuclease activity has been characterized in *P. aeruginosa* and additional nucleic acid-targeting effectors have been identified in other species that may be active in the cytoplasm [32, 45, 46].

While it was previously thought that the T6SS was only active against Gram-negative bacteria, it was recently shown that *A. baumanii* ATCC 17978 can kill Gram-positives [47]. This isolate of *A. baumanii* secretes D-Lysine, thereby raising the extracellular pH and enhancing the activity if its peptidoglycan degrading effector, TseH, such that killing of Gram-positive bacteria occurs [47]. Indeed, abiotic factors such as Ca2+, Mg2+, and temperature have been shown to alter *V. cholerae* effector activity as well [48]. More specifically, divalent cations appear to enhance the activity of *V. cholerae* TseH and TseL. In addition, VasX and VgrG-3 play a more prominent role in E. coli killing at 30C while TseL is more active at 37C [48]. While the exact mechanism of divalent cation and temperature-dependent sensitivity of prey strains to T6SS attacks remain unclear, preliminary work suggests that the PhoPQ, BaeSR, and Rcs two-component systems are involved in protection from T6SS attacks in E. coli.

Table 1.1: Type VI Secretion System (T6SS) Effector Proteins from Pandemic *Vibrio cholerae* Strains

Effector	Target kingdom	Adaptor	Immunity	Effector activity	Effector class	Refs
VgrG1	Eukaryotes	–	–	Actin crosslinking	C-terminal extension	3
TseL	Prokaryotes	Tap-1	TsiV1	Putative lipase	Cargo effector	29, 38
VasX	Prokaryotes Eukaryotes	VasW	TsiV3	Pore forming	Cargo effector	30, 38
VgrG3	Prokaryotes	–	TsiV3	Peptidoglycan	C-terminal extension	19
TseH	Prokaryotes	–	TsiH	Peptidoglycan	Cargo effector	36

In addition, it was shown that the VxrAB two-component system is also important in defending against T6SS attacks [36, 48]. Together this suggests that pathways involved in the envelope stress response play a role in mitigating T6SS effector toxicity. Over the past decade, a plethora of effector classes have been identified in Gram-negative bacteria and it is likely more will be discovered. The study of T6SS effectors has illuminated the versatility and limitations of *V. cholerae*'s T6SS during antagonistic interactions with competing microorganisms. The continued identification and characterization of T6SS effectors will remain an important means of enhancing our understanding of the role the T6SS plays in bacterial and host interactions.

1.2 T6SS Genetic Organization and Regulation

Pandemic *V. cholerae* T6SS genes are encoded in one large operon (VCA0105-VCA0124), known as the large or major cluster, and at least three smaller operons known as auxiliary clusters 1, 2, and 3 (VCA0017-VCA0021, VC1415-VC1419, and VCA0284-VCA0286) (Figure 1.3) [1, 49, 50].

The large cluster encodes the majority of the T6SS structural components,

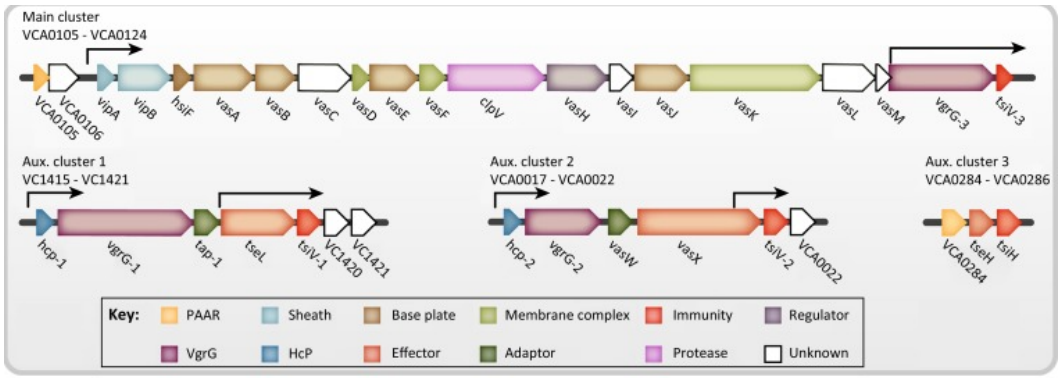

Figure 1.3: Genetic Loci of the *Vibrio cholerae* Type VI Secretion System (T6SS). The genes of the T6SS are organized into one main cluster and at least three auxiliary clusters. Genes are color-coded based on predicted function and labeled with *V. cholerae* gene annotations. Black arrows denote known transcriptional start sites.

with the exception of the essential secreted inner tube component Hcp, two of the VgrG proteins, and one PAAR-motif protein (VCA0284) [1, 50]. Auxiliary clusters 1 and 2 encode for the nearly identical hcp1 (VC1417) and hcp2 (VCA0017) genes, either of which is sufficient to produce Hcp and form the inner tube [50, 51]. Auxiliary clusters 1 and 2 also encode for the VgrG-1 (VC1416) and VgrG-2 (VCA0018) tip components respectively, as well as unique effector sets and their cognate immunity proteins [40, 50]. The third auxiliary cluster encodes for one PAAR motif protein (VCA0284) and a unique effector-immunity pair (VCA0285-86) [35, 49]. In addition to the promoters found upstream of each operon, internal promoter activity has been identified within the large cluster and auxiliary clusters 1 and 2 that lie just upstream of the immunity genes [40, 52]. The transcriptional regulators that drive expression from these internal promoters are not well understood; however it has been hypothesized that they may allow immunity proteins to be constitutively expressed, thus ensuring protection from

neighbouring kin cells even in the absence of an active T6SS [52]. Finally, additional auxiliary clusters (auxiliary clusters 4, 5, and 6) have been identified in environmental isolates [53]. Each auxiliary cluster possesses a copy of hcp, vgrG, and unique effector and immunity genes.

Significant advancements have been made in discerning the complex regulatory networks that govern the transcription and activation of the T6SS in *V. cholerae*. The transcriptional regulator VasH, which is encoded in the large T6SS cluster (VCA0117), was among the first T6SS regulators to be identified [1, 54]. VasH is a bacterial enhancer binding protein that complexes with the alternative sigma factor RpoN and coordinates transcription from the upstream promoters of auxiliary clusters 1 and 2 (Figure 1.4) [1, 55, 56, 57, 58]. The genetic organization of the T6SS clusters provides a mechanism by which activation of the large cluster prompts transcription from the auxiliary clusters and the production of an assembled T6SS. In addition, free Hcp can bind directly to the N-terminus of VasH and inhibit its activity. This provides a post-translational mechanism that limits expression of the auxiliary clusters when excess T6SS components have been produced [59]. Since the discovery of VasH, numerous additional regulators have been identified and diverse signalling pathways that feed into T6SS activation in response to various environmental cues have been characterized. For example, the T6SS is now known to be controlled via the quorum sensing and catabolite repression pathways [56, 58]. These signalling cascades are additionally integrated into the chitin induced competency cascade, which coordinates co-expression of the T6SS and competency genes [11, 60]. Finally, the T6SS is influenced by a number of additional

environmental and host signals including, but not limited to, temperature, osmolarity, the secondary messenger cyclic dimeric (3' → 5') GMP (c-di-GMP), mucin, and bile [52, 61, 62, 63]. Together, these regulatory mechanisms provide insights into how *V. cholerae* coordinates its T6SS activity in both the aquatic and host environments.

1.2.1 Quorum Sensing

Quorum sensing (QS) is a form of bacterial communication that occurs through the production, secretion, and sensing of small molecules known as autoinducers [64, 65]. This communication allows alterations in gene expression to occur across a population of bacteria in response to changing cell density, which is signaled by increasing levels of autoinducers. QS is known to regulate a variety of behaviors important for *V. cholerae*'s aquatic and intestinal life cycles including biofilm formation, motility, natural competency, and virulence factor production [60, 66, 67]. It is now recognized that QS also coordinates T6SS activation by repressing the T6SS at low cell density (LCD) and upregulating the T6SS at high cell density (HCD) (Figure 1.4) [68]. In *V. cholerae*, QS-mediated gene regulation occurs through a phosphorelay cascade modulated by four sensor histidine kinases, CqsS, LuxPQ, CqsR, and VpsS. CqsS and LuxPQ sense the levels of cholerae autoinducer 1 (CAI-1) and autoinducer 2 (AI-2), respectively, while the ligands for CqsR and VpsS have not been identified [69, 70]. At LCD, these four histidine kinases phosphorylate the phosphotransfer protein LuxU, which in turn phosphorylates LuxO [69, 70]. Phosphorylated LuxO activates the expression of four small RNAs known as Qrr1-4, which bind to and destabilize the mRNA transcripts of the

large cluster of the T6SS and HapR. At HCD, however, LuxO is unphosphorylated, and transcription of qrr1-4 is inactive, thus permitting the translation of the large T6SS cluster and HapR [68]. HapR positively regulates transcription of auxiliary clusters 1 and 2, likely via direct binding to HapR binding motifs [71].

1.2.2 Chitin-Induced Competency Pathway

V. cholerae spends much of its life cycle in the aquatic environment, where it is frequently found associated with chitinous surfaces, such as the exoskeletons of zooplankton. Mounting evidence suggests that growth on zooplankton facilitates *V. cholerae*'s persistence, transmission, and virulence [72, 73]. Thus, mechanisms and strategies that promote *V. cholerae*'s successful colonization of chitinous surfaces are of great interest. *V. cholerae* has evolved several signaling cascades that are influenced by the presence of chitin, including the ability to utilize chitin as a carbon source, natural competency, and activation of the T6SS [11, 74, 75, 76].

Chitin is an insoluble polymer consisting of repeating β-1,4-linked N-acetylglucosamine (GlcNAc) residues. Upon growth on chitin, the histidine kinase (HK) ChiS, senses GlcNac polymers and initiates a regulatory cascade that results in the expression of genes important for the transport, degradation and utilization of chitin, as well as those required for natural competency [75, 76]. Natural competency allows bacteria to import extracellular DNA (eDNA) from the environment, which can act as either a nutritional resource or be recombined into the genome, facilitating horizontal gene transfer [75, 76]. In *V. cholerae*, the signaling cascade initiated by ChiS couples natural

competency to the induction of the T6SS via the transcriptional regulator TfoX (Figure 1.4) [11]. The ability of TfoX to activate competency and T6SS genes is dependent upon the presence of the QS and TfoX-dependent regulator, QstR, which is required for the production of T6SS structural components [11, 60]. Thus, QS signals also appear to feed into the chitin competency pathway to initiate activation of the T6SS; however, the molecular mechanisms underlying this activation have not been characterized. Additionally, the nucleoside scavenging regulator CytR is essential for natural transformation and contributes to T6SS gene activation; however, the means by which it regulates the T6SS remain unclear (Figure 1.4) [77]. During chitin-induced co-activation of the T6SS and natural competency, *V. cholerae* uses its T6SS to kill non-immune, incompatible bacterial cells, freeing eDNA that is then taken up by its competency machinery [11]. Thus, the T6SS may facilitate genetic diversity and the evolution of *V. cholerae* strains in the environment via the acquisition of new genetic information through horizontal gene transfer, in addition to promoting *V. cholerae*'s colonization and persistence on chitinous surfaces through targeted killing of competing microbes (Figure 1.2A).

1.2.3 Carbon Catabolite Repression

The T6SS is positively regulated by the small molecule cyclic adenosine monophosphate (cAMP) and global regulator cAMP receptor protein CRP (Figure 1.4) [58]. The cAMP-CRP complex is essential for the carbon catabolite repression (CCR) response. CCR is a form of global regulation that facilitates the efficient uptake and metabolism of preferred carbon sources by repressing secondary metabolic pathways in

the presence of a preferred carbon source. The CCR response is mediated through the phosphotransferase system (PTS), which coordinates the passage and phosphorylation of preferred carbohydrates, such as glucose, into the cell. When preferred carbon sources are exhausted or unavailable, transcription of the adenylate cyclase gene, cyaA, is up-regulated, which leads to increased levels of cAMP [78, 79]. Free cAMP binds to CRP and the resulting complex acts as a transcriptional regulator, controlling the activation and repression of a number of essential *V. cholerae* pathways, including carbon uptake, QS, chitin utilization and chitin induced natural competency, as well as the T6SS [58, 80, 81]. Deletion of either cyaA or crp prevents production of Hcp, indicating that the cAMP-CRP complex is essential for T6SS production [58]. The mechanism by which cAMP-CRP regulates the T6SS is unclear; however, it is possible that cAMP-CRP influences T6SS production through its regulation of QS and chitin-induced competency [80, 81]. Additional studies are needed to determine whether cAMP-CRP controls T6SS production through these pathways or through alternative regulatory mechanisms.

1.2.4 Post-Translational Regulation

Little is known about the post-translational regulation of T6SS protein production, assembly, and activation in *V. cholerae*. However, the Lon (or LonA) protease was recently identified as a negative regulator of the T6SS (Figure 1.4) [82]. Lon belongs to the AAA+ superfamily of proteins and couples ATP-hydrolysis with the binding, unwinding, and degradation of targeted proteins. While a major role of the Lon protease is to degrade misfolded or otherwise aberrant proteins, it also has the ability to

degrade specific protein targets [83]. This targeted degradation by Lon provides post-translational regulation of a wide array of processes in a variety of bacteria, including *E. coli*, *P. aeruginosa*, and *B. subtilis*, though *V. cholerae* is the only bacteria in which the Lon protease has been shown to regulate the T6SS. In the absence of Lon, transcription of hcp1 and 2 are upregulated 5-fold while 2-fold increases are observed in transcripts from the main cluster. Additionally, production and secretion of Hcp is increased, and killing of *E. coli* prey is increased by 2-fold in a standard killing assay [82]. At the time I began my PhD research, the Yildiz lab had demonstrated that Lon was a key regulator of T6SS gene expression and killing, however, the molecular mechanisms that governed this regulatory pathway were unknown.

Since my dissertation research focuses on characterizing Lon-dependent regulatory mechanisms in *V. cholerae*, I was especially interested in determining how the Lon protease controls the T6SS. Using a combination of proteomic, molecular genetics, and biochemical techniques we determined the Lon inhibits T6SS-dependent gene expression and killing by controlling steady state levels of TfoY [84]. Furthermore, we provide evidence that Lon is a c-di-GMP receptor protein and that c-di-GMP inhibits Lon-dependent proteolysis of TfoY [84]. Finally, our data supports a model where T6SS activity is elevated when c-di-GMP is high, indicating that TfoY may play a role in T6SS-mediated competition in biofilms [84]. This work is fully discussed in Chapter 2.

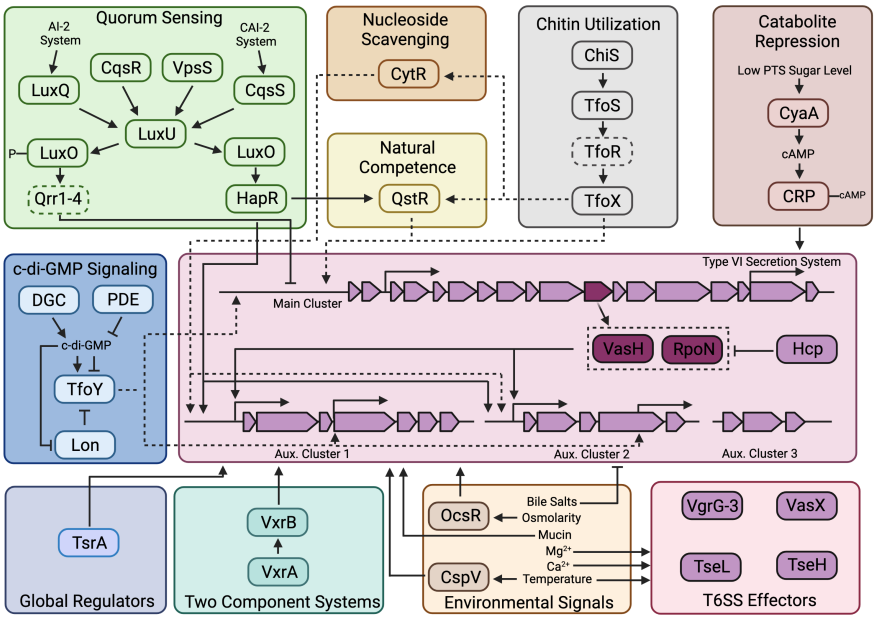

Figure 1.4: The Regulatory Network of the T6SS in *V. cholerae*. Activation is indicated by arrow-headed lines while inhibition is indicated by bar-headed lines. Lines that do not enter the Type VI Secretion System bubble represent regulation through an unknown mechanism. Regulators that directly bind to promoters are designated with solid lines while those that activate through as of yet unknown mechanisms have dashed lines. At low cell density, the quorum sensing small RNAs (sRNAs, denoted by a dashed outline) Qrr1-4 inhibit translation of hapR and the main T6SS cluster mRNAs. At high cell density, this inhibition is relieved. The chitin utilization cascade induces expression of TfoX, which acts in concert with HapR to activate QstR. TfoX and QstR facilitate transcription of the main cluster while HapR activates transcription of auxiliary clusters 1 and 2. When preferred carbohydrates are absent, CRP-cAMP accumulates and activates T6SS gene expression. At low nucleoside levels, CytR activates T6SS gene expression. Cyclic-di-GMP (c-di-GMP) is produced by diguanylate cyclases (DGCs) and degraded by phosphodiesterases (PDEs). TfoY can be produced through low and high c-di-GMP pathways. When c-di-GMP levels are low, Lon-dependent proteolysis of TfoY occurs efficiently. When c-di-GMP levels are high, Lon-depedent proteolysis of TfoY occurs inefficiently. Activation of auxiliary clusters 1 and 2 requires the VasH-RpoN complex. High levels of Hcp can inhibit VasH-RpoN-dependent transcription of the T6SS. The VxrAB two component system (TCS) senses an unknown signal and activates T6SS gene expression. OscR represses the T6SS under conditions of low osmolarity. CspV is required for activation of the T6SS at temperatures between 25°C and 37°C. Mucins activate the T6SS while bile salt metabolites inhibit T6SS tube formation. Mg^{2+}, Ca^{2+}, and temperature can enhance the effectiveness of T6SS effectors. The H-NS-like protein TsrA and the LonA protease inhibit the T6SS. These regulatory cascades are described in detail within the main text. This figure was generated using BioRender (https://app.biorender.com/)

1.2.5 Regulation of the T6SS in the Host

Infection by *V. cholerae* occurs through the ingestion of contaminated food or water. The invading bacteria navigate through the digestive system to the epithelial surface of the small intestine where *V. cholerae* produces virulence factors that promote colonization and disease onset. Recent studies have shown that the T6SS is active in the host and contributes to virulence and intestinal colonization [6, 13, 15, 18, 19, 17, 20]. The regulatory mechanisms that govern T6SS expression during pathogenesis remain poorly defined. It is likely that many of the regulators and signaling pathways mentioned earlier contribute to T6SS induction during pathogenesis; however, most in vivo assays have focused on the function of the T6SS within the host rather than its regulation. QS is known to play an essential role in coordinating *V. cholerae*'s virulence cascade and current data suggests that the T6SS remains under the control of HapR and LuxO during infection [6, 66]. Additionally, the H-NS-like protein TsrA was shown to repress virulence factors, including the T6SS; however, its mechanism of action remains unknown [6]. A recently identified two component system (TCS), VxrAB, was demonstrated to positively regulate intestinal colonization in a T6SS-dependent manner; however, the mechanism by which it regulates *in vivo* T6SS activity and the signal that feeds into this TCS is unknown [15]. The important role the T6SS appears to play in pathogenesis prompts additional studies of T6SS regulation within the host, which may aid in our understanding of this system.

1.2.6 Influence of Environmental Signals on T6SS Regulation

The T6SS of *V. cholerae* is also influenced by a number of environmental signals encountered in the aquatic environment or the host, though many of the key regulators that mediate these signals have not yet been identified. The cyclic antimicrobial peptide known as polymyxin B has been shown to result in increased T6SS gene expression and killing of D. discoideum, although the exact mechanism of this regulation remains unclear [85].

Osmolarity is known to be an important signal that influences the T6SS through the osmoregulator OscR, which represses T6SS gene expression at low osmolarities (85mM NaCl). The repressive effect of OscR is relieved when *V. cholerae* is placed in high osmotic conditions (340mM NaCl) (Figure 1.4) [62, 86]. Temperature additionally modulates the activity and expression of the T6SS, repressing T6SS gene expression at low temperatures (15°C) and activating T6SS gene expression at high temperatures (25°C – 37°C) (Figure 1.4) [61, 62]. The activation of the T6SS in response to elevated temperature appears to be regulated in part by the cold shock protein CspV. Deletion of cspV, significantly decreases the transcription of hcp, resulting in less killing of bacterial prey at 25°C and 37°C [61]. While the mechanisms through which OscR and CspV regulate the T6SS remain unclear, some studies have shown that T6SS gene induction and activity is optimal at osmolarities of 340mM NaCl and temperatures of 25°C [61, 62]. These conditions are similar to those found in the estuarine habitats where *V. cholerae* resides [87, 88, 89]. Thus, the regulatory mechanisms described here may have adapted

to facilitate competition and survival within this niche.

The *V. cholerae* T6SS is also responsive to host signals, such as mucin, bile, and indole (Figure 1.4). Mucins, the main component of the mucus layer in the intestine, are known to increase T6SS-mediated killing of bacterial prey, while the bile salt deoxycholic acid represses T6SS killing via inhibition of T6SS tube formation [63]. The production of deoxycholic acid is facilitated by the commensal bacterium Bifidobacterium bifidium, which is capable of metabolizing certain bile acids to deoxycholic acid [63]. Additionally, in vitro exposure to indole, a signaling molecule found in large concentrations in the mammalian intestinal tract, was shown to activate T6SS gene expression and may feed into in-vivo control of the T6SS [90]. Given that efficient colonization of the intestinal tract is known to be significantly influenced by the peptidoglycan degrading effector VgrG-3, the *V. cholerae*'s T6SS may target commensal bacteria to facilitate intestinal colonization (Figure 1.2C) [14, 15]. Signals produced by the microbiota may serve to inhibit or activate *V. cholerae*'s T6SS and may influence host susceptibility to disease. Indeed, host microbial communities are known to increase colonization resistance against many pathogens by preventing access to desirable niches, limiting nutrient availability, and producing inhibitory compounds [91, 92, 93] Thus, *V. cholerae* may overcome these obstacles through T6SS killing of the host's microbiota; however, additional work is required to characterize the influence of the microbial community on *V. cholerae* pathogenesis and T6SS activity.

1.3 Concluding Remarks

Over the past 15 years, significant advancements have been made on the structural and mechanistic properties of the T6SS, as well as the signals and regulatory pathways that govern its activation in *V. cholerae*. It is now understood that *V. cholerae* can use its T6SS on chitinous surfaces and co-regulates T6SS activation with natural competency pathways [11]. This provides a mechanism that likely increases the survival and persistence of *V. cholerae* in the aquatic environment through the direct killing of microbial competitors and may contribute to the evolution of *V. cholerae* through horizontal acquisition of new genetic information from killed cells (Figure 1.2A). In addition, *V. cholerae* uses its T6SS as a colonization and virulence determinant by targeting the host's epithelial cells as well as the commensal microbial population (Figure 1.2C).

While numerous insights have been made into the structure, function, and regulation of this bacterial weapon, substantial gaps remain. For example, the extent to which the T6SS facilitates inter- and intra-species competition and the biologically relevant targets of the T6SS require further exploration. Furthermore, the regulatory mechanisms and pathways important for T6SS activation in the host are poorly characterized. Indeed, additional research is required to identify the activating signals and mechanisms through which most regulators function.

Finally, it is important to note that while all sequenced *V. cholerae* isolates encode for T6SS genes, not all strains regulate their T6SS identically [1, 6, 94]. Many environmental isolates have a constitutively active T6SS, while all characterized pan-

demic strains exercise more controlled regulation of the T6SS [1, 94]. These differences are most apparent within the QS pathway. In constitutively active strains, HapR has relatively little influence on T6SS gene expression, while the influence of QS on strains that heavily regulate their T6SS differs, with some strains requiring the removal of LuxO for activation under standard laboratory conditions [6, 68]. This diversity of regulatory strategies may be indicative of evolutionary adaptations that are advantageous to the specific isolate's niche. So far, all studied isolates belonging to the O1 and O139 serogroups, which are responsible for pandemic outbreaks of cholera, tightly control expression of the T6SS [1, 6, 68, 94]. This may facilitate the timely activation of the T6SS when it is most needed for colonization of the host or survival in the aquatic environment, while repressing it when it is disadvantageous. Given the wealth of knowledge revealed about the T6SS in the past 15 years, it is exciting to consider what future study of the T6SS will yield as we continue to explore the complexities of the T6SS in *V. cholerae* and other important human pathogens.

Bibliography

[1] Stefan Pukatzki, Amy T Ma, Derek Sturtevant, Bryan Krastins, David Sarracino, William C Nelson, John F Heidelberg, and John J Mekalanos. Identification of a conserved bacterial protein secretion system in *Vibrio cholerae* using the *Dictyostelium* host model system. *Proceedings of the National Academy of Sciences*, 103(5):1528–1533, 2006.

[2] Joseph D Mougous, Marianne E Cuff, Stefan Raunser, Aimee Shen, Min Zhou, Casey A Gifford, Andrew L Goodman, Grazyna Joachimiak, Claudia L Ordoñez, Stephen Lory, et al. A virulence locus of *Pseudomonas aeruginosa* encodes a protein secretion apparatus. *Science*, 312(5779):1526–1530, 2006.

[3] Stefan Pukatzki, Amy T Ma, Andrew T Revel, Derek Sturtevant, and John J Mekalanos. Type vi secretion system translocates a phage tail spike-like protein into target cells where it cross-links actin. *Proceedings of the National Academy of Sciences*, 104(39):15508–15513, 2007.

[4] Lewis EH Bingle, Christopher M Bailey, and Mark J Pallen. Type vi secretion: a beginner's guide. *Current opinion in microbiology*, 11(1):3–8, 2008.

[5] Sandra Schwarz, Pragya Singh, Johanna D Robertson, Michele LeRoux, Shawn J Skerrett, David R Goodlett, T Eoin West, and Joseph D Mougous. Vgrg-5 is a burkholderia type vi secretion system-exported protein required for multinucleated giant cell formation and virulence. *Infection and immunity*, 82(4):1445–1452, 2014.

[6] Jun Zheng, Ok S Shin, D Ewen Cameron, and John J Mekalanos. Quorum sensing and a global regulator tsra control expression of type vi secretion and virulence in *Vibrio cholerae*. *Proceedings of the National Academy of Sciences*, 107(49):21128–21133, 2010.

[7] Richelle C Charles and Edward T Ryan. Cholera in the 21st century. *Current opinion in infectious diseases*, 24(5):472–477, 2011.

[8] World Health Organization. Cholera fact sheet. shorturl.at/jwAO9, February 2021.

[9] Mohammad Ali, Anna Lena Lopez, Young You, Young Eun Kim, Binod Sah, Brian Maskery, and John Clemens. The global burden of cholera. *Bulletin of the World Health Organization*, 90:209–218, 2012.

[10] Daniel Unterweger, Sarah T Miyata, Verena Bachmann, Teresa M Brooks, Travis Mullins, Benjamin Kostiuk, Daniele Provenzano, and Stefan Pukatzki. The *Vibrio cholerae* type vi secretion system employs diverse effector modules for intraspecific competition. *Nature communications*, 5(1):1–9, 2014.

[11] Sandrine Borgeaud, Lisa C Metzger, Tiziana Scrignari, and Melanie Blokesch. The type vi secretion system of *Vibrio cholerae* fosters horizontal gene transfer. *Science*, 347(6217):63–67, 2015.

[12] Mary-Jane Lombardo, Jane Michalski, Hector Martinez-Wilson, Cara Morin, Tamara Hilton, Carlos G Osorio, James P Nataro, Carol O Tacket, Andrew Camilli, and James B Kaper. An in vivo expression technology screen for *Vibrio cholerae* genes expressed in human volunteers. *Proceedings of the National Academy of Sciences*, 104(46):18229–18234, 2007.

[13] Amy T Ma and John J Mekalanos. In vivo actin cross-linking induced by *Vibrio cholerae* type vi secretion system is associated with intestinal inflammation. *Proceedings of the National Academy of Sciences*, 107(9):4365–4370, 2010.

[14] Yang Fu, Matthew K Waldor, and John J Mekalanos. Tn-seq analysis of *Vib-*

rio cholerae intestinal colonization reveals a role for t6ss-mediated antibacterial activity in the host. *Cell host & microbe*, 14(6):652–663, 2013.

[15] Andrew T Cheng, Karen M Ottemann, and Fitnat H Yildiz. *Vibrio cholerae* response regulator vxrb controls colonization and regulates the type vi secretion system. *PLoS pathogens*, 11(5):e1004933, 2015.

[16] Savannah L Logan, Jacob Thomas, Jinyuan Yan, Ryan P Baker, Drew S Shields, Joao B Xavier, Brian K Hammer, and Raghuveer Parthasarathy. The *Vibrio cholerae* type vi secretion system can modulate host intestinal mechanics to displace gut bacterial symbionts. *Proceedings of the National Academy of Sciences*, 115(16):E3779–E3787, 2018.

[17] Wenjing Zhao, Florence Caro, William Robins, and John J Mekalanos. Antagonism toward the intestinal microbiota and its effect on *Vibrio cholerae* virulence. *Science*, 359(6372):210–213, 2018.

[18] David Fast, Benjamin Kostiuk, Edan Foley, and Stefan Pukatzki. Commensal pathogen competition impacts host viability. *Proceedings of the National Academy of Sciences*, 115(27):7099–7104, 2018.

[19] David Fast, Kristina Petkau, Meghan Ferguson, Minjeong Shin, Anthony Galenza, Benjamin Kostiuk, Stefan Pukatzki, and Edan Foley. *Vibrio cholerae*-symbiont interactions inhibit intestinal repair in drosophila. *Cell reports*, 30(4):1088–1100, 2020.

[20] Paul Breen, Andrew D Winters, Kevin R Theis, and Jeffrey H Withey. The *Vibrio cholerae* t6ss is dispensable for colonization but affects pathogenesis and the structure of zebrafish intestinal microbiome. *Infection and Immunity*, pages IAI–00151, 2021.

[21] áM Basler and JJ Mekalanos. Type 6 secretion dynamics within and between bacterial cells. *Science*, 337(6096):815–815, 2012.

[22] Yannick R Brunet, Abdelrahim Zoued, Frédéric Boyer, Badreddine Douzi, and Eric Cascales. The type vi secretion tssefgk-vgrg phage-like baseplate is recruited to the tssjlm membrane complex via multiple contacts and serves as assembly platform for tail tube/sheath polymerization. *PLoS genetics*, 11(10):e1005545, 2015.

[23] Teresa M Brooks, Daniel Unterweger, Verena Bachmann, Benjamin Kostiuk, and Stefan Pukatzki. Lytic activity of the *Vibrio cholerae* type vi secretion toxin vgrg-3 is inhibited by the antitoxin tsab. *Journal of Biological Chemistry*, 288(11):7618–7625, 2013.

[24] Losee L Ling, Tanja Schneider, Aaron J Peoples, Amy L Spoering, Ina Engels, Brian P Conlon, Anna Mueller, Till F Schäberle, Dallas E Hughes, Slava Epstein, et al. A new antibiotic kills pathogens without detectable resistance. *Nature*, 517(7535):455–459, 2015.

[25] áM Basler, áM Pilhofer, GP Henderson, GJ Jensen, and JJ3527127 Mekalanos.

Type vi secretion requires a dynamic contractile phage tail-like structure. *Nature*, 483(7388):182–186, 2012.

[26] Jing Wang, Maximilian Brackmann, Daniel Castano-Diez, Mikhail Kudryashev, Kenneth N Goldie, Timm Maier, Henning Stahlberg, and Marek Basler. Cryo-em structure of the extended type vi secretion system sheath–tube complex. *Nature microbiology*, 2(11):1507–1512, 2017.

[27] Gabriele Bönemann, Aleksandra Pietrosiuk, Alexander Diemand, Hanswalter Zentgraf, and Axel Mogk. Remodelling of vipa/vipb tubules by clpv-mediated threading is crucial for type vi protein secretion. *The EMBO journal*, 28(4):315–325, 2009.

[28] Aleksandra Pietrosiuk, Esther D Lenherr, Sebastian Falk, Gabriele Bönemann, Jürgen Kopp, Hanswalter Zentgraf, Irmgard Sinning, and Axel Mogk. Molecular basis for the unique role of the AAA+ chaperone clpv in type vi protein secretion. *Journal of Biological Chemistry*, 286(34):30010–30021, 2011.

[29] Brian T Ho, Tao G Dong, and John J Mekalanos. A view to a kill: the bacterial type vi secretion system. *Cell host & microbe*, 15(1):9–21, 2014.

[30] Julie M Silverman, Danielle M Agnello, Hongjin Zheng, Benjamin T Andrews, Mo Li, Carlos E Catalano, Tamir Gonen, and Joseph D Mougous. Haemolysin coregulated protein is an exported receptor and chaperone of type vi secretion substrates. *Molecular cell*, 51(5):584–593, 2013.

[31] Chacko Jobichen, Smarajit Chakraborty, Mo Li, Jun Zheng, Lissa Joseph, Yu-

Keung Mok, Ka Yin Leung, and J Sivaraman. Structural basis for the secretion of evpc: a key type vi secretion system protein from edwardsiella tarda. *PloS one*, 5(9):e12910, 2010.

[32] Abderrahman Hachani, Luke P Allsopp, Yewande Oduko, and Alain Filloux. The vgrg proteins are "a la carte" delivery systems for bacterial type vi effectors. *Journal of Biological Chemistry*, 289(25):17872–17884, 2014.

[33] Daniel Unterweger, Benjamin Kostiuk, Rina Ötjengerdes, Ashley Wilton, Laura Diaz-Satizabal, and Stefan Pukatzki. Chimeric adaptor proteins translocate diverse type vi secretion system effectors in *Vibrio cholerae*. *The EMBO journal*, 34(16):2198–2210, 2015.

[34] Xiaoye Liang, Richard Moore, Mike Wilton, Megan JQ Wong, Linh Lam, and Tao G Dong. Identification of divergent type vi secretion effectors using a conserved chaperone domain. *Proceedings of the National Academy of Sciences*, 112(29):9106–9111, 2015.

[35] Mikhail M Shneider, Sergey A Buth, Brian T Ho, Marek Basler, John J Mekalanos, and Petr G Leiman. Paar-repeat proteins sharpen and diversify the type vi secretion system spike. *Nature*, 500(7462):350–353, 2013.

[36] Steven J Hersch, Nobuhiko Watanabe, Maria Silvina Stietz, Kevin Manera, Fatima Kamal, Brianne Burkinshaw, Linh Lam, Alexander Pun, Meixin Li, Alexei Savchenko, et al. Envelope stress responses defend against type six secretion system

attacks independently of immunity proteins. *Nature microbiology*, 5(5):706–714, 2020.

[37] Xiaoye Liang, Fatima Kamal, Tong-Tong Pei, Ping Xu, John J Mekalanos, and Tao G Dong. An onboard checking mechanism ensures effector delivery of the type vi secretion system in *Vibrio cholerae*. *Proceedings of the National Academy of Sciences*, 116(46):23292–23298, 2019.

[38] Paul C Kirchberger, Daniel Unterweger, Daniele Provenzano, Stefan Pukatzki, and Yan Boucher. Sequential displacement of type vi secretion system effector genes leads to evolution of diverse immunity gene arrays in *Vibrio cholerae*. *Scientific reports*, 7(1):1–12, 2017.

[39] Tao G Dong, Brian T Ho, Deborah R Yoder-Himes, and John J Mekalanos. Identification of t6ss-dependent effector and immunity proteins by tn-seq in *Vibrio cholerae*. *Proceedings of the National Academy of Sciences*, 110(7):2623–2628, 2013.

[40] Sarah T Miyata, Daniel Unterweger, Sydney P Rudko, and Stefan Pukatzki. Dual expression profile of type vi secretion system immunity genes protects pandemic *Vibrio cholerae*. *PLoS pathogens*, 9(12):e1003752, 2013.

[41] Dana L MacIntyre, Sarah T Miyata, Maya Kitaoka, and Stefan Pukatzki. The *Vibrio cholerae* type vi secretion system displays antimicrobial properties. *Proceedings of the National Academy of Sciences*, 107(45):19520–19524, 2010.

[42] Megan JQ Wong, Xiaoye Liang, Matt Smart, Le Tang, Richard Moore, Brian

Ingalls, and Tao G Dong. Microbial herd protection mediated by antagonistic interaction in polymicrobial communities. *Applied and environmental microbiology*, 82(23):6881–6888, 2016.

[43] Francis J Santoriello, Paul Kirchberger, Yann Boucher, and Stefan Pukatzki. Pandemic *Vibrio cholerae* acquired competitive traits from an environmental vibrio species. *bioRxiv*, 2021.

[44] David Bruce Borenstein, Peter Ringel, Marek Basler, and Ned S Wingreen. Established microbial colonies can survive type vi secretion assault. *PLoS computational biology*, 11(10):e1004520, 2015.

[45] Sanna Koskiniemi, James G Lamoureux, Kiel C Nikolakakis, Claire t'Kint de Roodenbeke, Michael D Kaplan, David A Low, and Christopher S Hayes. Rhs proteins from diverse bacteria mediate intercellular competition. *Proceedings of the National Academy of Sciences*, 110(17):7032–7037, 2013.

[46] Dor Salomon, Lisa N Kinch, David C Trudgian, Xiaofeng Guo, John A Klimko, Nick V Grishin, Hamid Mirzaei, and Kim Orth. Marker for type vi secretion system effectors. *Proceedings of the National Academy of Sciences*, 111(25):9271–9276, 2014.

[47] Nguyen-Hung Le, Victor Pinedo, Juvenal Lopez, Felipe Cava, and Mario F Feldman. Killing of gram-negative and gram-positive bacteria by a bifunctional cell wall-targeting t6ss effector. *BioRxiv*, 2021.

[48] Ming-Xuan Tang, Tao Dong, Tong-tong Pei, Zeng-Hang Wang, Han Luo, and Xing-Yu Wang. Abiotic factors modulate interspecies competition mediated by the type vi secretion system effectors in *Vibrio cholerae*. *bioRxiv*, 2021.

[49] Emrah Altindis, Tao Dong, Christy Catalano, and John Mekalanos. Secretome analysis of *Vibrio cholerae* type vi secretion system reveals a new effector-immunity pair. *MBio*, 6(2):e00075–15, 2015.

[50] Jun Zheng, Brian Ho, and John J Mekalanos. Genetic analysis of anti-amoebae and anti-bacterial activities of the type vi secretion system in *Vibrio cholerae*. *PloS one*, 6(8):e23876, 2011.

[51] SG Williams, LT Varcoe, Stephen Richard Attridge, and Paul Alexander Manning. *Vibrio cholerae* hcp, a secreted protein coregulated with hlya. *Infection and immunity*, 64(1):283–289, 1996.

[52] Lisa C Metzger, Sandrine Stutzmann, Tiziana Scrignari, Charles Van der Henst, Noémie Matthey, and Melanie Blokesch. Independent regulation of type vi secretion in *Vibrio cholerae* by TfoX and TfoY. *Cell reports*, 15(5):951–958, 2016.

[53] Cristian V Crisan, Aroon T Chande, Kenneth Williams, Vishnu Raghuram, Lavanya Rishishwar, Gabi Steinbach, Samit S Watve, Peter Yunker, I King Jordan, and Brian K Hammer. Analysis of *Vibrio cholerae* genomes identifies new type vi secretion system gene clusters. *Genome biology*, 20(1):1–14, 2019.

[54] Christophe S Bernard, Yannick R Brunet, Marthe Gavioli, Roland Lloubès, and

Eric Cascales. Regulation of type vi secretion gene clusters by σ54 and cognate enhancer binding proteins. *Journal of bacteriology*, 193(9):2158–2167, 2011.

[55] Maya Kitaoka, Sarah T Miyata, Teresa M Brooks, Daniel Unterweger, and Stefan Pukatzki. Vash is a transcriptional regulator of the type vi secretion system functional in endemic and pandemic *Vibrio cholerae*. *Journal of bacteriology*, 193(23):6471–6482, 2011.

[56] Tao G Dong and John J Mekalanos. Characterization of the rpon regulon reveals differential regulation of t6ss and new flagellar operons in *Vibrio cholerae* o37 strain v52. *Nucleic acids research*, 40(16):7766–7775, 2012.

[57] Jörg Schumacher, Nicolas Joly, Mathieu Rappas, Xiaodong Zhang, and Martin Buck. Structures and organisation of AAA+ enhancer binding proteins in transcriptional activation. *Journal of structural biology*, 156(1):190–199, 2006.

[58] Takahiko Ishikawa, Pramod Kumar Rompikuntal, Barbro Lindmark, Debra L Milton, and Sun Nyunt Wai. Quorum sensing regulation of the two hcp alleles in *Vibrio cholerae* o1 strains. *PloS one*, 4(8):e6734, 2009.

[59] Kevin Manera, Florence Caro, Hao Li, Tong-Tong Pei, Steven J Hersch, John J Mekalanos, and Tao G Dong. Sensing of intracellular hcp levels controls t6ss expression in *Vibrio cholerae*. *Proceedings of the National Academy of Sciences*, 118(25), 2021.

[60] Mirella Lo Scrudato and Melanie Blokesch. A transcriptional regulator linking quo-

rum sensing and chitin induction to render *Vibrio cholerae* naturally transformable. *Nucleic acids research*, 41(6):3644–3658, 2013.

[61] Loni Townsley, Marilou P Sison Mangus, Sanjin Mehic, and Fitnat H Yildiz. Response of *Vibrio cholerae* to low-temperature shifts: Cspv regulation of type vi secretion, biofilm formation, and association with zooplankton. *Applied and environmental microbiology*, 82(14):4441–4452, 2016.

[62] Takahiko Ishikawa, Dharmesh Sabharwal, Jeanette Bröms, Debra L Milton, Anders Sjöstedt, Bernt Eric Uhlin, and Sun Nyunt Wai. Pathoadaptive conditional regulation of the type vi secretion system in *Vibrio cholerae* o1 strains. *Infection and immunity*, 80(2):575–584, 2012.

[63] Verena Bachmann, Benjamin Kostiuk, Daniel Unterweger, Laura Diaz-Satizabal, Stephen Ogg, and Stefan Pukatzki. Bile salts modulate the mucin-activated type vi secretion system of pandemic *Vibrio cholerae*. *PLoS neglected tropical diseases*, 9(8):e0004031, 2015.

[64] Martin Schuster, D Joseph Sexton, Stephen P Diggle, and E Peter Greenberg. Acyl-homoserine lactone quorum sensing: from evolution to application. *Annual review of microbiology*, 67:43–63, 2013.

[65] ST Rutherford and BL Bassler. Cold spring harbor perspect. *Med*, 2(11):1, 2012.

[66] Jun Zhu, Melissa B Miller, Russell E Vance, Michelle Dziejman, Bonnie L Bassler, and John J Mekalanos. Quorum-sensing regulators control virulence gene ex-

pression in *Vibrio cholerae*. *Proceedings of the National Academy of Sciences*, 99(5):3129–3134, 2002.

[67] Brian K Hammer and Bonnie L Bassler. Quorum sensing controls biofilm formation in *Vibrio cholerae*. *Molecular microbiology*, 50(1):101–104, 2003.

[68] Yi Shao and Bonnie L Bassler. Quorum regulatory small rnas repress type vi secretion in v ibrio cholerae. *Molecular microbiology*, 92(5):921–930, 2014.

[69] Sarah A Jung, Christine A Chapman, and Wai-Leung Ng. Quadruple quorum-sensing inputs control *Vibrio cholerae* virulence and maintain system robustness. *PLoS pathogens*, 11(4):e1004837, 2015.

[70] Melissa B Miller, Karen Skorupski, Derrick H Lenz, Ronald K Taylor, and Bonnie L Bassler. Parallel quorum sensing systems converge to regulate virulence in *Vibrio cholerae*. *Cell*, 110(3):303–314, 2002.

[71] Amy M Tsou, Tao Cai, Zhi Liu, Jun Zhu, and Rahul V Kulkarni. Regulatory targets of quorum sensing in *Vibrio cholerae*: evidence for two distinct hapr-binding motifs. *Nucleic acids research*, 37(8):2747–2756, 2009.

[72] Anwar Huq, R Bradley Sack, Azhar Nizam, Ira M Longini, G Balakrish Nair, Afsar Ali, J Glenn Morris Jr, MN Huda Khan, A Kasem Siddique, Mohammed Yunus, et al. Critical factors influencing the occurrence of *Vibrio cholerae* in the environment of bangladesh. *Applied and environmental microbiology*, 71(8):4645–4654, 2005.

[73] Luigi Vezzulli, Carla Pruzzo, Anwar Huq, and Rita R Colwell. Environmental reservoirs of *Vibrio cholerae* and their role in cholera. *Environmental microbiology reports*, 2(1):27–33, 2010.

[74] Mirella Lo Scrudato, Sandrine Borgeaud, and Melanie Blokesch. Regulatory elements involved in the expression of competence genes in naturally transformable *Vibrio cholerae*. *BMC microbiology*, 14(1):1–13, 2014.

[75] Karin L Meibom, Xibing B Li, Alex T Nielsen, Cheng-Yen Wu, Saul Roseman, and Gary K Schoolnik. The *Vibrio cholerae* chitin utilization program. *Proceedings of the National Academy of Sciences*, 101(8):2524–2529, 2004.

[76] Karin L Meibom, Melanie Blokesch, Nadia A Dolganov, Cheng-Yen Wu, and Gary K Schoolnik. Chitin induces natural competence in *Vibrio cholerae*. *Science*, 310(5755):1824–1827, 2005.

[77] Samit S Watve, Jacob Thomas, and Brian K Hammer. Cytr is a global positive regulator of competence, type vi secretion, and chitinases in *Vibrio cholerae*. *PloS one*, 10(9):e0138834, 2015.

[78] Laetitia Houot, Sarah Chang, Bradley S Pickering, Cedric Absalon, and Paula I Watnick. The phosphoenolpyruvate phosphotransferase system regulates *Vibrio cholerae* biofilm formation through multiple independent pathways. *Journal of bacteriology*, 192(12):3055–3067, 2010.

[79] Josef Deutscher, Christof Francke, and Pieter W Postma. How phosphotransferase

system-related protein phosphorylation regulates carbohydrate metabolism in bacteria. *Microbiology and molecular biology Reviews*, 70(4):939–1031, 2006.

[80] Weili Liang, Alberto Pascual-Montano, Anisia J Silva, and Jorge A Benitez. The cyclic amp receptor protein modulates quorum sensing, motility and multiple genes that affect intestinal colonization in *Vibrio cholerae*. *Microbiology*, 153(9):2964–2975, 2007.

[81] Melanie Blokesch. Chitin colonization, chitin degradation and chitin-induced natural competence of *Vibrio cholerae* are subject to catabolite repression. *Environmental microbiology*, 14(8):1898–1912, 2012.

[82] Andrew Rogers, Loni Townsley, Ana L Gallego-Hernandez, Sinem Beyhan, Laura Kwuan, and Fitnat H Yildiz. The LonA protease regulates biofilm formation, motility, virulence, and the type vi secretion system in *Vibrio cholerae*. *Journal of bacteriology*, 198(6):973–985, 2016.

[83] Laurence Van Melderen and Abram Aertsen. Regulation and quality control by Lon-dependent proteolysis. *Research in microbiology*, 160(9):645–651, 2009.

[84] Avatar Joshi, Samar A Mahmoud, Soo-Kyoung Kim, Justyne L Ogdahl, Vincent T Lee, Peter Chien, and Fitnat H Yildiz. c-di-gmp inhibits LonA-dependent proteolysis of TfoY in *Vibrio cholerae*. *PLoS genetics*, 16(6):e1008897, 2020.

[85] Annabelle Mathieu-Denoncourt and Marylise Duperthuy. Secretome analysis reveals a role of subinhibitory concentrations of polymyxin b in the survival of *Vibrio*

cholerae mediated by the type vi secretion system. *Environmental Microbiology*, 2021.

[86] Nicholas J Shikuma and Fitnat H Yildiz. Identification and characterization of oscr, a transcriptional regulator involved in osmolarity adaptation in *Vibrio cholerae*. *Journal of bacteriology*, 191(13):4082–4096, 2009.

[87] Erin K Lipp, Anwar Huq, and Rita R Colwell. Effects of global climate on infectious disease: the cholera model. *Clinical microbiology reviews*, 15(4):757–770, 2002.

[88] Valérie R Louis, Estelle Russek-Cohen, Nipa Choopun, Irma NG Rivera, Brian Gangle, Sunny C Jiang, Andrea Rubin, Jonathan A Patz, Anwar Huq, and Rita R Colwell. Predictability of *Vibrio cholerae* in chesapeake bay. *Applied and environmental microbiology*, 69(5):2773–2785, 2003.

[89] Rita R Colwell, James Kaper, and SW Joseph. *Vibrio cholerae*, vibrio parahaemolyticus, and other vibrios: occurrence and distribution in chesapeake bay. *Science*, 198(4315):394–396, 1977.

[90] Ryan S Mueller, Sinem Beyhan, Simran G Saini, Fitnat H Yildiz, and Douglas H Bartlett. Indole acts as an extracellular cue regulating gene expression in *Vibrio cholerae*. *Journal of bacteriology*, 191(11):3504–3516, 2009.

[91] Charlie G Buffie and Eric G Pamer. Microbiota-mediated colonization resistance against intestinal pathogens. *Nature Reviews Immunology*, 13(11):790–801, 2013.

[92] Ivaylo I Ivanov, Koji Atarashi, Nicolas Manel, Eoin L Brodie, Tatsuichiro Shima,

Ulas Karaoz, Dongguang Wei, Katherine C Goldfarb, Clark A Santee, Susan V Lynch, et al. Induction of intestinal th17 cells by segmented filamentous bacteria. *Cell*, 139(3):485–498, 2009.

[93] Koji Atarashi, Takeshi Tanoue, Tatsuichiro Shima, Akemi Imaoka, Tomomi Kuwahara, Yoshika Momose, Genhong Cheng, Sho Yamasaki, Takashi Saito, Yusuke Ohba, et al. Induction of colonic regulatory t cells by indigenous clostridium species. *Science*, 331(6015):337–341, 2011.

[94] Eryn E Bernardy, Maryann A Turnsek, Sarah K Wilson, Cheryl L Tarr, and Brian K Hammer. Diversity of clinical and environmental isolates of *Vibrio cholerae* in natural transformation and contact-dependent bacterial killing indicative of type vi secretion system activity. *Applied and environmental microbiology*, 82(9):2833–2842, 2016.

Chapter 2

c-di-GMP Inhibits LonA-dependent Proteolysis of TfoY in *V. cholerae*

2.1 Introduction

Regulated proteolysis is a critical cellular mechanism that helps cells maintain homeostasis and regulate diverse processes [1, 2, 3]. The LonA (or Lon) protease is present across all domains of life and plays a central role in maintaining cellular homeostasis. LonA facilitates the turnover of misfolded, damaged, or unused proteins, a process which frees amino acids for use in other cellular machinery [1, 2, 3]. LonA's central role in governing cellular behaviors is highlighted by the gross dysregulation of wide-ranging cellular processes in its absence. For example, in many bacterial species, loss of *lonA* results in aberrant cell division, susceptibility to stressors such as UV irradiation and heat shock, as well as aberrant control of motility, biofilm formation,

quorum sensing, virulence factor production, and host colonization. Indeed, deletion of *lonA* significantly reduces the *in vivo* fitness of every pathogenic bacteria in which it has been tested [4, 5, 6, 7, 8, 9, 10, 11, 12].

LonA belongs to the superfamily of ATPases associated with diverse cellular activities (AAA+ ATPases) [1, 2, 3]. LonA monomers assemble into a barrel shaped hexamer, which utilizes successive rounds of ATP-hydrolysis to bind, unwind, and translocate proteins into a central chamber where catalytic serine and lysine residues irreversibly proteolyze substrates [1, 2, 3, 13, 14]. Because proteolysis is irreversible, the selectivity of AAA+ proteases must be carefully controlled [1, 2, 3, 13, 15]. In some cases, AAA+ proteases recognize their substrates directly, via recognition of conserved motifs known as degrons [1, 2, 3, 13, 14]. In other cases, additional specificity factors, known as adaptors, or other small signaling molecules can modulate the rate of proteolysis. To date, only two LonA adaptor proteins have been identified [16, 17]. The first LonA adaptor, known as SmiA, was identified in *Bacillus subtilis* and coordinates proteolysis of the swarming motility master regulator SwrA [16]. The second adaptor, known as HspQ, is a specificity-enhancing factor that allosterically activates *Yersinia pestis* Lon protease against diverse substrates including a small histone-like protein YmoA, which controls activation of the type III secretion system [17]. LonA has also been shown to respond to diverse signals *in vitro*, such as polyphosphate, cyclic AMP, guanosine tetraphosphate, c-di-GMP, and DNA; however, relatively little is known regarding the physiological consequences of these molecules *in vivo*[18, 19, 20].

LonA plays a critical role in the infection cycle of *Vibrio cholerae*, the facul-

tative human pathogen responsible for the acute diarrheal disease cholera. *V. cholerae* remains a threat to global public health. There are estimated to be 1.3–4.0 million cases of cholera and 21,000–143,000 deaths worldwide each year [21]. We previously demonstrated LonA's importance in *V. cholerae* pathogenesis as deletion of *lonA* results in a severe colonization defect in the infant mouse model [4]. LonA positively regulates biofilm formation but negatively regulates motility, the toxin co-regulated pilus and cholera toxin [4, 8]. In addition, LonA negatively regulates the type VI secretion system (T6SS), a contact dependent contractile spear that translocates toxins into neighboring prokaryotic and eukaryotic cells [4, 22]. LonA also functions as an activator and a repressor of c-di-GMP pools in planktonic and biofilm grown cells, respectively [4]. Finally, deletion of *lonA* results in filamentation of cells, suggesting it plays a role in cell septation [4]. Collectively, these phenotypes demonstrate the significance of LonA regulated cellular processes in *V. cholerae* pathogenesis and environmental survival. To date, only two known LonA substrates have been identified in *V. cholerae*. The first is FliA, an alternative sigma factor (σ28) that coordinates the activation of late stage flagellar genes and the repression of virulence gene expression [8]. The second is the quorum sensing master regulator HapR, which is proteolyzed by LonA upon heat shock in order to induce biofilm formation [23]. LonA proteolysis of FliA or HapR is highly condition dependent and is not sufficient to explain a majority of the phenotypes observed in a *lonA* mutant.

In the current study, using a quantitative proteomics approach, we identify the T6SS and motility regulator TfoY as a LonA target. We show that the hyper activation

of motility and T6SS-dependent killing in the Δ*lonA* strain are due to the absence of LonA-mediated degradation of TfoY. Further, we find that c-di-GMP represses LonA proteolysis of TfoY *in vivo* and show that c-di-GMP directly binds to LonA and inhibits its activity *in vitro*. Finally, we demonstrate the significance of LonA and TfoY mediated regulation of motility and T6SS-dependent killing phenotypes in strains with high and low cellular levels of c-di-GMP relative to WT. Our work provides the first *in vivo* evidence that LonA is a true c-di-GMP receptor protein and suggests how this second messenger can temper the levels of TfoY through changes in regulated degradation.

2.2 Results

2.2.1 Whole proteome analysis identifies TfoY as a putative LonA substrate

The substrates controlled by LonA in *V. cholerae* remain poorly characterized. Since the stability of a protein targeted for degradation is directly dependent upon the protease or proteases that degrade it, we sought to perform a global analysis of the relative enrichment of proteins in wild-type (WT) and Δ*lonA* strains. To identify proteins whose stability are dependent upon LonA, we used tandem mass tag (TMT)-labeling coupled with liquid chromatography tandem mass spectrometry (LC-MS/MS) to quantify the proteomes of WT and a Δ*lonA* mutant one hour after treatment with the translational inhibitor chloramphenicol. We reasoned that these conditions would reveal the most striking differences for LonA substrates (Fig 2.1). We identified 80 proteins

to be significantly enriched in the Δ*lonA* strain (Table A.1), suggesting that these proteins are either proteolyzed by LonA or are regulated in a LonA-dependent pathway. In addition, we identified 38 proteins to be significantly enriched in WT relative to the Δ*lonA* strain (Table A.2), suggesting that LonA positively impacts production of these proteins through indirect means.

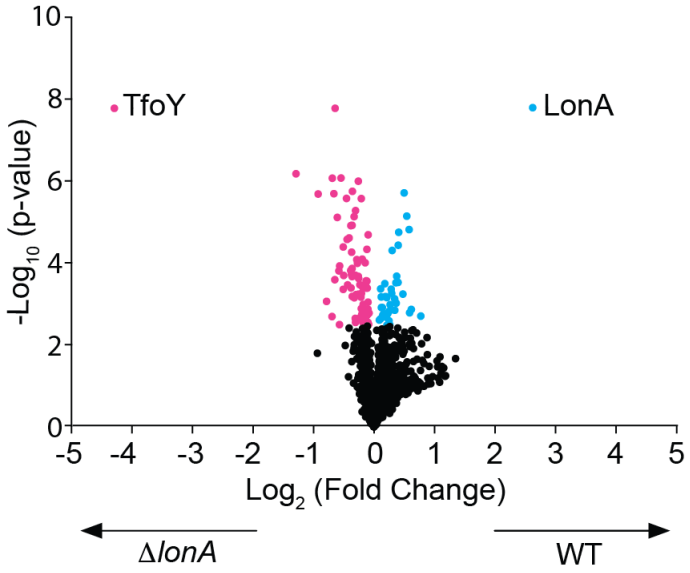

Figure 2.1: TfoY is significantly enriched in the Δ*lonA* mutant relative to wild-type. A volcano plot of proteins enriched in WT and Δ*lonA* mutant after translational inhibition. The proteomes of WT and Δ*lonA* strains (n = 5) that had been grown to an OD_{600} = 1.0 and exposed to the translational inhibitor chloramphenicol for 1-hour were analyzed by TMT-labeling and LC-MS/MS. A student's t-test using a Benjamini-Hochberg FDR cutoff of 5% was used to identify proteins that were statistically significantly enriched. Proteins enriched in Δ*lonA* relative to WT are shown in pink. Proteins enriched in WT relative to Δ*lonA* are shown in blue.

The proteins identified in our analysis are predicted to be involved in a wide array of metabolic activities such as amino acid and protein biosynthesis, central intermediary metabolism, energy metabolism, fatty acid and phospholipid biosynthesis,

the synthesis of nucleosides and nucleotides, and DNA metabolism. In addition, there was significant enrichment of hypothetical proteins and those involved in protein fate, secretion, or predicted to have regulatory functions. The most significantly enriched protein identified in our analysis was the transcriptional regulator TfoY (4.28 $\log_2$ fold increase), which was recently shown to lead to significant increases in motility and the T6SS, two behaviors that LonA represses [24]. Given that TfoY was the most abundant protein identified in our analysis and LonA control over TfoY could explain multiple $\Delta lonA$ phenotypes, we chose to focus our analysis on TfoY.

2.2.2 TfoY stability is controlled by LonA

To validate that TfoY stability is dependent upon LonA, we performed an *in vivo* protein stability assay. Since the conditions that lead to TfoY production remain to be fully elucidated, we placed the *tfoY* gene under the control of the Ptac promoter at the Tn7 locus on the chromosome in both WT and $\Delta lonA$ strains [25]. We then induced TfoY production via the addition of IPTG and tested TfoY stability as a function of time after translational inhibition. We observed that TfoY is highly unstable in the WT genetic background, with the majority of TfoY protein degraded within 15 minutes (Fig 2.2). In contrast, TfoY was stabilized in the absence of LonA (Fig 2.2). Indeed, we observed little to no signs of degradation for at least two hours, suggesting that LonA is the major factor governing TfoY protein stability in *V. cholerae*.

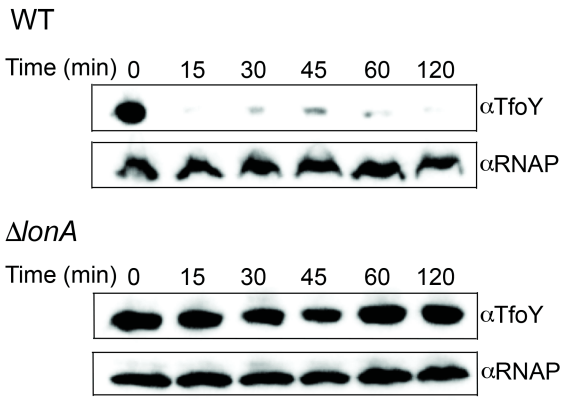

Figure 2.2: TfoY stability depends on the LonA protease. *In vivo* stability of TfoY after translational inhibition. TfoY was overproduced from the Tn7 locus in WT and a Δ*lonA* strains. Stability of TfoY was analyzed by western blot using an antibody against TfoY at the indicated time points. RNAP was used as a biomass loading control.

2.2.3 LonA represses motility and the type VI secretion system via TfoY

LonA is a repressor of motility and the T6SS, while TfoY enhances both pathways [4, 24]. Given that TfoY stability is dependent upon LonA, one explanation for the hypermotility and increased T6SS-dependent killing observed in the Δ*lonA* background is the increased abundance and stability of TfoY protein. To determine if dysregulation of TfoY could account for the increased activation of motility and T6SS-dependent killing observed in the Δ*lonA* strain, we assessed the motility and T6SS-dependent killing phenotypes of WT, Δ*tfoY*, Δ*lonA*, and Δ*lonA* Δ*tfoY* as well as in a *tfoY* overproducing strain (Fig 2.3A–2.3D).

The lack of *tfoY* did not result in statistically significant differences in motility or T6SS mediated killing relative to WT, suggesting that TfoY production is tightly

regulated under these conditions. Consistent with our previous work, the Δ*lonA* strain exhibited increased motility and T6SS killing [4]. Furthermore, strains harboring a mutation in the active site of LonA, where the catalytic serine is replaced with an alanine (LonAS678A), exhibited motility and T6SS-dependent killing phenotypes similar to a Δ*lonA* strain, indicating that LonA's proteolytic activity is necessary for repression of motility and T6SS-dependent killing. Consistent with our hypothesis, we observed that deletion of *tfoY* in the Δ*lonA* strain restored motility and T6SS-dependent killing to WT levels. We also observed that overproduction of TfoY leads to enhanced motility and T6SS-dependent killing, which is consistent with TfoY's known role as an activator of the T6SS and motility (Fig 2.3B and 2.3D) [24, 26]. In addition, we assessed levels of TfoY in *lonA* and *tfoY* mutant strains relative to WT (Fig 2.3E). We observed that detection of TfoY is dependent upon the presence of a functional LonA and that complementation of *tfoY* in the Δ*lonA*Δ*tfoY* mutant restored detection of TfoY. The high levels of TfoY in the complemented strain, which harbors 500 base pairs of the upstream regulatory sequence, suggests that additional regulatory factors may be present at the native locus of *tfoY*.

Finally, overexpression of *tfoY* from the Ptac promoter leads to large increases in TfoY. Taken together, these findings suggest that LonA tempers motility and T6SS-dependent killing in *V. cholerae* by controlling cellular levels of TfoY.

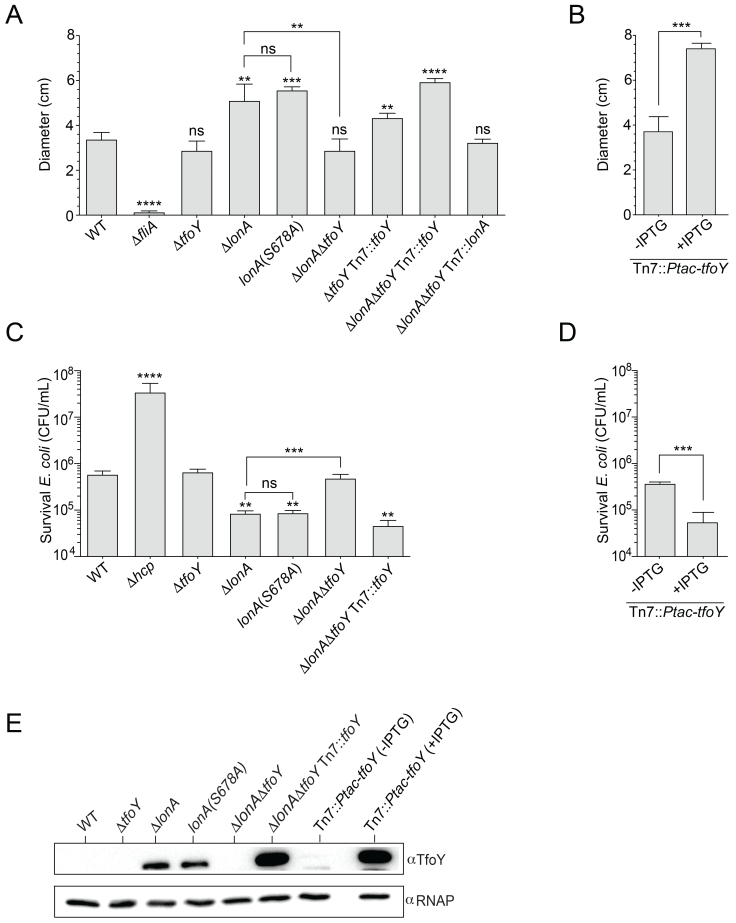

Figure 2.3: LonA represses motility and the T6SS through TfoY. Quantification of flagellar motility and T6SS killing experiments. For motility assays, single colonies were stabbed into LB soft agar plates (0.3% agar) and incubated at 30°C for approximately 18 hours. (A) Swimming motility phenotypes of WT, ΔfliA (negative control) and various Δ*lonA* and/or Δ*tfoY* deletions as well as their complementation strains from the Tn7 site. (B) Overexpression of *tfoY* from the Ptac promoter in plates with and without IPTG. (C) The T6SS killing phenotypes of various *tfoY* and *lonA* deletion mutants as well as their complementation strains were analyzed. T6SS killing was determined by enumerating the survival of *E. coli* strain MC4100, which is susceptible to T6SS attack. In addition, Δ*hcp* was included as a negative control for T6SS dependent killing and *lonA*(S678A) as a control for LonA-dependent proteolysis. (D) Overexpression of *tfoY* from the Ptac promoter on plates with or without IPTG. Motility and T6SS-dependent killing experiments represent the average and SD of at least three independent experiments. Statistical analysis was performed using an unpaired Student's t-test. Statistical values indicated are (**p<0.01, ***p < .001, and ****p < 0.0001). (E) Abundance of natively produced TfoY as well as overexpressed TfoY from the Ptac promoter.

2.2.4 LonA controls multiple cellular processes independently of TfoY

In addition to regulating motility and the T6SS, LonA is also responsible for modulating cellular processes that contribute to biofilm formation, intracellular pools of c-di-GMP, and intestinal colonization [4]. We wondered what role, if any, TfoY may play in these Δ*lonA* phenotypes. We evaluated the impact of TfoY on *lonA* biofilm formation using fluorescently labeled *V. cholerae* WT, Δ*tfoY*, Δ*lonA*, and Δ*lonA*Δ*tfoY* strains and confocal laser scanning microscopy (CLSM) (Fig 2.4A). We found that the biofilm-forming ability of the Δ*tfoY* strain is not altered, and that Δ*lonA* and Δ*lonA*Δ*tfoY* strains formed biofilms with similar properties (S3 Table) suggesting that LonA regulation of *tfoY* is not responsible for the aberrant biofilm formation observed in Δ*lonA*. In addition, TfoY appears to be dispensable for biofilm formation under the conditions used in this study.

Deletion of *lonA* also results in decreased levels of global c-di-GMP during exponential growth [4]. Intracellular pools of c-di-GMP are elevated through enzymes known as diguanylate cyclases (DGC) and decreased by phosphodiesterases (PDE). Thus, we wondered whether in the absence of *lonA*, TfoY may accumulate and lead to lower levels of c-di-GMP. We used LC-MS/MS to quantify global pools of c-di-GMP in WT, Δ*tfoY*, Δ*lonA*, and Δ*lonA*Δ*tfoY* strains (Fig 2.4B). Consistent with our previous analysis, we found that strains lacking *lonA* had lower levels of c-di-GMP [4]. However, we did not observe statistically significant differences between WT and Δ*tfoY* or between Δ*lonA* and Δ*lonA*Δ*tfoY* strains. This suggests that LonA's control over

c-di-GMP levels under these conditions occurs through a TfoY-independent pathway.

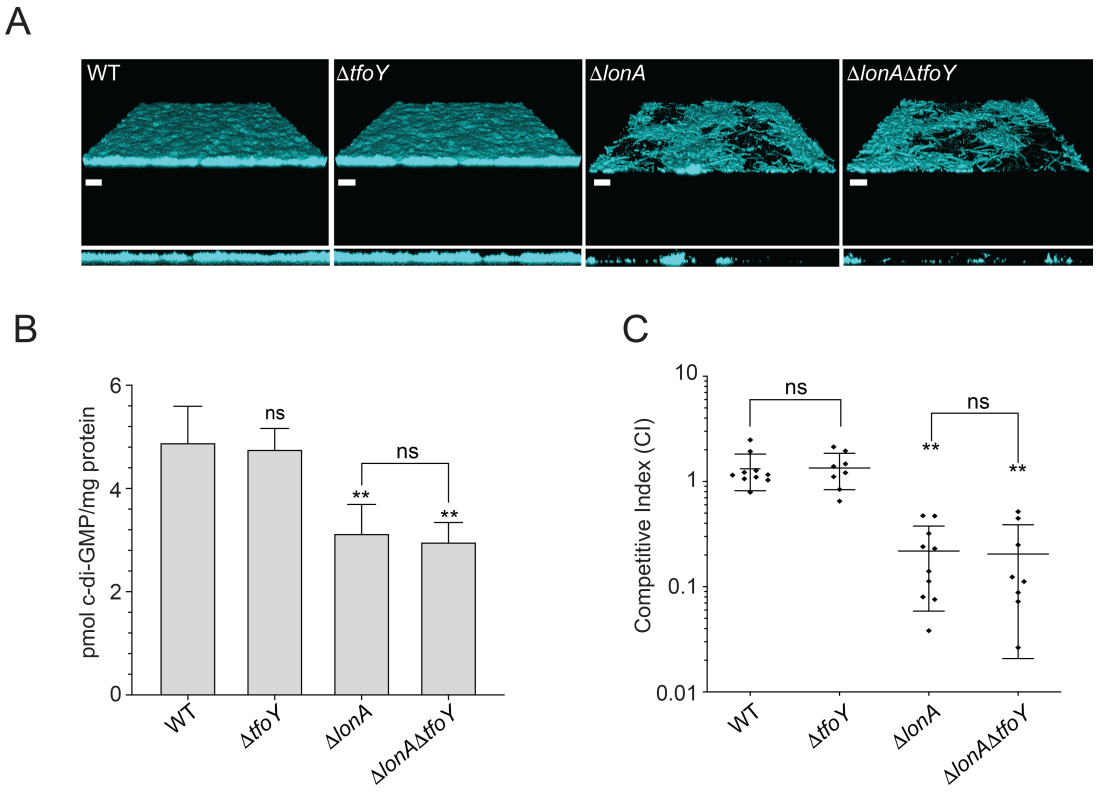

Figure 2.4: LonA regulates biofilm formation, cellular c-di-GMP levels, and intestinal colonization through TfoY independent mechanisms. Analysis of biofilm formation by CLSM, cellular c-di-GMP levels by LC-MS/MS, and intestinal colonization by *in vivo* competition assays. (A) Top-down and orthogonal views of mature biofilms formed by WT, Δ*tfoY*, Δ*lonA*, Δ*lonA*Δ*tfoY* mutants that contained *gfp* at the Tn7 locus. Scale bars are 40μm. (B) Cellular levels of c-di-GMP in WT, Δ*tfoY*, Δ*lonA*, Δ*lonA*Δ*tfoY* that had been grown to exponential phase (OD600 = 0.4) and analyzed for global c-di-GMP by LC-MS/MS. (C) Competitive index of *V. cholerae* strains. Otherwise WT strain (Δ*lacZ*) was co-inoculated with the strains indicated at a 1:1 ratio into 5-day old infant mice. The number of bacteria per intestine was determined 20 to 22 h post inoculation. The competitive index (CI) was determined as the output ratio of mutant to WT cells divided by the input ratio of mutant to WT cells per gram of intestine. Statistical analysis for panel B used a One-way ANOVA with Tukey's post-hoc analysis. Statistical analysis for panel C used Wilcoxon's signed rank test (*p<0.05, **p<0.01).

Finally, to determine what role the LonA and TfoY regulatory circuit might

play during intestinal colonization, we performed an *in vivo* competition experiment by competing WT, Δ*tfoY*, Δ*lonA*, and Δ*lonA*Δ*tfoY* strains against a lacZ- WT strain in the infant mouse intestinal colonization model (Fig 2.4C). We did not observe a statistically significant difference between the Δ*lonA* Δ*tfoY* strain relative to the Δ*lonA* strain. In addition, Δ*tfoY* did not exhibit any competition defect relative to WT. We conclude that TfoY is not a significant factor involved during intestinal colonization of the infant mouse in either WT or Δ*lonA* genetic backgrounds.

2.2.5 LonA activity and TfoY stability are modulated by c-di-GMP *in vivo*

Because c-di-GMP is known to regulate TfoY expression, we next explored whether TfoY abundance and stability is influenced by c-di-GMP levels *in vivo* [24, 26]. We reasoned that DGCs and PDEs that impact *V. cholerae* motility could participate in the LonA-TfoY-c-di-GMP regulatory module and used strains lacking four diguanylate cyclases (Δ4DGC; Δ*cdgD*Δ*cdgH*Δ*cdgK*Δ*cdgL*) and two phosphodiesterases (Δ2PDE; Δ*rocS*Δ*cdgJ*) that impact *V. cholerae* motility to evaluate TfoY stability. We first assessed if natively produced TfoY would be detectable in WT, Δ*lonA*, Δ2PDE, and Δ4DGC strains using a Δ*lonA*Δ*tfoY* mutant as a negative control for TfoY production (Fig 2.5A). We were able to detect significant accumulation of TfoY in Δ*lonA*. In addition, we also observed the presence of TfoY in the Δ2PDE strain but not in WT, Δ4DGC, or Δ*lonA*Δ*tfoY* strains, suggesting that high levels of c-di-GMP in the Δ2PDE background stabilized TfoY, possibly by inhibiting LonA. Given that c-di-GMP can reg-

ulate the production of TfoY at both transcriptional and post-transcriptional levels, we assessed TfoY abundance in WT, Δ*lonA*, Δ*lonA*Δ2PDE, and Δ*lonA*Δ4DGC mutants to better understand how the LonA regulatory mechanism functions to control cellular levels of TfoY (Fig 2.5B) [24, 26]. In the absence of *lonA*, TfoY levels were increased in all backgrounds relative to WT. Notably, levels of TfoY were significantly enriched in the low c-di-GMP strain in the absence of *lonA*. It was previously shown that c-di-GMP limits production of TfoY protein by binding to a riboswitch (Vc2) located in the 5'UTR of *tfoY* mRNA [24, 27, 28]. Thus, this result is consistent with prior analyses, which have shown that decreasing levels of c-di-GMP results in enhanced TfoY translation, and suggests that LonA plays a more significant role in regulating levels of TfoY when c-di-GMP levels are low [24, 26]. In addition, we also observed a small but consistent increase in TfoY in the Δ*lonA*Δ2PDE relative to the Δ*lonA* strain (Fig 2.5B, Table A.2). Notably, levels of LonA did not significantly differ in WT, Δ2PDE, and Δ4DGC strains (Fig 2.5C), suggesting that LonA quantity is not regulated by c-di-GMP. To determine if LonA turnover of TfoY might be influenced by c-di-GMP, we introduced the Tn7::Ptac-*tfoY* construct into the Δ4DGC and Δ2PDE strains and assessed TfoY stability relative to WT (Fig 2.5D). In addition, we simultaneously assessed global levels of c-di-GMP from these strains when *tfoY* was overproduced. We determined that cellular c-di-GMP levels are decreased 4.4-fold in the Δ4DGC and increased 2.2-fold in the Δ2PDE strains (Fig 2.5E). Interestingly, we found that TfoY stability is enhanced and decreased in Δ2PDE and in Δ4DGC strains, respectively suggesting that TfoY stability is positively correlated with cellular c-di-GMP. Taken together, our data demonstrates

that c-di-GMP mediated inhibition of LonA proteolysis is a central factor governing levels of TfoY.

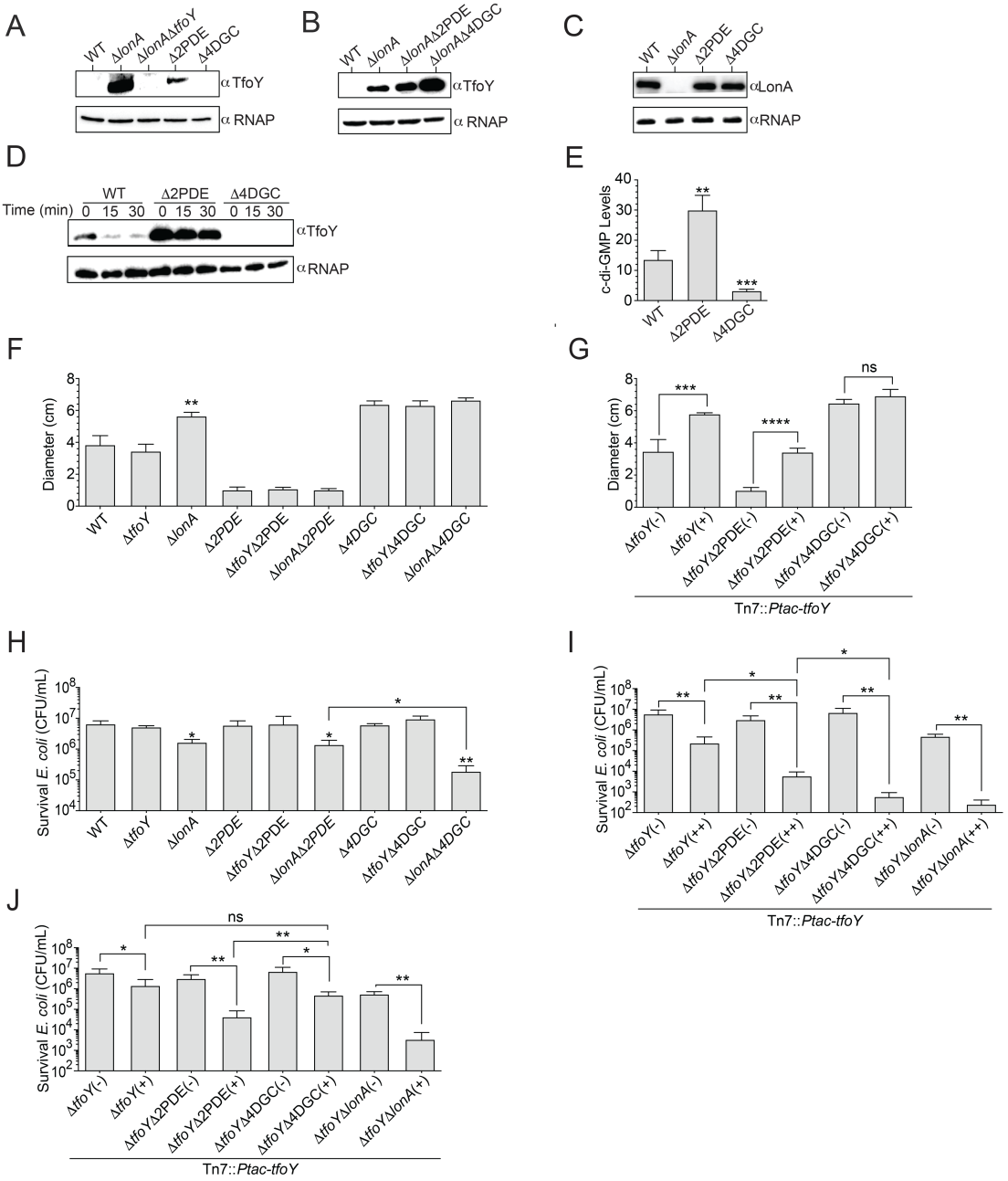

Figure 2.5: TfoY stability is influenced by c-di-GMP. *In vivo* abundance and stability of TfoY in high and low c-di-GMP genetic backgrounds relative to WT. (A) Abundance

of natively produced TfoY in WT, ΔlonA, a mutant lacking two phosphodiesterases (Δ2PDE; Δ*rocS*Δ*cdgJ*) as well as a strain lacking four diguanylate cyclases (Δ4DGC; Δ*cdgD*Δ*cdgH*Δ*cdgK*Δ*cdgL*).(B) Abundance of TfoY in WT, Δ*lonA*, Δ*lonA*Δ2PDE, Δ*lonA*Δ4DGC strains. (C) Abundance of LonA in WT, Δ2PDE, and Δ4DGC strains. (D) TfoY was overproduced from the Tn7 locus in WT, Δ2PDE and Δ4DGC strains. Overproduction of TfoY was achieved via the addition of 0.1mM IPTG for 2 hours. Levels of TfoY were assessed immediately before and after translational inhibition via chloramphenicol. (E) Prior to translational inhibition, 40mLs of culture was spun down and analyzed for global c-di-GMP by LC-MS/MS. A One-way ANOVA using Dunnet's multiple comparisons test was used for statistical analysis (**p<0.01, ***p<0.001). Abundance and stability of TfoY was analyzed by western blot using an TfoY antibody. RNAP was used as a control for sample loading in all western blots. Levels of LonA were analyzed by western blot using a LonA antibody. (F) Swimming motility phenotypes of Δ*tfoY* and Δ*lonA* deletions in WT, Δ2PDE, and Δ4DGC strains. (G) Overexpression of *tfoY* from the Ptac promoter in plates with (+) and without (-) IPTG. For motility assays, single colonies were stabbed into LB soft agar plates (0.3% agar) and incubated at 30C for approximately 18 hours. (H) The T6SS killing phenotypes of Δ*tfoY* and Δ*lonA* deletions in WT, Δ2PDE, and Δ4DGC strains. (I) Overexpression of *tfoY* from the Ptac promoter in liquid culture and on plates (++) relative to uninduced (-). (J) Overexpression of *tfoY* from the Ptac promoter in liquid culture (+). Cells were then washed to remove the inducer and spotted onto plates lacking IPTG. T6SS-dependent killing was determined by enumerating the survival of *E. coli* strain MC4100, which is susceptible to T6SS attack. Statistical analysis was performed using an unpaired Student's t-test. Statistical values indicated are (*p<0.05, **p<0.01, ***p<0.001, and ****p<0.0001).

2.2.6 c-di-GMP levels govern LonA and TfoY-dependent regulation of motility and the T6SS

Given that LonA and c-di-GMP coordinate TfoY stability, we wondered how these two factors might function to influence TfoY-mediated phenotypes. We first assessed how the deletion of *tfoY* and of *lonA* in WT, Δ2PDE, and Δ4DGC strains would alter motility and T6SS-dependent killing (Fig 2.5F and 2.5H). We did not observe any changes in motility or T6SS-dependent killing in Δ*tfoY*, Δ*tfoY*Δ2PDE, and Δ*tfoY*Δ4DGC strains relative to WT, Δ2PDE and Δ4DGC strains (Fig 2.5F

and 2.5H). We also did not observe altered motility in Δ*lonA*Δ2PDE relative to the Δ2PDE strain or Δ*lonA*Δ4DGC relative to the Δ4DGC strain (Fig 2.5F). Both Δ*lonA* and Δ*lonA*Δ2PDE exhibited increased T6SS-dependent killing relative to WT; however, T6SS-dependent killing was not different between these strains (Fig 2.5F). In contrast, the Δ*lonA*Δ4DGC strain exhibited increased T6SS-dependent killing relative to Δ*lonA* and Δ*lonA*Δ2PDE strains (Fig 2.5F). Collectively, these results show that LonA regulates T6SS-dependent killing in WT, Δ2PDE, and Δ4DGC strains and that LonA-dependent regulation is most prominent when cellular c-di-GMP levels are low. These T6SS-dependent killing phenotypes correlate with the levels of TfoY observed in these strains (Fig 2.5E).

We next explored how overproduction of TfoY would impact motility and T6SS-dependent killing (Fig 2.5G and 2.5I). We analyzed these phenotypes in Δ*tfoY*, Δ*tfoY*Δ2PDE, and Δ*tfoY*Δ4DGC strains containing the Tn7::Ptac-*tfoY* construct. As expected, overexpression of *tfoY* led to increased motility in the Δ*tfoY* background (Fig 2.5G) [24]. Overproduction of TfoY also enhanced motility in the Δ*tfoY*Δ2PDE strain but not in the Δ*tfoY*Δ4DGC strain. It is noteworthy that the increase in TfoY-induced motility was 1.7-fold in Δ*tfoY*, 3.3-fold in Δ*tfoY*Δ2PDE, and 1.1-fold in Δ*tfoY*Δ4DGC strains. Together, these data suggest that as cellular levels of c-di-GMP increase, TfoY is able to play a more pronounced role in regulating motility. To analyze the impact of TfoY overproduction on T6SS-dependent killing, we induced TfoY production in cells grown in liquid cultures and on agar plates (Fig 2.5I). Overproduction of TfoY led to increased killing in all strains tested (Fig 2.5I). We observed greater T6SS-dependent

killing in Δ*tfoY*Δ2PDE and Δ*tfoY*Δ*lonA* strains, conditions where TfoY is more stable and accumulates to higher levels (Fig 2.5A, 2.5B and 2.5D and A.2A and A.2B Fig). However, we also observed a significant increase in T6SS-dependent killing when TfoY was overproduced in the Δ*tfoY*Δ4DGC strain. The increase in T6SS-dependent killing was 26-fold in Δ*tfoY*, a 1,575-fold in Δ*tfoY*Δ2PDE, a 13,336-fold Δ*tfoY*Δ4DGC and 1,944-fold Δ*tfoY*Δ*lonA* strain. The large increase in TfoY-dependent killing of *E. coli* in the Δ*tfoY*Δ4DGC strain was unexpected given that TfoY accumulates to substantially lower levels in this strain relative to the others tested (A.2A and A.2B Fig).

To determine if the increase in T6SS-dependent killing could be mediated by increased transcription of T6SS gene clusters, we assessed TfoY-mediated transcriptional activation of the T6SS by introducing transcriptional reporters of the large T6SS operon (*vipA-lux*) and of auxiliary cluster 2 (*hcp2-lux*) into the TfoY overproduction strains. TfoY overproduction led to increased T6SS gene expression in each of these strains (Fig. A.3A and A.3B). However, we only observed very small increases in T6SS promoter activity between Δ*tfoY*Δ2PDE and Δ*tfoY*Δ4DGC strains relative to the Δ*tfoY* strain (Fig. A.3A and A.3B). Such modest increases in transcription from these promoters are unlikely to account for the substantial increases in T6SS-dependent killing observed.

To further evaluate the impact of LonA and c-di-GMP regulation of TfoY stability on T6SS-dependent killing, we modified our experimental conditions in such a way that pools of TfoY were controlled before the onset of the T6SS-dependent killing assay. To do this, we first overproduced TfoY in Δ*tfoY*, Δ*tfoY*Δ*lonA*, Δ*tfoY*Δ2PDE, and

$\Delta tfoY\Delta$4DGC strains in liquid-grown culture. We then collected cells and resuspend them in a buffer without inducer; the T6SS-dependent killing experiment were then performed on agar plates without inducer (Fig 2.5J). Overproduction of TfoY in the $\Delta tfoY\Delta$2PDE strain resulted in increased T6SS-dependent killing compared to $\Delta tfoY$ or $\Delta tfoY\Delta$4DGC strains (Fig 2.5J). However, in the $\Delta lonA\Delta tfoY$ strain killing was restored to levels comparable to the $\Delta tfoY\Delta$2PDE strain (Fig 2.5J), indicating that LonA is the governing factor regulating TfoY-induced T6SS-dependent killing under the conditions tested.

2.2.7 LonA activity can be directly regulated by c-di-GMP

Prior work has shown that c-di-GMP can inhibit Lon protease activity *in vitro*; however, this work was restricted to *E. coli* Lon [19]. Based on our *in vivo*work, we hypothesized that c-di-GMP may also function to reduce LonA activity in *V. cholerae*. In order to test this, we purified LonA and assessed how c-di-GMP influences LonA proteolysis of the model substrate casein. We found that addition of c-di-GMP substantially reduced the ability of LonA to degrade casein with approximately 60% reduction in activity at the highest c-di-GMP concentration tested (Fig 2.6A and 2.6B) with no effects on ATP hydrolysis in the conditions used (Fig 2.6C and 2.6D). We next tested direct binding of c-di-GMP, using a radiolabeled nucleotide DRaCALA assay and found that purified LonA bound c-di-GMP (Fig 2.6E), albeit with weak affinity [29]. We confirmed this result by using a c-di-GMP derivative (MANT-c-di-GMP) that increases fluorescence when bound [30]. Fluorescence of MANT-c-di-GMP increased when incubated

with LonA and less so with heat denatured LonA, suggesting that a structured motif of LonA is likely important for c-di-GMP binding (Fig 2.6F). Taken together, these data show that LonA can weakly bind c-di-GMP directly and, most importantly for our model of TfoY regulation, that the *V. cholerae* LonA protease activity can be inhibited by c-di-GMP.

2.3 Discussion

LonA is a pleiotropic regulator in *V. cholerae* governing diverse behaviors such as cell morphology, biofilm formation, motility, c-di-GMP pools, the T6SS, virulence gene expression, and intestinal colonization [4]. In the current study, we fill significant gaps regarding the mechanism by which LonA controls these processes. We identified the T6SS and motility regulator TfoY as a LonA substrate and demonstrated that LonA-mediated proteolysis of TfoY functions to temper *V. cholerae*'s activation of flagellar mediated motility and T6SS-dependent killing. We determined that c-di-GMP reduces LonA-dependent proteolysis of a model substrate *in vitro*. In addition, we observed that cellular levels of TfoY are enhanced and stable when cellular c-di-GMP levels are high, providing evidence that c-di-GMP inhibits LonA proteolysis *in vivo*. Furthermore, we show how LonA and TfoY influence motility and T6SS-dependent killing phenotypes differently in strains with high and low levels of c-d-GMP relative to WT.

Prior to this study only two LonA substrates had been identified in *V. cholerae* [8, 23]. The first is the alternative sigma factor FliA, which helps coordinate the acti-

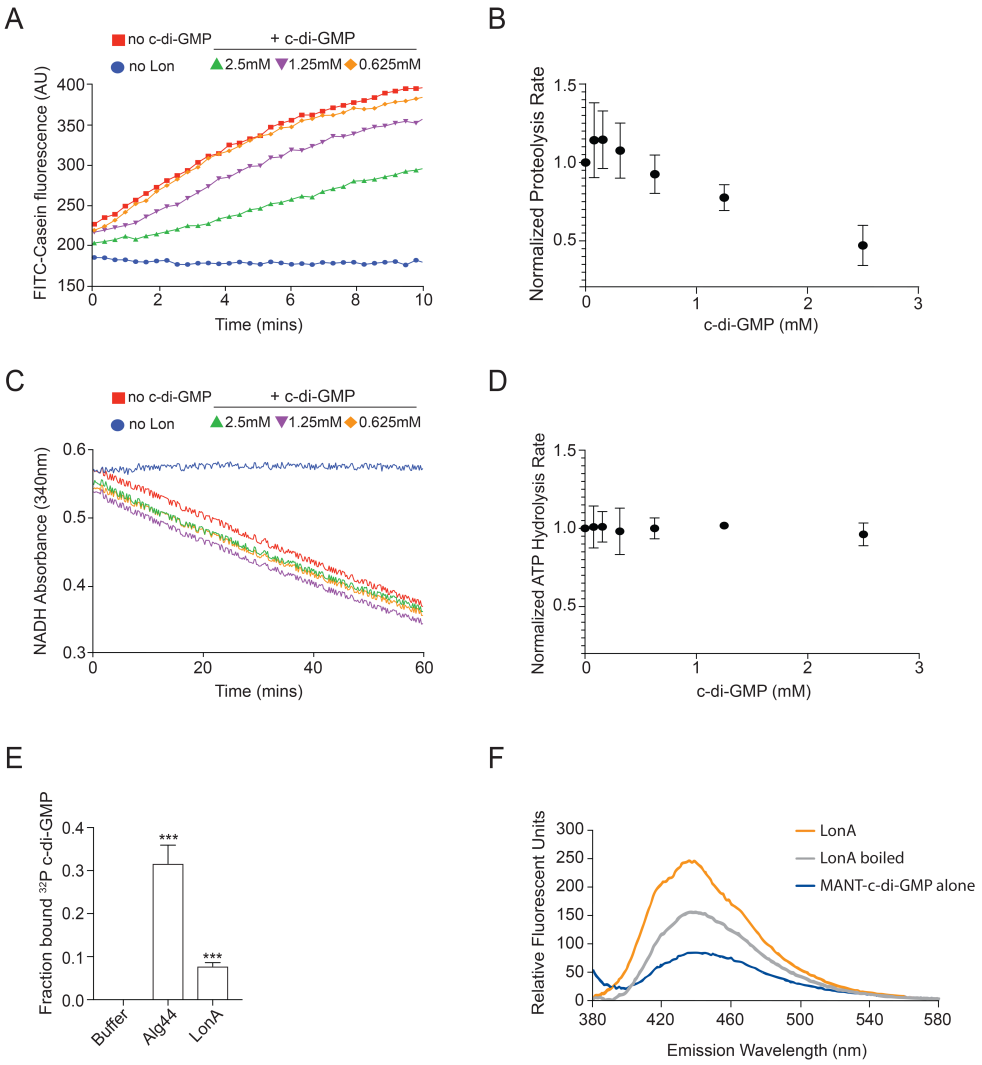

Figure 2.6: LonA proteolysis is directly regulated by c-di-GMP. *In vitro* proteolysis and protein ligand binding assays are shown. (A) Proteolysis of FITC-casein by purified LonA results in increased fluorescent signal. (B) Initial rate of substrate degradation as

vation of late stage flagellar genes and also acts to repress virulence factor production [8, 31]. Upon assembly of the hook, or shearing of the flagellar filament, the anti-sigma factor FlgM is secreted through the flagella, permitting FliA to activate the genes necessary for flagellar function and the repression of virulence gene expression [8, 31, 32].

a function of c-di-GMP. (C) ATP hydrolysis for LonA alone and in the presence of c-di-GMP was monitored by loss of NADH, which is consumed stoichiometrically with ATP. (D) Rate of ATP hydrolysis as a function of c-di-GMP. Representative curves for (A) and (C) are shown with different concentrations of c-di-GMP. (E) Quantification of fraction bound of ^{32}P-c-di-GMP to LonA by DRaCALA. Binding data shown represent the average and SD of triplicate independent experiments. Fraction bound by LonA and Alg44 were compared to buffer control by Student's t-test. *** indicate p value of 0.0005, respectively. (F) Purified LonA or heat denatured LonA (boiled) were incubated with MANT-c-di-GMP. Representative emission fluorescence spectrum (excitation at 355 nm) is shown. Emission spectrum of MANT-c-di-GMP alone is also shown as a control.

The release of FliA by FlgM, however, also causes FliA to become highly unstable due to proteolysis by LonA [8]. Thus, LonA's control of FliA in the host may be important for derepressing virulence factor production. The second substrate is the quorum sensing master regulator HapR, which is proteolyzed by LonA during heat shock in order to activate biofilm formation [23]. We note that neither FliA nor HapR were identified in our proteome analysis, however, this is likely due to the physiological conditions required for LonA proteolysis of these regulators.

TfoY belongs to a class of proteins that contain TfoX-like N- and C-terminal domains. Proteins with TfoX-like domains are transcription factors that are frequently found in gamma-proteobacteria and are involved in the regulation of natural competency, the T6SS, and motility. Homologues of TfoY, such as TfoX of *V. cholerae*, Sxy-1 of Haemophilus influenzae, and Sxy of *E. coli* are regulators of DNA uptake and natural transformation in their respective organisms [24, 33, 34, 35, 36]. Prior studies have shown that TfoY does not control competency; TfoY is, however, an activator of motility in diverse *Vibrio* species and frequently controls T6SS-dependent killing as well [24, 37].

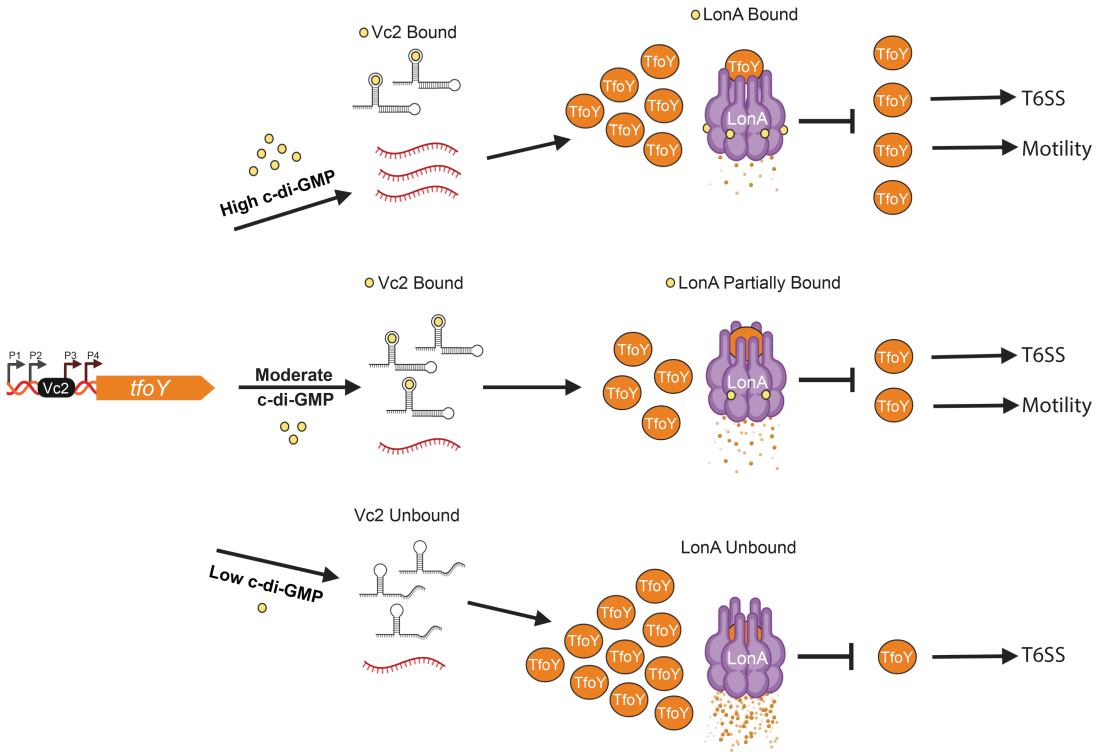

Figure 2.7: Model of LonA and c-di-GMP regulation of TfoY. Regulation of *tfoY* by c-di-GMP takes place at multiple regulatory points. TfoY production is regulated at the transcriptional level via a c-di-GMP binding transcriptional factor; at the post-transcriptional level via a c-di-GMP dependent riboswitch; and the post-translational level via c-di-GMP modulated proteolysis. The upstream regulatory region of *tfoY* contains 4 promoters. Promoters P1 and P2 (black bent arrows) produce transcript that contains the Vc2 riboswitch (close stem loop), which functions as an off switch when bound by c-di-GMP (yellow circle) and prevents translation [24,26,28]. In contrast, transcripts produced from promoters P3 and P4 (red bent arrows), driven by the c-di-GMP binding transcriptional activator VpsR, do not contain the Vc2 riboswitch [26]. In this model, we present our current understanding of post-transcriptional and post-translational regulation of TfoY (orange circles) by LonA (purple barrel) and c-di-GMP. At high c-di-GMP levels, transcripts without the Vc2 riboswitch accumulate at high levels. Transcript containing the Vc2 riboswitch are not translated. This results in moderate levels of TfoY. At the same time, high levels of c-di-GMP greatly reduce LonA-dependent proteolysis of TfoY, which results in TfoY activation of motility and T6SS-dependent killing. At intermediate c-di-GMP concentrations, transcripts with and without the Vc2 aptamer are present and LonA activity is reduced. This leads to low levels of TfoY production and the activation of motility and T6SS-dependent

killing. At low c-di-GMP conditions, transcripts with the Vc2 aptamer are not inhibited by c-di-GMP. In addition, LonA activity is also not repressed by c-di-GMP, thereby leading to increased TfoY degradation. Under these conditions, TfoY activates T6SS-dependent killing but not motility. This figure was generated using BioRender (https://app.biorender.com/).

It is important to note that the stability of Sxy of *E. coli* is also dependent upon LonA, which suggests that LonA proteolysis of TfoX-like domain containing proteins may be a common regulatory mechanism in diverse bacterial species [33].

While we did not observe TfoY to play a role in modulating an increase or decrease in c-di-GMP levels in the Δ*lonA* strains, transcriptomic analysis revealed that TfoY overproduction leads to significant transcriptional changes in a wide array of DGCs and PDEs [24]. Thus, it is possible that under certain conditions TfoY functions to alter levels of c-di-GMP within the cell by modulating the production of specific DGCs and PDEs. Of the c-di-GMP enzymes regulated by TfoY, the motility repressor CdgD appears to be the most significantly impacted [24, 38, 39, 40]. Specifically, overproduction of TfoY leads to significant repression of *cdgD* [24]. Notably, we found that CdgD levels were elevated in WT relative to the *lonA* mutant. Thus, elevated TfoY in the *lonA* mutant may function to lower levels of CdgD in the cell. It is therefore possible that the enhanced motility observed in the *lonA* mutant and in *tfoY* overexpressing strains is at least in part due to repression of cdgD.

While the environmental signals that govern the production of TfoY remain unclear, it has become increasingly apparent that sustained sensing of c-di-GMP by multiple c-di-GMP receptors is critical in controlling TfoY synthesis and turnover (Fig

2.7) [24, 26, 27, 37, 41, 42, 43]. For example, TfoY is regulated at the transcriptional level via a c-di-GMP binding transcriptional factor; at the post-transcriptional level via a c-di-GMP dependent riboswitch; and at the post-translational level via c-di-GMP modulated proteolysis. The upstream regulatory region of *tfoY* contains 4 promoters. Promoters P1 and P2 produce transcript that contains the Vc2 riboswitch, which restricts translation when bound by c-di-GMP [24, 27, 28]. Decreasing levels of c-di-GMP derepresses the Vc2 inhibitory mechanism and permits translation of *tfoY* mRNA into TfoY protein [24, 26, 27, 28]. However, elevated levels of c-di-GMP also permit the productio[26]. This occurs through the master regulator of biofilm formation, VpsR, which binds to *tfoY* promoter elements P3 and P4 within and downstream of the Vc2 riboswitch, respectively, resulting in transcript lacking the Vc2 inhibitory mechanism [26]. It is important to note that decreasing levels of c-di-GMP leads to greater production of TfoY than elevating c-di-GMP does [24, 26, 37]. We note that these studies utilized TfoY fluorescent fusions to evaluate TfoY production. It has been previously shown that fluorescent fusions with sfGFP can severely limit LonA proteolysis unless circular permuted variants of sfGFP are used [44]. Thus, the translational reporters utilized in prior studies may have prevented LonA-mediated proteolysis of TfoY, and would therefore reflect TfoY protein production but not TfoY turnover [24, 26, 37]. Consistent with this hypothesis, we observe that a greater amount of TfoY accumulates in the Δ4DGC strain relative to the Δ2PDE strain in mutants where *lonA* has been deleted.

Our findings suggest the presence of an additional regulatory module governing

TfoY stability in a c-di-GMP dependent manner. Specifically, when c-di-GMP levels are decreased, the Vc2 regulatory mechanism is bypassed and TfoY protein is produced efficiently. However, because LonA is unimpeded by c-di-GMP, it proteolyzes TfoY efficiently as well. On the other hand, when c-di-GMP levels are high, TfoY production occurs less efficiently and LonA proteolysis of TfoY is similarly scaled back by c-di-GMP. Therefore, the same ligand that drives large changes in transcriptional and translational control of TfoY expression also buffers steady state levels of TfoY through proteolysis.

Our genetic and phenotypic analyses also suggest that TfoY may play different roles under high and low c-di-GMP conditions. For example, we observed that TfoY is increasingly important in driving motility when c-di-GMP levels are increased. Levels of c-di-GMP are elevated in biofilms, thus it is possible that TfoY may aid in dispersal from biofilms by enhancing motility. Conversely, we did not observe TfoY to significantly influence motility when c-di-GMP levels were low, which is consistent with a prior analysis that analyzed TfoY-dependent motility when a phosphodiesterase was overproduced [24]. TfoY also enhances T6SS-dependent killing when c-di-GMP levels are increased, indicating that TfoY may have a role in mediating T6SS-dependent competition in biofilms. Similarly, overproduction of TfoY resulted in robust T6SS-dependent killing in strains with low cellular levels of c-di-GMP. We found that the increases in T6SS-dependent killing in strains with high and low c-di-GMP levels are likely independent of TfoY's ability to activate transcription from the two T6SS operons tested. Thus, it is possible that TfoY functions synergistically with additional c-di-GMP dependent regulatory factors to enhance *V. cholerae* fitness against its competitors. An

intriguing observation from this analysis is that overproduction of TfoY led to the most significant T6SS-dependent killing phenotype in a strain with low cellular levels of c-di-GMP, despite levels of TfoY also being lowest under in this background. While the physiological significance of this regulation remains to be fully elucidated, these findings suggests that TfoY is capable of mounting a particularly powerful T6SS-dependent assault when cellular c-di-GMP levels are reduced. It was previously hypothesized that activation of TfoY could be part of a danger sensing system utilized in a defensive escape response [24]. The results of our genetic and phenotypic analysis suggest that the production of TfoY could be important for launching a T6SS-mediated counter-attack in the presence of a c-di-GMP reducing "danger signal," and that LonA and c-di-GMP would be central regulators controlling the magnitude and longevity of this output.

Our finding that c-di-GMP limits LonA proteolysis in *V. cholerae* is consistent with a previous report that found addition of c-di-GMP inhibits degradation of α-casein by *E. coli* Lon in an endpoint assay [19]. The same study also found that binding of c-di-GMP to Lon could be indirectly monitored by loss of HPLC signal [19]. In our current work, we extend upon those findings by using kinetic assays to monitor degradation in real-time. We also demonstrate c-di-GMP weakly binds to LonA using a radiolabeled assay and a fluorescent assay. It remains to be determined how LonA binds c-di-GMP, how selective this binding is, and how binding of this ligand reduces LonA activity. It will be important to assess how c-di-GMP modulates LonA proteolysis against a wide range of substrates in order to determine if c-di-GMP functions solely as a repressor or if it can also function to enhance proteolysis by altering LonA target specificity.

2.4 Methods

2.4.1 Ethics statment

All animal procedures used were in strict accordance with the Guide for the Care and Use of Laboratory Animals [45] and were approved by the University of California (UC), Santa Cruz, Institutional Animal Care and Use Committee, Santa Cruz, CA (approval number Yildf1206).

2.4.2 Bacterial strains, growth conditions and antibody generation

The bacterial strains used in this study can be found in S4 Table. *V. cholerae* and *E. coli* strains were grown aerobically in Lysogeny Broth (LB) broth (1% tryptone, 0.5% yeast extract, 1% NaCl, pH 7.5) at 30°C and 37°C, respectively. LB agar contained granulated agar (Difco) at 1.5% (wt/vol). Antibiotics were used when necessary at the following concentrations: rifampin, 100 μg/ml; ampicillin, 100 μg/ml; gentamycin, 15 μg/ml; and chloramphenicol, 2.5μg/ml, 5μg/ml, or 100 μg/ml as indicated in the text.

2.4.3 Strain and plasmid generation

Plasmids were constructed using standard cloning methods or the Gibson Assembly recombinant DNA technique (New England BioLabs, Ipswich, MA). Gene deletions were carried out using allelic exchange of the native open reading frame (ORF) with a truncated ORF, as previously described [39]. The generation of complementation and overexpressing mutants was carried out using a Tn7-based system, as previously

described [4, 25]. For the *tfoY* complementation construct, the open reading frame of *tfoY*, as well as 500bp upstream, were cloned into pGP704-Tn7 plasmid. For the *tfoY* overexpression construct, the open reading frame of *tfoY* was cloned into pMMB67EH, which contains the IPTG inducible Ptac system. The Ptac-*tfoY* fusion was then cloned into the pGP704-Tn7 plasmid. Triparental matings with donor *E. coli* S17λpir carrying the pGP704-Tn7 plasmid with the gene of interest, helper *E. coli* S17λpir harboring pUX-BF13, and *V. cholerae* deletion strains were carried out by mixing all three strains and incubating mating mixtures on LB agar plates for 18 h at 30°C. Transconjugants were selected on LB media containing rifampicin and gentamycin at 30°C. Insertion of the complementation construct to the Tn7 site was verified by PCR. *V. cholerae* WT and mutant strains were tagged with green fluorescent protein (GFP) according to a previously described procedure [46]. The GFP-tagged *V. cholerae* strains were verified by PCR and used in biofilm analyses. Transcriptional reporters were generated by cloning the upstream of the regulatory region as well as a portion of the open reading frame of VCA0107 (*vipA*) or VCA0017 (*hcp2*) into the pBBRlux plasmid using established methodologies [47]. The exact lengths of the regulatory region used can be found in the supplementary material (S4 Table).

2.4.4 Whole proteome analysis

V. cholerae WT and Δ*lonA* strains that lacked the genes for cholera toxin (*ctxAB*) were grown aerobically at 30°C overnight. The cultures were diluted 1:500 and grown to OD_{600} = 1.0, at which point 100μg/mL of chloramphenicol was added

to stop translation. After 1-hour of chloramphenicol treatment, cells were collected by centrifugation and flash frozen in liquid nitrogen, and then stored in -80°C. Five biological replicates for WT and $\Delta lonA$ were collected. These samples were processed at NYU Proteomics Facility for analysis by liquid chromatography coupled with mass spectrometry.

2.4.5 Proteome extraction and sample preparation for mass spectrometry analysis

Cell pellets were resuspended in 8M urea in 100 mM HEPES buffer (pH 8.0) and 250μg of each protein lysates were reduced using dithiothreitol (5μl of 0.2M) for 1-hour at 55°C. The reduced cysteines were subsequently alkylated with iodoacetamide (5μl of 0.5M) for 45 min in the dark at room temperature. Next, 20mM HEPES (pH 8.0) were added to dilute the urea concentration to 2M and the protein lysates were digested with Trypsin (Promega) at a 100:1 (protein:enzyme) ratio overnight at room temperature. The pH of the digested protein lysates was lowered to pH<3 using trifluoroacetic acid (TFA). The digested lysates were desalted using C18 solid-phase extraction (Sep-Pak, Waters). 40% acetonitrile (ACN) in 0.5% acetic acid followed by 80% acetonitrile (ACN) in 0.5% acetic acid was used to elute the desalted peptides. The peptide eluate was concentrated in the SpeedVac and stored at -80°C.

2.4.6 Tandem Mass Tag (TMT) labeling

The dried peptide mixture was re-suspended in 100mM TEAB (pH 8.5) using a volume of 100μl. Isobaric mass tag labeling was performed used the TMT 10plex reagent set from ThermoFisher. Each sample was labeled with TMT reagent according to the manufacturer's protocol. In brief, each TMT reagent vial (0.8mg) was dissolved in 41 μL of anhydrous ethanol and was added to each sample. The reaction was allowed to proceed for 60min at room temperature and then quenched using 8μL of 5% w/v hydroxylamine. The samples were combined at a 1:1 ratio and the pooled sample was subsequently desalted using SCX and SAX solid-phase extraction columns (Strata, Phenomenex) as described [48].

2.4.7 Global proteome analysis

A 500 μg aliquot of pooled sample was fractionated using basic pH reverse-phase HPLC using previously established procedures [49]. Briefly, the sample was loaded onto a 4.6mm×250mm Xbridge C18 column (Waters, 3.5μm bead size) using an Agilent 1260 Infinity Bio-inert HPLC and separated over a 70min linear gradient from 10 to 50% solvent B at a flow rate of 0.5ml/min (Buffer A = 10mM ammonium formate, pH 10.0; Buffer B = 90% ACN, 10mM ammonium formate, pH 10.0). A total of 40 fractions were collected throughout the gradient. The early, middle and late eluting fractions were concatenated and combined into 10 final fractions. The combined fractions were concentrated in the SpeedVac and stored at -80(^{c}irc)C until further analysis.

2.4.8 LC-MS/MS analysis

An aliquot of each sample was loaded onto a trap column (Acclaim PepMap 100 pre-column, 75 μm×2cm, C18, 3μm, 100$\mathring{A}$, Thermo Scientific) connected to an analytical column (EASY-Spray column, 50m×75μm ID, PepMap RSLC C18, 2μm, 100$\mathring{A}$, Thermo Scientific) using the autosampler of an Easy nLC 1000 (Thermo Scientific) with solvent A consisting of 2% acetonitrile in 0.5% acetic acid and solvent B consisting of 80% acetonitrile in 0.5% acetic acid. The peptide mixture was gradient eluted into the QExactive mass spectrometer (Thermo Scientific) using the following gradient: a 5%-23% solvent B in 100min, 23% -34% solvent B in 20 min, 34% -56% solvent B in 10 min, followed by 56%- 100% solvent B in 20 min. The full scan was acquired with a resolution of 70,000 (@ m/z 200), a target value of 1e6 and a maximum ion time of 120ms. After each full scan 10 HCD MS/MS scans were acquired using the following parameters: resolution 35,000 (@m/z 200), isolation window of 1.5m/z, target value of 1e5, maximum ion time of 250ms, normalized collision energy (NCE) of 30, and dynamic exclusion of 30s.

2.4.9 Data analysis

Raw mass spectrometry data were processed using Proteome Discoverer 2.1. Proteins and peptides were searched against the PATRIC *V. cholerae* using the Byonic with a protein score cut-off of 300, using the following settings: oxidized methionine (M), and deamidation (NQ) were selected as variable modifications, and carbamidomethyl (C) as fixed modifications; precursor mass tolerance 10ppm; fragment mass tolerance

0.02 Da. The following filters and criteria were used for quantification: Proteins identified with less than two unique peptides were excluded from analysis. Bioinformatics analysis was performed with Perseus, Microsoft Excel and R statistical computing software. Student's t-test using Benjamini-Hochberg FDR cutoff of 5% was then used to identify proteins that were differentially enriched.

2.4.10 *in vivo* proteolysis and protein abundance assays

Overnight cultures of *V. cholerae* were diluted 1:500 in 100mL of LB medium. Cells were grown until an $OD_{600} = 0.1$ was reached, 0.1mM IPTG was added to induce transcription of *tfoY* from the Ptac promoter. Induction proceeded for 2-hours, 2mL aliquots were taken immediately prior, and then at the time points indicated after the addition of 100x the minimum inhibitory concentration of chloramphenicol (100μg/mL). Protein abundance assays were performed similarly with minor modifications noted in the figure legends. BCA analysis was used to quantify total protein loaded. Relative levels of TfoY, LonA, and RNAP were assessed by western blot analysis. The TfoY antibody was used at 1μg/mL concentration, the LonA antibody at 0.5μg/mL, and the RNAP antibody was used at 0.625μg/mL. At least three independent biological replicates were performed for all *in vivo* protein abundance and stability assays. For densitometric analysis, software from Image Lab v6.01 (Bio Rad Laboratories) was used to quantify band intensity of TfoY from western blots. Adjusted total band intensity was calculated by subtracting the background intensity values from the total band intensity value.

2.4.11 Swimming motility assays

Flagellar motility was determined by inoculating a single overnight colony into the center of LB soft agar plates (0.3% wt/vol). For overexpression experiments, the soft agar plates were supplemented with 0.1mM IPTG to induce expression from the Ptac promoter. The plates were moved to 30(^{c}irc)C and the swimming diameter was recorded 18-hours post inoculation. The motility phenotype of each mutant was assessed using at least three independent biological replicates. Statistical analysis of motility was performed using an unpaired Student's t-test.

2.4.12 Interbacterial killing assays

V. cholerae WT and mutant strains and the *E. coli* strain MC4100 were grown overnight in LB medium at 30(^{c}irc)C and 37(^{c}irc)C respectively. Overnight grown cultures of *V. cholerae* and *E. coli* strains were diluted 1:200 in LB medium supplemented with 340mM NaCl. *V. cholerae* strains were grown to an OD_{600} = 0.8–1.0 while *E. coli* was grown to an OD_{600} = 0.4–0.8. Approximately 10^9 *V. cholerae* and 10^8 *E. coli* cells were mixed and 25μL of this mixture was spotted in technical triplicate onto nitrocellulose membrane that had been placed on LB agar supplemented with 340mM NaCl. For overexpression experiments, 0.1mM IPTG was included in the liquid media and/or plates as indicated in the text. In the interbacterial competition assay that addressed TfoY stability on T6SS-dependent killing (Fig 2.5J), 0.1mM IPTG was included in liquid media, the cells were then washed twice with 1x PBS, and then *V. cholerae* and *E. coli* were mixed and spotted onto 340mM NaCl agar plates lacking IPTG. Interbacterial

competition was allowed to proceed for approximately 4-hours at 37(^{c}irc)C, at which point the filter membranes were removed and resuspended in 1mL of 1x PBS. Cells were resuspended and serial dilutions were generated and spotted onto LB plates containing 100μg/mL of streptomycin, grown overnight, and the surviving *E. coli* was enumerated. Statistical analysis of T6SS killing was performed using an unpaired Student's t-test.

2.4.13 Biofilm assays

Flow cell chambers were inoculated with 200μL of overnight-grown cultures of GFP-tagged *V. cholerae* strains that had been diluted to an OD_{600} of 0.02. Once inoculated, the bacteria were allowed to adhere at room temperature for 1 hr without flow. Next, the flow of 2% (vol/vol) LB (0.2 g/liter tryptone, 0.1 g/liter yeast extract, 1% NaCl) was initiated at a rate of 7.5 ml/h and continued for 24 h. Confocal laser scanning microscopy (CLSM) images of the biofilms were captured with the Zeiss 880 microscope using an excitation wavelength of 488 nm and an emission wavelength of 543 nm. Three-dimensional images of the biofilms were reconstructed and analyzed using Imaris software (Bitplane). Biofilm analysis was performed using COMSTAT2. Statistical analysis of biofilms was performed with ANOVA, utilizing Tukey's multiple comparison analysis.

2.4.14 Intestinal colonization assays

Colonization of the infant mouse was performed as previously described [4]. Briefly, a WT strain, a WT strain lacking *lacZ* ($\Delta lacZ$), $\Delta lonA$, $\Delta tfoY$, and $\Delta lonA\Delta tfoY$

mutants were grown overnight at 30°C in LB media. The mutant strains (*lacZ+*) strains were competed against otherwise WT Δ*lacZ* strain at a 1:1 ratio in 1xPBS containing Evan's blue dye. The input inoculum was serial diluted and plated onto LB agar plates supplemented with X-gal such that *lacZ* containing strains could be visually differentiated from the ΔlacZ WT. Approximately 10^5 CFU were intragastrically administered to groups of 5-day-old CD-1 mice (Charles River Laboratories, Hollister, CA). At 20hrs post infection, the small intestine was removed, weighed, and homogenized. The ratio of the ΔlacZ WT and the respective competing strains were determined by serial diluting and plating the homogenized intestine onto LB agar plates containing rifampicin and X-gal. Statistical analyses were performed using the Wilcoxon's signed-ranked test.

2.4.15 DRaCALA measurment of ligand binding

For binding assay, final concentrations of the following are used: 2 μM Vc Lon was mixed with in 1x binding buffer (10 mM Tris, pH 8.0, 100 mM NaCl) and added to 3.3 nM ^{32}P-c-di-GMP in a 20 μL reaction. The entire reaction was incubated for 1 min at room temperature and 2 μL of the reaction was applied to dry nitrocellulose paper to perform DRaCALA. Once dried and imaged, the fraction bound quantified using Fujifilm Multi Gauge software v3.0. The assays were performed in triplicate [29].

2.4.16 Measurement of MANT-c-di-GMP binding

MANT-c-di-GMP (2'-O-(N'-Methylanthraniloyl)-cyclic diguanosine monophosphate; BioLog, Germany) was added at 2.5 μM to LonA at 0.7 μM hexamer either native

or denatured by heating at 95°C for 20 minutes. Fluorescence was measured by excitation at 355 nm and scanning emission from 380–600 nm. Assays were performed in triplicate [30].

2.4.17 Protein purification and *in vitro* proteolysis assays

Full length *lonA* from *V. cholerae* was cloned into a pBAD33 expression vector and transformed into BL21DE3. Overnight cultures grown at 37°C were back diluted into 6 L of LB + 100 μg/ml ampicillin, grown to mid-log phase, and induced by addition of 0.2% L-arabinose for 3 hours. Cells were pelleted by centrifugation then pellets were resuspended in lysis buffer (100 mM potassium phosphate at pH 6.5, 1 mM DTT, 1 mM EDTA, 10% glycerol). Following microfluidization disruption, the lysate was clarified by centrifugation (15,000 g / 30 minutes), and supernatant was applied to 10 ml of washed hydroxyapatite resin (Sigma). Following batch binding for 1 hour at 4°C, bound resin was washed twice (3 column volumes each) with buffer A (100 mM potassium phosphate at pH 6.5, 1 mM DTT, 1 mM EDTA, 10% glycerol), then twice (3 column volumes each) with buffer B (200 mM potassium phosphate at pH 6.5, 1 mM DTT, 1 mM EDTA, 10% glycerol), centrifuging at 2000 g for 10 minutes following each wash to separate the resin. Protein was eluted by 3 washes (1 column volume each) with elution buffer (400 mM potassium phosphate at pH 6.5, 1 mM DTT, 1 mM EDTA, 10% glycerol). Elutions were filtered using 0.22 um filters, then concentrated to 5 ml using centrifugal concentrators (10 kDa cutoff). Concentrate was loaded onto a Sephacryl S-200 (120 ml) equilibrated in 50 mM Tris (pH 8), 1 mM DTT, 1 mM EDTA, and 20% glycerol and eluted with the

same buffer. Activity was monitored by testing fractions using FITC-casein (see below). Active fractions were pooled and loaded onto a 1ml Mono-Q equilibrated in Qbuffer A (25 mM Tris pH 8, 50 mM KCl, 10% glycerol, 1 mM DTT), washed extensively and eluted with a 30 CV (0–100%) gradient using Qbuffer B (25 mM Tris pH 8, 1M KCl, 20% glycerol, 1 mM DTT). Final active fractions were concentrated, snap frozen in liquid nitrogen, and stored at -80°C. Standard proteolysis reactions contain 100–200 nM LonA (hexamer concentration) in degradation buffer (20 mM Tris pH 8, 100 mM KCl, 10 mM MgCl2) with 4 mM ATP, 5 mM creatine phosphate, 7.5 μg/ml creatine kinase (for ATP regeneration) and 10 μg/ml FITC-Casein (Sigma). Increases in fluorescence (ex 460 nm / em 520 nm) due to degradation of the labeled substrate was monitored using a Spectramax M5 (Molecular Devices) in 384-well nonbinding surface plates (Corning) incubated at 30°C. ATP hydrolysis was monitored using a coupled NADH-based assay where loss of NADH corresponds 1:1 with hydrolysis of ATP [50].

2.4.18 Analysis of promoter activity of T6SS operons

Luminescence assays were performed as previously described with minor alterations [4, 38, 51]. Briefly, overnight cultures of *V. cholerae* were grown in LB media containing 5μg/mL of chloramphenicol. Cells were diluted 1:500 in LB media containing 2.5μg/mL chloramphenicol and grown to late exponential phase (OD_{600} = 1.0). Cells were diluted 1:10 in LB and luminescence was measured in technical triplicate. Relative luminescence was quantified across at least 3 biological replicates. Statistical analysis was performed using an unpaired Student's t-test.

Bibliography

[1] Samar A Mahmoud and Peter Chien. Regulated proteolysis in bacteria. *Annual review of biochemistry*, 87:677–696, 2018.

[2] Adrian O Olivares, Tania A Baker, and Robert T Sauer. Mechanistic insights into bacterial AAA+ proteases and protein-remodelling machines. *Nature Reviews Microbiology*, 14(1):33, 2016.

[3] Eyal Gur, Dvora Biran, and Eliora Z Ron. Regulated proteolysis in gram-negative bacteria—how and when? *Nature Reviews Microbiology*, 9(12):839–848, 2011.

[4] Andrew Rogers, Loni Townsley, Ana L Gallego-Hernandez, Sinem Beyhan, Laura Kwuan, and Fitnat H Yildiz. The LonA protease regulates biofilm formation, motility, virulence, and the type vi secretion system in *Vibrio cholerae*. *Journal of bacteriology*, 198(6):973–985, 2016.

[5] the Lon protease homologue LonA, not LonC, contributes to the stress tolerance and biofilm formation of *Actinobacillus pleuropneumoniae*.

[6] Lihong He, Manoj Kumar Mohan Nair, Yuling Chen, Xue Liu, Mengyun Zhang, Karsten RO Hazlett, Haiteng Deng, and Jing-Ren Zhang. The protease locus of *Francisella tularensis* lvs is required for stress tolerance and infection in the mammalian host. *Infection and immunity*, 84(5):1387–1402, 2016.

[7] Elena BM Breidenstein, Laure Janot, Janine Strehmel, Lucia Fernandez, Patrick K Taylor, Irena Kukavica-Ibrulj, Shaan L Gellatly, Roger C Levesque, Joerg Over-

hage, and Robert EW Hancock. The Lon protease is essential for full virulence in *Pseudomonas aeruginosa*. *PloS one*, 7(11):e49123, 2012.

[8] Katharina Pressler, Dina Vorkapic, Sabine Lichtenegger, Gerald Malli, Benjamin P Barilich, Fatih Cakar, Franz G Zingl, Joachim Reidl, and Stefan Schild. AAA+ proteases and their role in distinct stages along the *Vibrio cholerae* lifecycle. *International Journal of Medical Microbiology*, 306(6):452–462, 2016.

[9] Akiko Takaya, Toshifumi Tomoyasu, Akane Tokumitsu, Mizue Morioka, and Tomoko Yamamoto. The ATP-dependent Lon protease of *Salmonella enterica* serovar Typhimurium regulates invasion and expression of genes carried on *Salmonella* pathogenicity island 1. *Journal of bacteriology*, 184(1):224–232, 2002.

[10] Lefu Lan, Xin Deng, Yanmei Xiao, Jian-Min Zhou, and Xiaoyan Tang. Mutation of Lon protease differentially affects the expression of *Pseudomonas syringae* type III secretion system genes in rich and minimal media and reduces pathogenicity. *Molecular plant-microbe interactions*, 20(6):682–696, 2007.

[11] Carly Ching, Brendan Yang, Chineme Onwubueke, David Lazinski, Andrew Camilli, and Veronica G Godoy. Lon protease has multifaceted biological functions in *Acinetobacter baumannii*. *Journal of bacteriology*, 201(2), 2019.

[12] Shengchang Su, Bonnie B Stephens, Gladys Alexandre, and Stephen K Farrand. Lon protease of the α-proteobacterium *Agrobacterium tumefaciens* is required for

normal growth, cellular morphology and full virulence. *Microbiology*, 152(4):1197–1207, 2006.

[13] Robert T Sauer and Tania A Baker. AAA+ proteases: ATP-fueled machines of protein destruction. *Annual review of biochemistry*, 80:587–612, 2011.

[14] Tania A Baker and Robert T Sauer. ATP-dependent proteases of bacteria: recognition logic and operating principles. *Trends in biochemical sciences*, 31(12):647–653, 2006.

[15] Susan Gottesman. Proteases and their targets in *Escherichia coli*. *Annual review of genetics*, 30(1):465–506, 1996.

[16] Sampriti Mukherjee, Anna C Bree, Jing Liu, Joyce E Patrick, Peter Chien, and Daniel B Kearns. Adaptor-mediated Lon proteolysis restricts *Bacillus subtilis* hyperflagellation. *Proceedings of the National Academy of Sciences*, 112(1):250–255, 2015.

[17] Neha Puri and A Wali Karzai. Hspq functions as a unique specificity-enhancing factor for the AAA+ Lon protease. *Molecular cell*, 66(5):672–683, 2017.

[18] Akio Kuroda, Kazutaka Nomura, Ryo Ohtomo, Junichi Kato, Tsukasa Ikeda, Noboru Takiguchi, Hisao Ohtake, and Arthur Kornberg. Role of inorganic polyphosphate in promoting ribosomal protein degradation by the Lon protease in *E. coli*. *Science*, 293(5530):705–708, 2001.

[19] Devon O Osbourne, Valerie WC Soo, Igor Konieczny, and Thomas K Wood.

Polyphosphate, cyclic AMP, guanosine tetraphosphate, and c-di-GMP reduce *in vitro* Lon activity. *Bioengineered*, 5(4):264–268, 2014.

[20] Chin Ha Chung and Alfred L Goldberg. DNA stimulates ATP-dependent proteolysis and protein-dependent ATPase activity of protease La from *Escherichia coli*. *Proceedings of the National Academy of Sciences*, 79(3):795–799, 1982.

[21] Mohammad Ali, Allyson R Nelson, Anna Lena Lopez, and David A Sack. Updated global burden of cholera in endemic countries. *PLoS neglected tropical diseases*, 9(6):e0003832, 2015.

[22] Avatar Joshi, Benjamin Kostiuk, Andrew Rogers, Jennifer Teschler, Stefan Pukatzki, and Fitnat H Yildiz. Rules of engagement: the type vi secretion system in *Vibrio cholerae*. *Trends in microbiology*, 25(4):267–279, 2017.

[23] Kyung-Jo Lee, You-Chul Jung, Soon-Jung Park, and Kyu-Ho Lee. Role of heat shock proteases in quorum-sensing-mediated regulation of biofilm formation by Vibrio species. *Mbio*, 9(1), 2018.

[24] Lisa C Metzger, Sandrine Stutzmann, Tiziana Scrignari, Charles Van der Henst, Noémie Matthey, and Melanie Blokesch. Independent regulation of type vi secretion in *Vibrio cholerae* by TfoX and TfoY. *Cell reports*, 15(5):951–958, 2016.

[25] Ying Bao, Douglas P Lies, Haian Fu, and Gary P Roberts. An improved tn7-based system for the single-copy insertion of cloned genes into chromosomes of gram-negative bacteria. *Gene*, 109(1):167–168, 1991.

[26] Benjamin R Pursley, Michael M Maiden, Meng-Lun Hsieh, Nicolas L Fernandez, Geoffrey B Severin, and Christopher M Waters. Cyclic di-GMP regulates TfoY in *Vibrio cholerae* to control motility by both transcriptional and posttranscriptional mechanisms. *Journal of bacteriology*, 200(7), 2018.

[27] Saki Inuzuka, Kei-Ichiro Nishimura, Hitoshi Kakizawa, Yuki Fujita, Hiroyuki Furuta, Shigeyoshi Matsumura, and Yoshiya Ikawa. Mutational analysis of structural elements in a class-i cyclic di-gmp riboswitch to elucidate its regulatory mechanism. *The Journal of Biochemistry*, 160(3):153–162, 2016.

[28] Saki Inuzuka, Hitoshi Kakizawa, Kei-ichiro Nishimura, Takuto Naito, Katsushi Miyazaki, Hiroyuki Furuta, Shigeyoshi Matsumura, and Yoshiya Ikawa. Recognition of cyclic-di-GMP by a riboswitch conducts translational repression through masking the ribosome-binding site distant from the aptamer domain. *Genes to Cells*, 23(6):435–447, 2018.

[29] Kevin G Roelofs, Jingxin Wang, Herman O Sintim, and Vincent T Lee. Differential radial capillary action of ligand assay for high-throughput detection of protein-metabolite interactions. *Proceedings of the National Academy of Sciences*, 108(37):15528–15533, 2011.

[30] Indra Mani Sharma, Thillaivillalan Dhanaraman, Ritta Mathew, and Dipankar Chatterji. Synthesis and characterization of a fluorescent analogue of cyclic di-GMP. *Biochemistry*, 51(27):5443–5453, 2012.

[31] Zhi Liu, Tim Miyashiro, Amy Tsou, Ansel Hsiao, Mark Goulian, and Jun Zhu. Mucosal penetration primes *Vibrio cholerae* for host colonization by repressing quorum sensing. *Proceedings of the National Academy of Sciences*, 105(28):9769–9774, 2008.

[32] Nidia E Correa, Jeffrey R Barker, and Karl E Klose. The *Vibrio cholerae* FlgM homologue is an anti-σ28 factor that is secreted through the sheathed polar flagellum. *Journal of bacteriology*, 186(14):4613–4619, 2004.

[33] Milena Jaskólska and Kenn Gerdes. CRP-dependent positive autoregulation and proteolytic degradation regulate competence activator Sxy of *Escherichia coli*. *Molecular Microbiology*, 95(5):833–845, 2015.

[34] Karin L Meibom, Melanie Blokesch, Nadia A Dolganov, Cheng-Yen Wu, and Gary K Schoolnik. Chitin induces natural competence in *Vibrio cholerae*. *Science*, 310(5755):1824–1827, 2005.

[35] Rosemary J Redfield. Sxy-1, a *Haemophilus influenzae* mutation causing greatly enhanced spontaneous competence. *Journal of bacteriology*, 173(18):5612–5618, 1991.

[36] Sunita Sinha and Rosemary J Redfield. Natural DNA uptake by *Escherichia coli*. *PLoS One*, 7(4):e35620, 2012.

[37] Lisa C Metzger, Noémie Matthey, Candice Stoudmann, Esther J Collas, and

Melanie Blokesch. Ecological implications of gene regulation by tfox and TfoY among diverse vibrio species. *Environmental microbiology*, 21(7):2231–2247, 2019.

[38] D Zamorano-Sánchez, W Xian, CK Lee, M Salinas, W Thongsomboon, L Cegelski, GCL Wong, and FH Yildiz. Functional specialization in *Vibrio cholerae* diguanylate cyclases: distinct modes of motility suppression and c-di-GMP production. mBio 10: e00670-19, 2019.

[39] Xianxian Liu, Sinem Beyhan, Bentley Lim, Roger G Linington, and Fitnat H Yildiz. Identification and characterization of a phosphodiesterase that inversely regulates motility and biofilm formation in *Vibrio cholerae*. *Journal of bacteriology*, 192(18):4541–4552, 2010.

[40] Bentley Lim, Sinem Beyhan, James Meir, and Fitnat H Yildiz. Cyclic-digmp signal transduction systems in *Vibrio cholerae*: modulation of rugosity and biofilm formation. *Molecular microbiology*, 60(2):331–348, 2006.

[41] N Sudarsan, ER Lee, Z Weinberg, RH Moy, JN Kim, KH Link, and RR Breaker. Riboswitches in eubacteria sense the second messenger cyclic di-GMP. *Science*, 321(5887):411–413, 2008.

[42] Benjamin R Pursley, Nicolas L Fernandez, Geoffrey B Severin, and Christopher M Waters. The Vc2 cyclic di-GMP-dependent riboswitch of *Vibrio cholerae* regulates expression of an upstream putative small RNA by controlling RNA stability. *Journal of bacteriology*, 201(21):e00293–19, 2019.

[43] Mona W Orr, Michael Y Galperin, and Vincent T Lee. Sustained sensing as an emerging principle in second messenger signaling systems. *Current opinion in microbiology*, 34:119–126, 2016.

[44] Matthew L Wohlever, Andrew R Nager, Tania A Baker, and Robert T Sauer. Engineering fluorescent protein substrates for the AAA+ Lon protease. *Protein Engineering, Design & Selection*, 26(4):299–305, 2013.

[45] National Institutes of Health et al. *Guide for the care and use of laboratory animals*. National Academies, 2012.

[46] Jiunn CN Fong, Kevin Karplus, Gary K Schoolnik, and Fitnat H Yildiz. Identification and characterization of RbmA, a novel protein required for the development of rugose colony morphology and biofilm structure in *Vibrio cholerae*. *Journal of bacteriology*, 188(3):1049–1059, 2006.

[47] David Zamorano-Sánchez, Jiunn CN Fong, Sefa Kilic, Ivan Erill, and Fitnat H Yildiz. Identification and characterization of VpsR and VpsT binding sites in *Vibrio cholerae*. *Journal of bacteriology*, 197(7):1221–1235, 2015.

[48] Jessica R Chapman, Olga Katsara, Rachel Ruoff, David Morgenstern, Shruti Nayak, Claudio Basilico, Beatrix Ueberheide, and Victoria Kolupaeva. Phosphoproteomics of fibroblast growth factor 1 (fgf1) signaling in chondrocytes: identifying the signature of inhibitory response. *Molecular & Cellular Proteomics*, 16(6):1126–1137, 2017.

[49] Amit Bhardwaj, Yanling Yang, Beatrix Ueberheide, and Susan Smith. Whole proteome analysis of human tankyrase knockout cells reveals targets of tankyrase-mediated degradation. *Nature communications*, 8(1):1–13, 2017.

[50] Kristina Jonas, Jing Liu, Peter Chien, and Michael T Laub. Proteotoxic stress induces a cell-cycle arrest by stimulating Lon to degrade the replication initiator DnaA. *Cell*, 154(3):623–636, 2013.

[51] Jennifer K Teschler, Andrew T Cheng, and Fitnat H Yildiz. The two-component signal transduction system vxrab positively regulates *Vibrio cholerae* biofilm formation. *Journal of bacteriology*, 199(18), 2017.

Chapter 3

Regulation of Biofilm Formation by the Lon Protease in *V. cholerae*

3.1 Introduction

Biofilms are aggregates of microbial cells encapsulated within a protective extracellular polymeric matrix. The biofilm growth mode is prevalent as it increases the fitness of resident microorganisms [1]. Biofilm formation is critical to the infectious cycle of *V. cholerae*, the Gram-negative facultative human pathogen responsible for the diarrheal disease cholera [2]. In the aquatic environment, biofilms protect *V. cholerae* from diverse environmental stressors as well as predatory bacteriophages and protozoans [3, 4]. *V. cholerae* biofilms are also primed for infection as they produce high levels of cholera toxin and the toxin co-regulated pilus, which are required for host colonization and the onset of cholera symptoms [5]. Furthermore, biofilms shed from the host are

hyperinfectious relative to their planktonic counterparts [5, 6, 7].

The transcriptional regulatory mechanisms governing biofilm formation in *V. cholerae* have been extensively studied, however, relatively little is known regarding how biofilm formation is regulated at the post-translational level. Proteolysis is a fundamental cellular process that maintains protein homeostasis through the targeted destruction of proteins [8]. Lon (or LonA) is a broadly conserved, energy-dependent protease that couples ATP hydrolysis with protein turnover [8, 9, 10]. Lon functions as a housekeeping protease that degrades aberrant or misfolded proteins and as a post-translational regulator that degrades specific protein targets. Lon substrates are often critical regulatory proteins controlling diverse cellular functions [8]. Thus, Lon-dependent regulation has far-reaching consequences in shaping the global protein content of the cell and, in turn, dictating various aspects of cellular physiology and behavior. Lon often regulates cell division, motility, and biofilm formation [8, 10]. Furthermore, Lon plays an important role in stress adaptation, enhancing a cell's fitness when faced with diverse genotoxic or proteotoxic stressors [8, 11, 12]. In the case of bacterial pathogens, Lon contributes to the production of virulence factors and host colonization [13, 14, 15, 16, 17]. Although the importance of Lon-dependent regulation is well established in bacteria, relatively few Lon substrates have been identified.

Lon regulates processes important for *V. cholerae*'s infectious cycle. Lon mutants poorly colonize the host intestinal tract and display abnormal expression patterns of cholera toxin and the toxin co-regulated pilus [13, 15]. Lon mutants are also highly motile and hyper-activate the type VI secretion system (T6SS), a contact-dependent

nanomachine that delivers anti-prokaryotic and anti-eukaryotic toxins to neighboring cells [18, 19]. Finally, Lon also plays an important role in regulating biofilm formation [13, 15, 20, 21]. Lon mutants form tangled, loosely packed biofilms composed primarily of hyperfilamentous cells that have altered c-di-GMP levels and biofilm gene expression [13, 15, 20].

Due to the irreversible nature of proteolysis, proteases must be strictly regulated. Indeed, diverse stressors, signaling molecules, adaptors, and anti-adaptors, as well as specificity altering factors modulate Lon activity [11, 15, 21, 22, 23]. Currently, three Lon targets have been identified in *V. cholerae*, and proteolysis of each target is condition-dependent. Lon represses motility as well as the expression of the toxin co-regulated pilus and cholera toxin through proteolysis of the alternative sigma factor (σ28) FliA [15]. However, Lon-dependent turnover of FliA is inhibited by the anti-sigma factor FlgM, which functions as a Lon anti-adaptor [15]. Lon also represses motility and T6SS-dependent killing through proteolysis of TfoY [13, 21, 24]. We previously showed that Lon-dependent proteolysis of TfoY is reduced by elevated levels of c-di-GMP [21]. Finally, Lon activates biofilm gene expression during heat shock by degrading the quorum-sensing master regulator HapR. However, since Lon-dependent turnover of HapR is contingent upon heat shock, Lon likely regulates biofilm formation and biofilm-associated processes independently of HapR in most other conditions [13, 15, 20, 21].

Most analyses on Lon have focused on Lon-dependent regulation in planktonic grown cells. Thus, relatively little is known regarding how Lon regulates processes im-

portant for biofilm formation. In the current study, we perform whole proteome and whole transcriptome analyses on WT and Δ*lon* biofilms grown at 25°C to identify potential Lon substrates and Lon-regulated pathways in biofilms. Our analyses indicates that Lon is important regulator of biofilm matrix production, virulence factor production, nucleotide pool homeostasis, iron homeostasis, and DNA repair pathways during the biofilm growth mode. Our analysis also found that PurH, NDK, and CspD were among the most enriched proteins in the Δ*lon* biofilm. We find that Lon regulates the steady-state levels of PurH and CspD, suggesting that these proteins are targeted by Lon. Furthermore, we provide preliminary data indicating that Lon-dependent regulation of CspD activates c-di-GMP biosynthesis while Lon-dependent regulation of PurH represes c-di-GMP biosynthesis. In addition, we find that Δ*lon* strains are more sensitive to streptonigrin, which induces cell death in the presence of free intracellular iron. In addition, our initial results suggest that PurH, NDK, and CspD may play a protective role in mitigating streptonigrin-induced cell death in Δ*lon* mutants. Finally, we show that Lon-deficient strains are hypersensitive to DNA damage inflicted by mitomycin C. The work outlined here provides valuable insights into how regulated proteolysis functions to control processes important for biofilm formation, biofilm-associated virulence factor production, c-di-GMP biosynthesis, and stress responses in *V. cholerae*.

3.2 Results and Discussion

3.2.1 The Lon protease shapes the global proteome and transcriptome during biofilm formation

The absence of proteolysis can lead to the enrichment of target proteins. To identify putative Lon targets and Lon-regulated pathways during biofilm formation, we compared the proteome and transcriptome of WT and Δ*lon* strains when grown as biofilms. For these studies, we grew WT and Δ*lon* biofilms in drip flow reactors and compared biofilm-associated phenotypes, including biofilm matrix production and cellular c-di-GMP levels. We found that the Δ*lon* mutant formed biofilms composed of hyperfilamentous cells (Fig 3.1A) with an overall reduction in cellular c-di-GMP (Fig 3.1B) and decreased abundance of the biofilm matrix proteins RbmA (Fig 3.1C) and RbmC (Fig 3.1D), suggesting that Lon functions to regulate various aspects of biofilm formation under these conditions. In addition, since the biofilm growth mode promotes hyperinfectivity through increased virulence factor production, we tested the expression of cholera toxin (Fig 3.1E) and toxin co-regulated pilus (Fig 3.1F). While we did not observe differences in CtxA production, we found that the Δ*lon* mutant had elevated levels of TcpA, the major pilin subunit of the toxin co-regulated pilus, indicating Lon represses toxin co-regulated pilus levels in biofilms.

The proteomic analysis was performed using TMT-labeling and LC-MS/MS. We applied a false discovery cutoff of 15% ($p<0.15$) to identify differentially regulated proteins. This analysis detected 198 differentially regulated proteins in WT and Δ*lon*

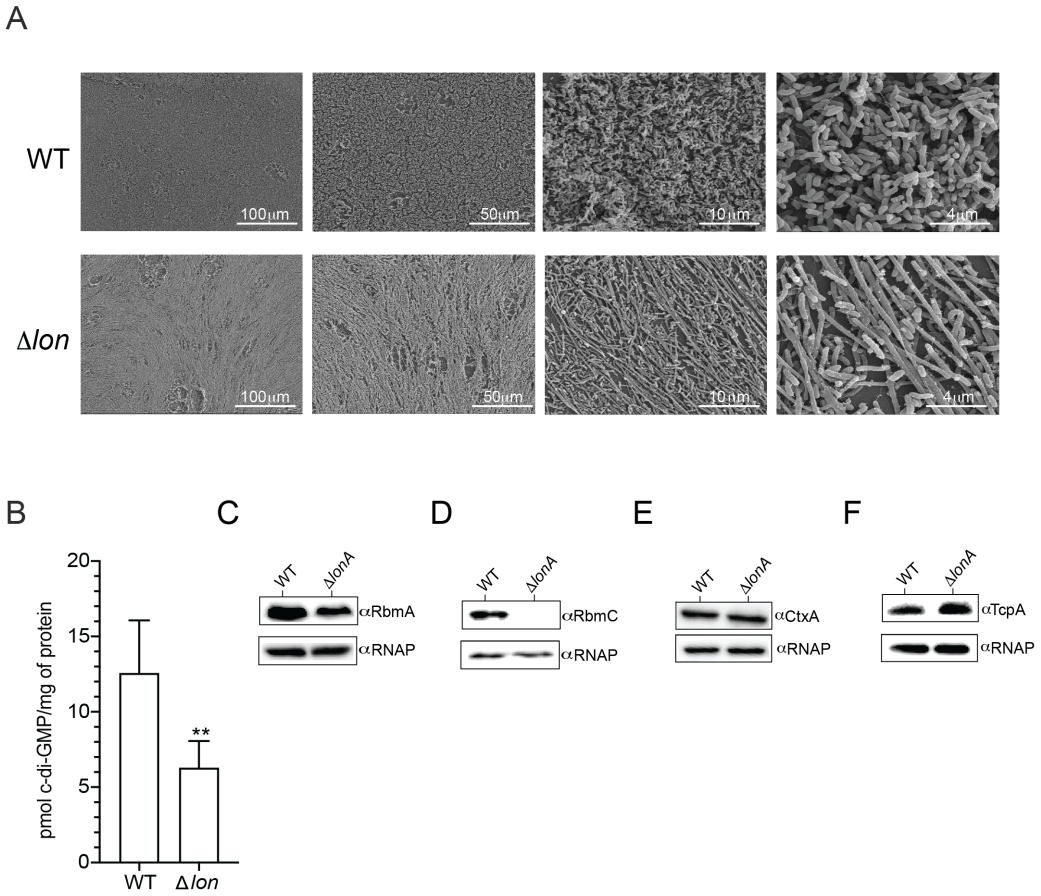

Figure 3.1: Lon regulates cell filamentation, c-di-GMP, biofilm matrix proteins, and virulence factor production in biofilms. Analysis of cell morphology, intracellular c-di-GMP, biofilm matrix proteins, and virulence factors in WT and Δ*lon* 48-hour drip flow reactor biofilms. (A) Scanning electron microscopy of *Vibrio cholerae* WT and Δ*lon* biofilms. Scale bars are provided for size reference. (B) Quantification of intracellular c-di-GMP by LC-MS/MS. Statistical analysis was performed using Student's t-test (**$p<0.01$). Western blot analysis of the biofilm matrix proteins (C) RbmA and (D) RbmC as well as the virulence factors (E) TcpA and (F) CtxA. RNA polymerase was used as a protein loading control.

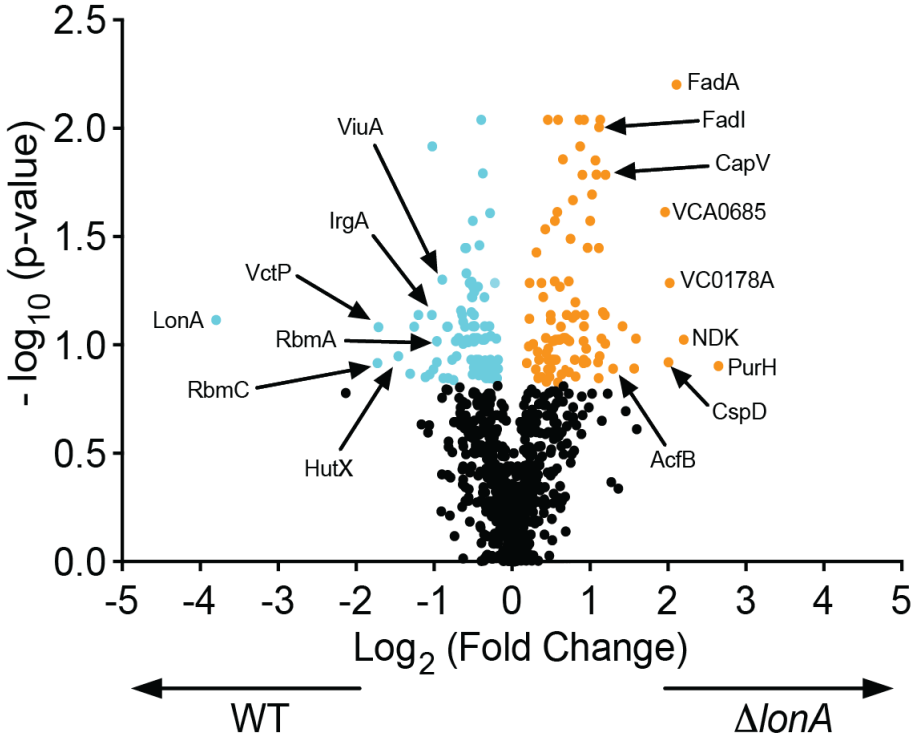

Figure 3.2: A volcano plot of proteins enriched in WT and Δ*lon* mutant biofilms. The proteomes of WT and Δ*lon* biofilms (n = 3) that had been grown for 48-hours in drip flow reactors were analyzed. A Student's t-test using Benjamini-Hochberg FDR cutoff of 15% was applied to identify proteins that were statistically significantly enriched. Proteins statistically significantly enriched in Δ*lon* are labeled in orange and proteins statistically significantly enriched in WT are labeled in cyan.

biofilms (Fig 3.2). Of these, 96 proteins were increased and 102 proteins decreased in abundance in the Δ*lon* biofilm relative to WT, respectively (Table B.1: Proteins Enriched in Δ*lon*) (Table B.2: Proteins Enriched in WT). The transcriptional profiling studies were performed using RNA-seq and a false discovery rate of 15% ($p<0.15$) was applied to identify differentially regulated transcripts. The transcriptomic profiling experiment identified 1,194 differentially regulated genes (Fig. 3.3). Of these, 883 transcripts increased in abundance and 1,111 decreased in abundance in Δ*lon* biofilm relative to WT, respectively. To better understand how Lon regulation impacts various cellular processes during biofilm formation, we analyzed our proteomic and transcriptomic data sets for genes involved in Lon-associated biofilm, motility, T6SS, virulence factor, and stress-related phenotypes.

3.2.2 Regulation of Biofilm Formation

Biofilm formation requires the biofilm matrix components *Vibrio* polysaccharide (VPS), encoded in *vps-I* and *vps-II* operons, and the matrix proteins RbmA, Bap1, and RbmC. A complex regulatory hierarchy governs the regulation of biofilm formation; however, VpsT and VpsR, transcriptional regulators whose activity is enhanced by c-di-GMP binding, function as the master regulators of biofilm gene expression [2, 25]. We observed a 1.9-fold reduction in RbmA protein levels and a 3.3-fold reduction in RbmC protein levels in the Δ*lon* mutant relative to WT. There were small but significant transcript abundance reductions in most biofilm matrix genes in the Δ*lon* mutant relative to WT (Fig 3.4A). We did not observe significant changes in protein and transcript

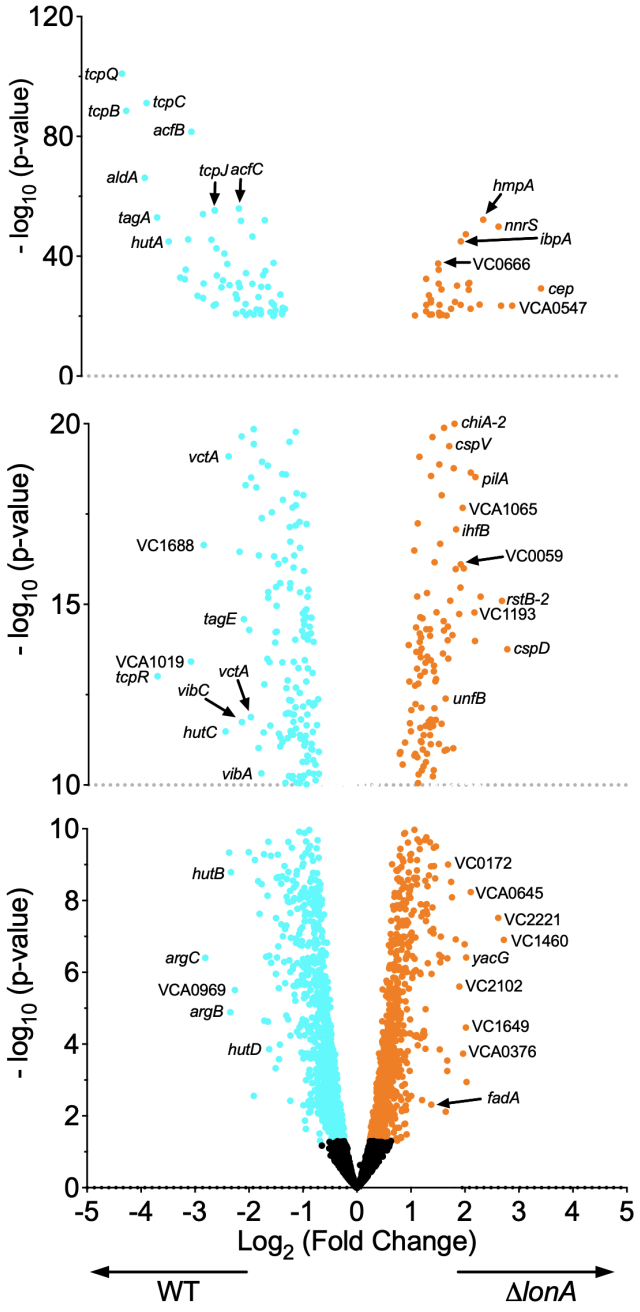

Figure 3.3: Whole transcriptome analysis of WT and Δ*lon* from biofilms. A volcano plot of differentially enriched transcripts from WT and Δ*lon* biofilms. The transcriptome of WT and Δ*lon* biofilms (n = 3) that had been grown for 48-hours in drip flow reactors were analyzed. An FDR cutoff of 0.5% was applied to identify transcripts that were differentially expressed. Transcripts significantly enriched in Δ*lon* are labeled in orange and transcripts significantly enriched in WT are labeled in cyan.

abundance of VpsT. While VpsR protein levels were not altered, VpsR transcript levels were elevated modestly (1.4-fold) in the Δ*lon* mutant relative to the WT strain. Levels of c-di-GMP change during biofilm formation and increase VpsR and VpsT activity. Since the Δ*lon* biofilm has significantly reduced c-di-GMP levels relative to the WT biofilm, lower c-di-GMP levels may result in reduced gene expression from VpsR and VpsT regulated promoters.

We also note that CsrA protein (1.5-fold enriched) and transcript (2.5-fold) levels were elevated relative to WT in the Δ*lon* biofilm. CsrA is an RNA binding protein that can impact the stability, elongation, and translation efficiency of RNA targets [26, 27, 28, 29]. Recent work suggests that CsrA positively regulates biofilm gene expression during the exponential phase but inhibits biofilm gene expression during the stationary phase. Furthermore, it was recently shown that *rbmA* transcript co-immunoprecipitates with CsrA, suggesting CsrA may directly regulate *rbmA* [30]. Thus, one possibility is that the elevated levels of CsrA in the Δ*lon* biofilm results in direct repression of RbmA and indirect repression of other biofilm matrix genes. Future studies using both genetic and biochemical assays will be required to establish the role of CsrA in *V. cholerae* biofilm formation and it's role in Lon-dependent phenotypes.

3.2.3 Regulation of Flagellar Assembly

Flagellar genes are categorized hierarchically based on their sequential activation by the transcriptional regulators FlrA, RpoN (σ 54), FlrC, and FliA [31]. FlrA is the lone class I gene and activates RpoN-dependent transcription of class II flagellar

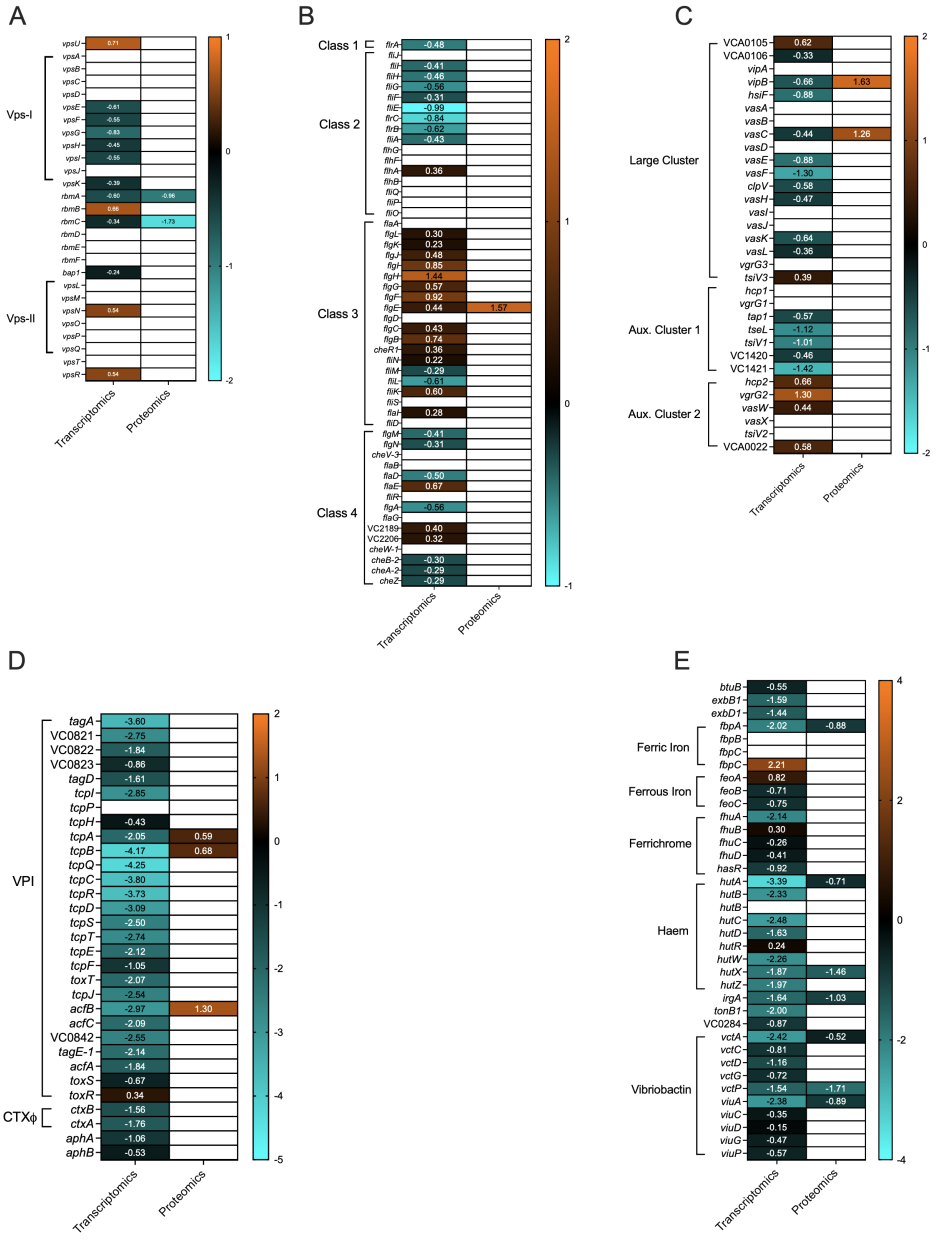

Figure 3.4: Heat maps of differentially expressed genes and proteins that are up-regulated or down-regulated in the Δ*lon* biofilm relative to WT. Shown are selected genes that encode for (A) biofilm matrix production, (B) flagellar assembly, (C) T6SS assembly, (D) virulence factor production, and (D) iron transport systems. Transcripts and proteins that increased in abundance are labeled in orange while those that decreased are labeled in cyan. The $\log_2$ fold change (Δ*lon*/WT) for each gene is shown on their respective cells.

genes. Class II flagellar genes include the FlrBC two-component system, promoting RpoN-dependent transcription of class III flagellar genes. When the anti-sigma factor FlgM is exported out of the flagellar hook, FliA activates class IV flagellar gene expression. FlrA functions as the master regulator of flagellar gene expression due to its placement at the top of the flagellar regulatory hierarchy, and *flrA* deficient mutants typically display reduced transcription from class II-IV flagellar genes.

We observed a 1.5-fold increase in the flagellar hook protein FlgE (VC2197) in the Δ*lon* mutant relative to WT. However, no other flagellar proteins were significantly different in the proteomics. The Δ*lon* mutant exhibited flagellar gene expression patterns atypical of the flagellar regulatory cascade (Fig 3.4B). Specifically, message abundance of class I, II, and IV genes are decreased; however, most class III genes are elevated. FlrC regulates class III flagellar genes; however, *flrC* transcript is reduced in the Δ*lon* mutant. This finding suggests that rather than abundance, the activity of FlrC may be altered. FlrC heptameric assembly is inhibited by c-di-GMP [32]. Thus, the reduced levels of c-di-GMP in the Δ*lon* biofilm might facilitate FlrC-dependent transcription of class III flagellar genes. It is important to note that c-di-GMP also directly inhibits FlrA activity, and the reduced c-di-GMP in the Δ*lon* mutant did not lead to an increase in FlrA-dependent gene expression [33]. This is likely because FlrA binds to c-di-GMP more tightly than FlrC and is therefore, more easily repressed by c-di-GMP [32, 33].

3.2.4 Regulation of Pathogenesis

Most genes required for *V. cholerae* pathogenesis are located on the *Vibrio* pathogenecity island (VPI) and the CTXΦ prophage [34]. The VPI, also known as the toxin co-regulated pilus island, contains the genes required for biogenesis of the toxin co-regulated pilus [34]. In addition, the VPI contains other genes that are known, or thought to, enhance fitness during infection such as accessory colonization factors (*acfABCD*), an aldehyde dehydrogenase (*aldA*), and the ToxR-activated genes (*tagA* and *tagE-1*) [35, 36, 37, 38]. The CTXΦ prophage contains the genes for cholera toxin biogenesis (*ctxAB*). The toxin co-regulated pilus and cholera toxin are required for efficient colonization, the onset of cholera symptoms, and biofilm hyperinfectivty [5, 39, 40]. Thus, the toxin co-regulated pilus and cholera toxin are considered the primary virulence determinants in *V. cholerae*. The proteomic analysis found that levels of pathogenesis-related proteins were higher in Δ*lon* compared to WT. More specifically, AcfB was 2.4-fold enriched, TcpA was 1.5-fold enriched, and TcpB was 1.6-fold increased in the Δ*lon* mutant relative to WT. The increased levels of TcpA in the Δ*lon* mutant are consistent with our earlier observations (Fig3.1 F). Interestingly, the transcript abundance of AcfB, TcpA, and TcpB were reduced 7.8-fold, 4.1-fold, and 16-fold, respectively. Indeed, all genes encoded on the VPI and CTXΦ showed decreased transcript abundance (Fig 3.4D). Together, this indicates that opposing transcriptional and post-transcriptional regulatory mechanisms are influencing virulence factor production in the Δ*lon* biofilm relative to WT.

In *V. cholerae*, transcriptional regulation of pathogenesis genes is under the control of TcpPH, ToxRS, HapR, FliA, AphAB, and ToxT [34, 41]. Transcriptional activation of the virulence regulon is controlled primarily by the TcpPH and ToxRS two-component signaling networks, which function to drive the expression of ToxT, the master regulator of virulence gene expression [39, 40, 42]. ToxT activation leads to the expression of virulence genes, including those located on the VPI and CTXΦ prophage [40]. Repression of the ToxT regulatory module can occur in several ways. First, at high cell density, the quorum-sensing regulator HapR can repress AphA and AphB, which leads to reduced transcription of *tcpPH* [43]. Reduced *tcpPH* transcription leads to reduced *toxT* transcription [43]. In addition, FliA is thought to function as both an activator and repressor of the virulence cascade by bridging motility and quorum sensing signaling networks [15, 31, 44]. Specifically, during penetration of the intestinal mucosa, the flagellar filament breaks, which permits secretion of the anti-sigma factor FlgM [44]. In the absence of FlgM, FliA represses virulence gene expression [16,31]. However, FliA also represses *hapR* transcription and this is thought to prime the activation of the virulence cascade by derpressing HapR control of *aphA* [44]. HapR is optimally produced at high cell density. Since the infectious dose of *V. cholerae* is relatively high (10^6 CFU/mL) levels of HapR are also likely high. Thus, it is thought that FliA repression of *hapR* transcription is important in resetting the quorum sensing regulatory module back to a low cell density state [44]. The absence of FlgM, however, also permits proteolysis of FliA by Lon [16]. Together, this regulatory circuit is thought to ensure virulence factor production occurs when *V. cholerae* is properly situated in the host

intestinal tract [44]. Since both HapR and FliA are targets of Lon, and both regulators can repress virulence factor production, the enrichment of either HapR or FliA in the transcriptomic or proteomic datasets would indicate their involvement in repressing the virulence regulon in the Δ*lon* biofilm [15, 20] [16,21]. However, neither HapR nor FliA were differentially regulated in the proteomics, and *hapR* and *fliA* transcripts were modestly decreased in the Δ*lon* biofilm. Together, this suggests that HapR and FliA-independent mechanisms function to repress virulence gene expression in the Δ*lon* biofilm.

Another mechanism that shuts down virulence gene expression is the accumulation of unsaturated fatty acids (UFA), which bind to and inhibit ToxT activity [45, 46]. When UFAs are high, fatty acid catabolic pathways are upregulated while fatty acid biosynthesis pathways are down regulated [47, 48]. The fatty acid catabolic genes FadA (4.3-fold enriched), FadB (2-fold enriched), and FadI (2.1-fold enriched) were among the most enriched proteins in the Δ*lon* biofilm, and the transcriptomics revealed similar trends in transcript abundance. Conversely, protein levels of the fatty acid biosynthesis genes FabF (1.5-fold decreased) and FabV (1.2-fold decreased) were reduced. Interestingly, it was recently shown that the dicyclic nucleotide cyclase, DncV (VC0179), and the phospholipase CapV (VC0178) positively regulate fatty acid catabolism and inhibit fatty acid biosynthesis [49]. It has been proposed that DncV/CapV may modulate ToxT activity by regulating intracellular UFA levels [49, 50]. More specifically, DncV produces cyclic GMP-AMP (cGAMP), a signaling molecule that binds to, and directly activates, CapV phospholipase activity. When bound to cGAMP, CapV functions to

remove long-chain fatty acids (LCFA) from the cell membrane. Thus, DncV and CapV may regulate ToxT activity by modulating fatty acid catabolism. Interestingly, CapV protein levels were 2.3-fold enriched and DncV protein levels were 1.4-fold enriched. In addition, we identified the hypothetical protein VC0178A (WP_001125591.1) to be 4-fold increased in the Δ*lon* biofilm. VC0178A is not annotated in the N16961 genome; however, it is located immediately upstream of the dncV/capV operon and may constitute an additional component of this system.

An intriguing question that remains is how protein levels of TcpA, TcpB, and AcfB are elevated despite the substantial decreases in their transcript abundance in the Δ*lon* biofilm. One possible explanation is that translation of these genes is enhanced through the action of translational regulators. RNA binding proteins are known to regulate translation efficiency and we identified elevated levels of two proteins that are known (CsrA) or are predicted (CspD) to be RNA binding proteins in the Δ*lon* -omics data sets. CsrA is known to positively impact the production of virulence-related genes by promoting the translation of *aphA*, a positive regulator of the virulence cascade. However, we did not detect increased levels of AphA protein in the proteomics data sets [30]. In addition, it is not known if CsrA directly controls of *tcpA*, *tcpB*, or *acfB*. The second translational regulator is CspD which was 4.0-fold enriched in the proteomics and 6.5-fold enriched in the transcriptomics. A function for CspD in virulence gene regulation has not been explored. Thus, additional analysis is required to determine what role, if any, CsrA and CspD have in virulence factor production.

3.2.5 Regulation of Iron Homeostasis

Among the most significantly reduced proteins in the Δ*lon* biofilm were those involved in the acquisition and transport of iron (Fig3.4 E). The abundance of proteins involved in the acquisition and transport of vibriobactin, enterobactin, heme, and ferric iron were significantly lower in the Δ*lon* biofilm relative to the WT strain. More specifically, VctP (VCA0227), which encodes a periplasmic vibriobactin binding protein, was 3.3-fold reduced in the Δ*lon* biofilm and ViuA (VC2211), which encodes a vibriobactin TonB-dependent receptor, was 1.8-fold reduced in the Δ*lon* biofilm. In addition, both IrgA (VCA0475) and VctA (VCA0232), which encode enterobactin TonB-dependent receptors, were 1.6 and 1.4-fold reduced in the Δ*lon* biofilm relative to WT. Furthermore, HutA (VCA0576), which encodes the TonB-dependent receptor for heme, and HutX, which encodes a heme cytosolic carrier protein, were 1.6-fold and 2.7-fold reduced, respectively. Finally, FbpA (VC0608), which encodes a periplasmic ferric iron-binding protein, was 1.8-fold reduced. Additional analysis of the operons encoding the vibriobactin and enterobactin permease systems VctPDGC (VCA0227-30), heme permease system HutBCD (VCA0914-VCA0916), and ferric iron permease system FbpABC (VC0608-VC0610), as well as their respective TonB-dependent receptors, revealed reductions in transcript abundance ranging from 1.5-10-fold in the Δ*lon* biofilm relative to WT. In *Vibrio cholerae*, the transcriptional regulator Fur represses these iron acquisition systems when intracellular iron levels are high. Thus, it seems likely that the cellular levels of iron are greater in the Δ*lon* biofilm than its WT counterpart. It is

also interesting to note that ToxT indirectly activates iron uptake genes [50]. Thus, it is possible that repression of ToxT by UFAs may also contribute to the repression of these iron uptake systems in the Δlon biofilm.

While iron is an essential cofactor in many enzymatic processes, cells need to balance intracellular iron levels to avoid generating reactive oxygen species (ROS), such as hydrogen peroxide and superoxide, which can lead to systemic cellular damage. For example, nucleobases, especially guanosine nucleotides, are highly susceptible to oxidation and can lead to DNA base mispairing, the formation of DNA lesions, and double-stranded DNA (dsDNA) breaks [51, 52, 53]. We know little regarding the consequences of RNA oxidation by ROS; the existing evidence suggests that tRNAs and ribosomes are susceptible to oxidative stress and that misincorporation of oxidized bases into mRNA can reduce translation efficiency [53, 54]. Furthermore, ROS can lead to the peroxidation of lipid molecules leading to their degradation [53]. Finally, oxidation of essential enzymatic cofactors or the amino acids methionine and cysteine can lead to loss of enzymatic activity, protein misfolding, and proteotoxic stress [53, 55, 56]. Interestingly, it was recently shown in *Salmonella enterica*, that loss of *lon* results in increased metal ion uptake and oxidative stress [57].

3.2.6 Regulation of Reactive Oxygen Stress Response Pathways

In *V. cholerae*, the SoxRS two component system as well as the transcriptional regulators OxyR-1 and OxyR-2 are involved in sensing and responding to ROS [58, 59, 60]. Both systems rely on regulators that become active in the presence of

oxidizing conditions [61, 62]. For example, SoxR (VCA0084) monomers each contain an iron sulfur [2Fe-2S] cluster and assemble into a homodimer. SoxR activation requires full oxidation of its iron sulfur cluster core (Fe^{3+} - Fe^{3+}). Fully oxidized SoxR activates SoxS (VC1825), which in turn leads to the expression of genes to cope with ROS such as the superoxide dismutases *sodA* (VC2694), *sodB* (VC2045), and *sodC* (VC1583) [63]. Similarly, OxyR-1 becomes active when a critical cysteine becomes oxidized [61]. The *V. cholerae* OxyR-2 is thought to be activated similarly and functions to regulates OxyR-1 activity [58,59,61]. Active OxyR-1 and OxyR-2 lead to the production of hydrogen peroxide scavenging genes such as alkylhydroperoxide reductase, *ahpC* (VC0731). Notably, hydrogen peroxide also activates the expression of the catalases *katG* (VC1560) and *katB* (VC1585), albeit independently of OxyR-1 [64]. None of the listed genes were identified in the proteomics analysis. Furthermore, all of these genes were either not differentially regulated or only modestly downregulated (1.2 to 1.5-fold reduced) in the Δ*lon* transcriptomic profiling experiment. The only exception to this was the transcript for *katG*, which was 1.5-fold increased in the Δ*lon* mutant. The SoxRS and OxyR-1 systems primarily respond to superoxide and hydrogen peroxide. Since these systems function as direct redox sensors of these stressors, it seems unlikely that intracellular superoxide or hydrogen peroxide are at high enough concentrations to activate these systems in the Δ*lon* biofilm.

3.2.7 Regulation of Reactive Nitrogen Stress Response Pathways

While ROS response pathways were only modestly different in WT and Δ*lon* biofilms, pathways that sense and respond to reactive nitrogen species (RNS) were among the most upregulated proteins and transcripts in the Δ*lon* biofilm. While SoxRS, OxyR-1, and OxyR-2 regulated genes were only modestly different in WT and Δ*lon* biofilms, proteins and transcripts of genes involved in the detoxification and response to reactive nitrogen species (RNS) were substantially different in WT and Δ*lon* biofilms. RNS exert systemic cellular damage. For example, nitric oxide can disrupt the function of proteins containing cysteine residues and can also damage proteins with haeme centers and labile 4Fe-4S iron sulfur clusters. Many enzymes involved in the electron transport chain (ETC) depend on cysteine, haeme, and iron sulfur clusters for electron transfer. Thus, RNS is often associated with growth inhibition due to the the collapse of the ETC. In addition, RNS can corrupt the nucleotide pool by reacting with nucleobases, particularly guanosine nucleotides, leading to DNA mutagenesis and impaired translation [65, 66].

In *V. cholerae*, the nitric oxide response is mediated through NorR (VCA0182), which contains a non haeme iron that forms a mononitrosyl iron complex in the presence of RNS [67, 68]. In *E. coli*, NorR activation occurs in the presence of nitric oxide, nitrite, and nitrate [68, 69, 70]. The formation of the mononitrosyl iron complex leads to NorR's activation. NorR proceeds to activate transcription of *hmpA* (VCA0183) and *nnrS* (VC2330), which detoxify RNS [67, 68]. In addition, NorR functions repress its

own transcription [67]. HmpA was one of the most enriched proteins in the Δ*lon* biofilm (4.5-fold enriched). In addition, *hmpA* and *nnrS* transcription were increased 5.4-fold and 6.5-fold respectively in the Δ*lon* biofilm. Finally, *norR* transcription was decreased by 1.7-fold in the Δ*lon* mutant relative to WT. Together, this suggests that the Δ*lon* mutant may be experiencing stress due to RNS.

3.2.8 Regulation of DNA Repair Pathways

We identified numerous enzymes involved in DNA repair to be upregulated in the Δ*lon* biofilm proteomics and transcriptomic datasets. Specifically, RecA (VC0543), which is involved in DNA recombination and repair, was 2.2-fold enriched in the Δ*lon* proteomics and 2-fold enriched in the Δ*lon* transcriptomics. Furthermore, RecN (VC0852) and RecX (VC0544) transcripts were 3-fold increased in the Δ*lon* biofilm. RecA, RecN, and RecX are members of the bacterial recombination system, which help repair stalled replication forks and DNA lesions through homologous recombination [71]. In addition, UvrA (VC0394), a nucleotide excision repair (NER) pathway component, was 1.6-fold enriched in both the Δ*lon* proteomics and transcriptomics [71]. NER functions to repair diverse genotoxic DNA lesions. In addition, Dps (VC0139), which encodes for a DNA-binding oxidative stress defense protein, was 1.7-fold enriched in the Δ*lon* proteomics and 2-fold increased in the Δ*lon* transcriptomics. Finally, there was a 2-fold enrichment of the transcript and protein abundance of VC0428, which belongs to the universal stress protein superfamily of proteins. Universal stress proteins protect cells from diverse stressors, including oxidative stress, though the protective mechanisms utilized by

these enzymes are poorly understood. Together, this suggests that Lon-deficient strains are likely coping with some sort of DNA damage. Indeed, inhibition of cell division and subsequent filamentation is often associated with DNA damage, nucleotide starvation, or corruption of the nucleotide pool [72, 73, 49, 74].

3.2.9 Analysis of Lon Targets

To identify Lon targets in biofilm-grown cells, we focused on three of the proteins with the highest abundance in the proteomics: PurH, NDK, and CspD. The two most enriched proteins identified in our proteomics were PurH (6.2-fold enriched) and NDK (4.6-fold enriched). PurH encodes for the bifunctional phosphoribosylaminoimidazolecarboximide formyl transferase/IMP cyclohydrolase; it catalyzes the final two steps in inosine monophosphate (IMP) biosynthesis, a precursor of purine nucleotides [75]. NDK encodes for nucleoside diphosphate kinase, a broadly conserved enzyme that plays an important role in regulating nucleotide homeostasis [76]. NDK catalyzes the reversible transfer of γ-phosphates from nucleoside triphosphates (NTPs) to nucleoside diphosphates (NDPs) as well as deoxynucleoside diphosphates (dNDPs) [77, 78]. NDK enzymatic activity results in the generation of nucleoside triphosphates (NTPs) and deoxynucleoside triphosphates (dNTPs), respectively. While NDK has broad substrate specificity, NDK acts most favorably on guanosine nucleotides [77, 78, 79]. Since diguanylate cyclases (DGCs) generate c-di-GMP from 2GTP, enzymes that alter the cellular pool of GTP are likely to influence c-di-GMP levels.

The most enriched regulatory protein identified in our analysis was CspD (4-

fold enriched), belonging to the CspA family of cold shock proteins. In *E. coli*, Lon regulates steady-state levels of CspD *in vivo* and *in vitro* [80]. The Lon protease encoded by *V. cholerae* Lon shares 82% identity to its *E. coli* homolog, indicating that there may be some conservation in the proteins they target. Indeed, *V. cholerae* and *E. coli* Lon have overlapping substrate profiles [15, 21, 81, 82]. A role for CspD in regulating *V. cholerae* cellular processes remains unexplored; however, its enrichment in the Δ*lon* biofilm suggests it may play an important role in regulating Lon-dependent processes.

3.2.10 The role of Lon on effecting steady-state levels of PurH, NDK, and CspD

To determine if PurH, NDK, or CspD might be Lon substrates, we generated FLAG tagged PurH, NDK, and CspD overproduction strains. An inducible promoter drove the expression of the tagged constructs at the neutral Tn-7 site in Δ*purH*, Δ*ndk*, and Δ*cspD* strains. In addition, we also generated a similar set of strains in Δ*lon* genetic backgrounds. To determine the impact of Lon on the stability of these proteins, we inhibited protein translation with chloramphenicol addition and then analyzed protein abundance over time. While we did not observe NDK stability to be regulated by Lon, we did find that PurH and CspD were more stable in the absence of Lon, suggesting that PurH and CspD are Lon targets. These assays should be repeated to validate that Lon affects PurH and CspD steady state levels.

It is important to note that this experiment was performed using planktonic cultures grown to stationary phase. These conditions are unlikely to reproduce the

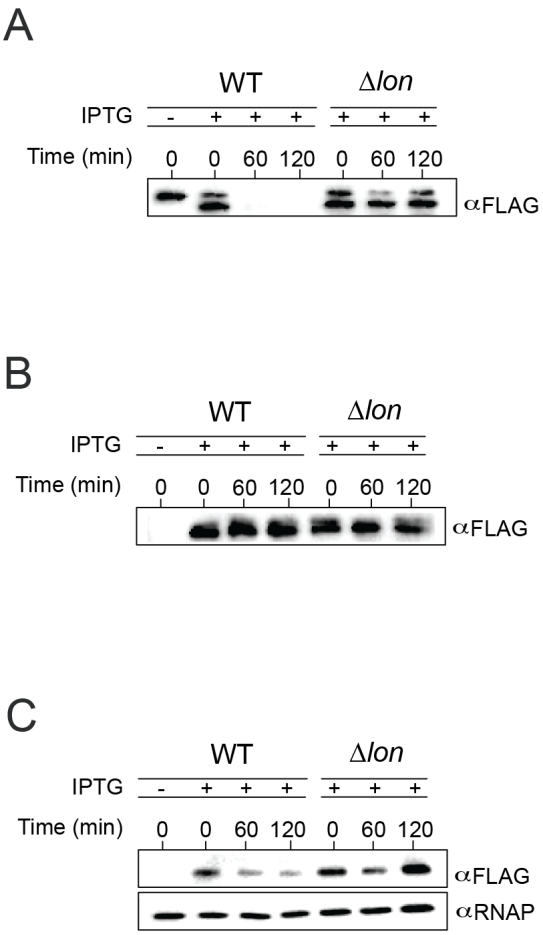

Figure 3.5: *In vivo* stability of PurH, NDK, and CspD. 3xFLAG tagged PurH, CspD, and NDK were placed under the control of the Ptac promoter at the Tn7 locus in the mutant strains indicated. Each mutant was grown aerobically overnight in the presence or absence of 0.1mM IPTG. Levels of each protein were assessed before and after translational inhibition. (A) Steady state levels of PurH in Δ*purH* and Δ*lon*Δ*purH* backgrounds. (B) Steady state levels of NDK in Δ*ndk* and Δ*lon*Δ*ndk*. (C) Steady state levels of CspD in Δ*cspD* and Δ*lon*Δ*cspD* backgrounds. PurH, NDK, and CspD were detected with FLAG antibody. Cells were normalized by optical density and by BCA. For CspD, RNA polymerase was included as an additional protein loading control. PurH and NDK possess a 3xFLAG tag on the C-terminal region while CspD possesses a 3xFLAG tag on the N-terminal region.

conditions found in a mature biofilm. Thus, we cannot definitively rule out NDK as a Lon target. Additional PurH, NDK, and CspD abundance analysis should be assessed from 48-hour biofilms in WT and Δ*lon* mutants. It is also important to note that while epitope tags are an efficient way of detecting a protein, some tags can interfere with Lon substrate acquisition [83]. Thus, these studies should be repeated using antibodies raised against PurH, NDK, and CspD.

3.2.11 The role of PurH, NDK, and CspD in c-di-GMP and biofilm matrix production during biofilm formation

Next, we sought to determine what role, if any, PurH, NDK, and CspD might have in c-di-GMP and biofilm matrix production in mature biofilms. Thus, we constructed *purH*, *ndk*, and *cspD* mutants in WT and Δ*lon* genetic backgrounds to determine their role in these processes during biofilm formation. To accommodate the number of mutant strains and to acquire sufficient biomass for mass spectrometry and western analysis, we grew mutants as tube biofilms for 48-hours. Our preliminary data indicate that the Δ*lon* mutant had significantly reduced c-di-GMP (3.6A) as well as reduced RbmA and RbmC (Fig 3.6B and 3.6C) relative to the WT strain. These results are consistent with our 48-hour drip flow reactor biofilms, suggesting that c-di-GMP regulation under these conditions is similar. PurH, NDK, and CspD single mutants did not alter c-di-GMP pools (Fig. 3.6A) or biofilm matrix production (Fig. 3.6B), indicating they are dispensable for these processes in the presence of Lon.

While deletion of *ndk* in the Δ*lon* mutant did not alter c-di-GMP, deletion

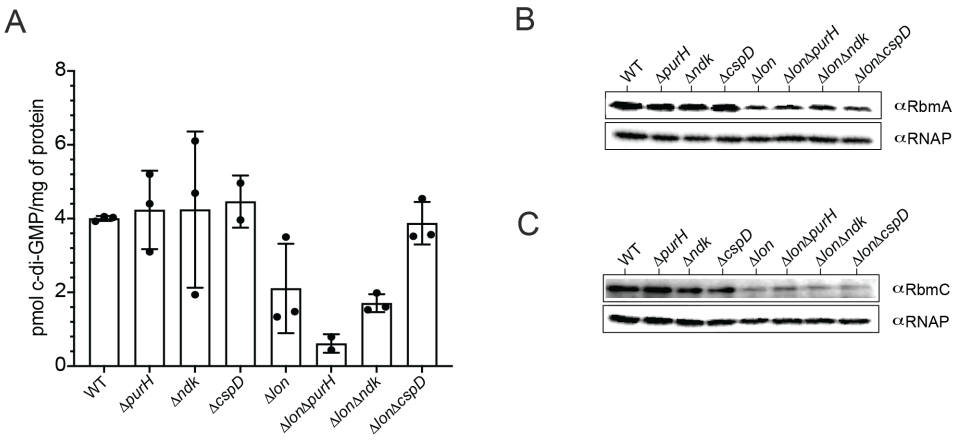

Figure 3.6: Quantification of intracellular c-di-GMP and biofilm matrix proteins from biofilms. *V. cholerae* WT and mutant strains were grown in silicone tubing under constant flow for 48-hours in LB. (A) The biofilms were harvested and c-di-GMP was extracted and then quantified by high performance liquid chromatography-tandem mass spectrometry (HPLC-MS/MS). The value of each individual replicate is shown. (B) RbmA and RbmC levels were also assessed by western blot. RNAP was used as a biomass loading control.

of *purH* in the Δ*lon* mutant significantly decreased c-di-GMP levels, indicating that PurH positively contributes to c-di-GMP biosynthesis in biofilm-grown Δ*lon* strains. Furthermore, deletion of *cspD* in the Δ*lon* mutant appears to restore c-di-GMP levels to those similar to WT, indicating that CspD functions to repress c-di-GMP biosynthesis in the Δ*lon* biofilm. We note that additional replicates are required to validate these findings. If these findings are reproducible, it would suggest that Lon represses c-di-GMP biosynthesis by regulating PurH and activates c-di-GMP biosynthesis by regulating CspD. Interestingly, loss of *purH* and *cspD* in the Δ*lon* mutant did not alter RbmA or RbmC levels. Since these two proteins are transcriptionally activated by c-di-GMP, we expected the levels of RbmA and RbmC protein to correspond with c-di-GMP pools. Thus, translational regulatory mechanisms may be involved in controlling RbmA

and RbmC production in the Δ*lon* mutant.

3.2.12 The role of PurH, NDK, and CspD in motility and T6SS-dependent killing phenotypes

We also wondered if PurH, NDK, and CspD might participate in other Lon-associated phenotypes. Specifically, we asked if they influenced motility or type VI secretion system (T6SS)-dependent killing. We did not observe differences in motility in the Δ*purH*, Δ*ndk*, or Δ*cspD* strains between WT (Fig. 3.6A). In addition, there were no differences in motility phenotypes of the Δ*lon*Δ*purH*, Δ*lon*Δ*ndk*, or Δ*lon*Δ*cspD* strains and Δ*lon* single mutant. We observed similar pattern for the T6SS-dependent killing assays (Fig. 3.6B). The lone exception was that deletion of *cspD* resulted in significantly increased killing relative to WT. However, deletion of *cspD* in the Δ*lon* background did not further increase killing in the Δ*lon* mutant. The enchanced T6SS-dependent killing observed in the Δ*lon* mutant is due to TfoY [21]. Since loss of *cspD* does not reduce T6SS-dependent killing in the Δ*lon* mutant, it is likely that CspD functions upstream of TfoY.

3.2.13 The role of PurH, NDK, and CspD in stress response phenotypes

The down regulation of iron transport systems in the Δ*lon* biofilm are consistent with Fur mediated repression under iron replete conditions [84]. Streptonigrin is an antibiotic that leads to DNA damage in the presence of oxygen and free intracellular iron

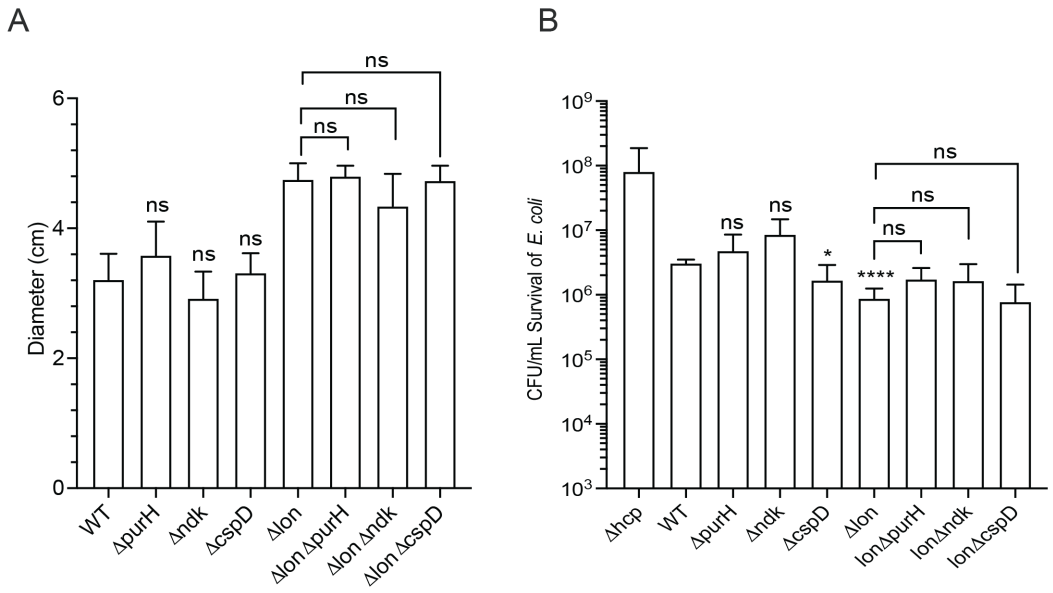

Figure 3.7: Quantification of flagellar motility and T6SS-dependent killing. For motility assays, single colonies were stabbed into LB soft agar plates (0.3% agar) and incubated at 30C for 18 hours. (A) The swimming motility phenotypes of WT, Δ*purH*, Δ*ndk*, Δ*cspD*, Δ*lon*, Δ*lon*Δ*purH*, Δ*lon*Δ*ndk*, and Δ*lon*Δ*cspD* were assessed. (B) The T6SS-dependent killing phenotypes of WT, Δ*purH*, Δ*ndk*, Δ*cspD*, Δ*lon*, Δ*lon*Δ*purH*, Δ*lon*Δ*ndk*, and Δ*lon*Δ*cspD* were determined by enumerating the survival of E. coli MC4100, which is susceptible to T6SS-mediated attacks. In addition, hcp was included as a negative control for T6SS-dependent killing.

[85]. Thus, we indirectly assessed free intracellular iron levels by quantifiying streptonigrin induced cell death of WT and Δ*lon* mutant strains (Fig. 3.7A). Our preliminary results indicate that mutants deficient in Lon are more susceptible to streptonigrin treatment than WT. In addition, loss of *ndk* in the WT genetic background resulted in decreased survival. In addition, loss of *ndk* in the Δ*lon* genetic background further decreased the fitness of this strain relative to the Δ*lon* single mutant. The Δ*purH* and Δ*cspD* single mutants strains did not appear to be more vulnerable to streptonigrin than the WT strain. However, loss of *purH* or *cspD* in the Δ*lon* genetic background

led to further decreases in survival. This data supports the hypothesis that levels of intracellular iron are elevated in the Δ*lon* mutant. Futhermore, it suggests that NDK, CspD, and PurH may play protective roles in defending against streptonigrin induced cell death.

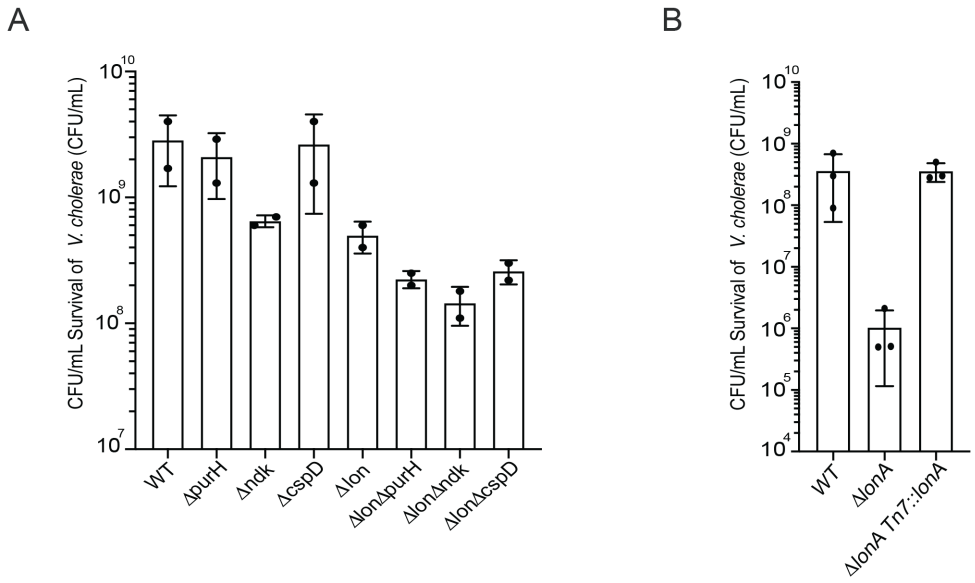

Figure 3.8: Survival of *V.cholerae* WT and mutant strains during streptonigrin and mitomycin C treatment. (A) *V. cholerae* WT and mutant strains were grown overnight at 37C in LB media supplemented with 1ug/mL of streptonigrin or (B) 0.025ug/mL of mitomycin C. The CFU/mL of surviving *V. cholerae* was enumerated.

Lon-deficient mutants are often more susceptible to DNA damage. Thus, we assessed the susceptibility of WT and Δ*lon* in the presence of mitomycin C (MMC); a cytotoxic DNA crosslinking agent (Fig 3.7B). We found that Δ*lon* was extraordinarily sensitive to MMC treatment. Complementation of *lon* at the Tn7 locus restored survival to WT levels. This indicates that Lon plays an important role in the DNA damage response in *V. cholerae*. Further analysis is required to determine what role PurH,

NDK, and CspD play in protecting cells from MMC. This would help establish if they function specifically in regulating iron homeostasis, or more generally in response to DNA damage. Furthermore, since RNS response pathways are upregulated in the Δlon biofilm, it would be interesting to explore if these enzymes also mitigate RNS toxicity.

3.2.14 Concluding Remarks

In this study, we used proteomic and transcriptomic analyses to identify Lon regulated processes in biofilms. Our data indicates that Lon controls biofilm matrix production, virulence factor production, nucleotide pool homeostasis, iron homeostasis, and DNA repair pathways; processes that are known to influence *V. cholerae*'s fitness in its environmental resevoirs and during infection [5, 84, 86]. Thus, future studies directed at understanding the mechanisms by which Lon controls these processes will be of considerable interest.

The data shown here suggests that PurH and CspD are likely Lon substrates and that Lon-dependent control of these enzymes influences c-di-GMP biosynthesis. Additional analysis of the role of these enzymes on biofilm development is warranted. Growth of fluorescently labled mutant strains in flow cell biofilms would allow the impact of PurH and CspD at different stages of biofilm development to be assessed. In addition, it will be interesting to determine if PurH, NDK, or CspD influence virulence factor transcription or translation and what role these enzymes play in host colonization. Finally, determing the mechanism by which PurH, NDK, and CspD mitigate streptonigrin induced toxicity will be of interest. Indeed, the hyperfilamentation of Δlon mutants

coupled with the upregulation of DNA repair and stress response pathways suggests that Δlon mutant is attempting to cope with genotoxic stress. The source of this stressor is currently unclear, however, the upregulation of RNS response enzymes indicates that nitrosative stress is the likely culprit.

It is interesting to note that purine nucleotides, especially guanosine bases, are especially susceptible to ROS and RNS. Oxidized and nitrated nucleotides such as 8-oxoguanine and 8-nitroguanosine are mutagenic. Thus, it seems paradoxical that PurH and NDK, enzymes that enhance the production of guanosine nucleotides, would function to preserve the viability of Lon-deficient mutants when challenged with genotoxic stress. One possibility is that the corruption of the nucleotide pool leads to the upregulation of enzymes that can replenish the pool useable nucleotides. Thus, PurH and NDK may ensure that uncorrupted purine nucleotides are available for DNA and RNA synthesis. It is also interesting to note that 8-nitroguanosine 3',5'-cyclic monophosphate (8-nitro-cGMP), functions as an important secondary messenger molecule in eukaryotic cells that modulates the cellular oxidative stress responses [87]. While a role for nitrated bases in prokaryotic secondary messenger signaling has not been explored, it is tempting to speculate similar systems exist. In either scenario, these enzymes would need to be strictly regulated in order to ensure their mutagenic properties don't outweigh their protective properties. Thus, Lon-dependent regulation of these enzymes may act as a control checkpoint to preserve nucleotide pool homeostasis.

3.3 Materials and Methods

3.3.1 Bacterial Strains and Growth Conditions

The bacterial strains used in this study can be found in S4 Table. *V. cholerae* and *E. coli* strains were grown aerobically in Lysogeny Broth (LB) broth (1% tryptone, 0.5% yeast extract, 1% NaCl, pH 7.5) at 30°C and 37°C, respectively. LB agar contained granulated agar (Difco) at 1.5% (wt/vol). Antibiotics were used when necessary at the following concentrations: rifampin, 100 μg/ml; ampicillin, 100 μg/ml; gentamycin, 15 μg/ml; streptonigrin, 1μg/mL, and mitomycin C, 0.0250μg/mL.

3.3.2 Strain and Plasmid Generation

Plasmids were constructed using standard cloning methods or the Gibson Assembly recombinant DNA technique (New England BioLabs, Ipswich, MA). Gene deletions were carried out using allelic exchange of the native open reading frame (ORF) with a truncated ORF, as previously described [88]. The generation of complementation and overexpressing mutants was carried out using a Tn7-based system, as previously described [14,89]. For overexpression of *purH*, *ndk*, and *cspD*, the open reading frames were cloned into pMMB67EH vectors designed to include either N- or C-terminal 3xFLAG tags. The vectors contain the IPTG inducible Ptac system. The Ptac-ORF fusions were then cloned into the pGP704-Tn7 plasmid. Triparental matings with donor *E. coli* S17λpir carrying the pGP704-Tn7 plasmid with the gene of interest, helper *E. coli* S17λpir harboring pUX-BF13, and *V. cholerae* deletion strains were carried out by mix-

ing all three strains and incubating mating mixtures on LB agar plates for 18 h at 30°C. Transconjugants were selected on LB media containing rifampicin and gentamycin at 30°C. Insertion of the complementation construct to the Tn7 site was verified by PCR.

3.3.3 Biofilm Assays

Drip flow reactor (DFR) biofilm experiments were performed using a 6-chamber drip flow reactor purchased from BioSurface Technologies Corporation (BST). Cell density was normalized to approximately 109 CFU/mL in 15mL, and 100μL of this was set aside for serial dilutions, which were used to verify equal loading of the chambers. The DFR was laid flat, and 15 mLs of bacterial culture was added to each chamber to promote initial attachment to uncoated glass slides. After 1-hr, the 15mL of bacterial culture was decanted to remove non-adherent cells. The DFR was then placed at a 10° angle, and a peristaltic pump was used to flow LB medium at a rate of 0.8mL/minute/channel (8.25 RPM) to each chamber. Biofilms were grown at 25°C for 42-hours. The entire biofilm was harvested in 2.5mLs of 1xPBS buffer. Then, 1mL of culture was spun down and used for proteome analysis, 1mL was used for c-di-GMP quantification, and 200μL was used for BCA quantification. In addition, 100μL of the remaining culture was serially diluted to enumerate the total CFU/mL of the biofilm. An unpaired Students t-test was used to assess statistical differences between the input and outputs from the DFR biofilms.

3.3.4 Proteome Analysis

For proteome analysis, DFR biofilms were grown as indicated above. The 1mL of bacterial culture taken for proteome analysis was spun down and resuspended in 500μL of 50mM Tris pH 8.0 containing 8M Urea. The samples were then immediately flash frozen and stored at -80°C. Isobaric mass tag labeling was prepared using the TMT 6-plex kit (Fisher Scientific). TMT labeling and LC-MS/MS were performed by Justyne Ogdahl from Peter Chien's lab at the University of Massachusetts, Amherst. Data analysis was performed using Protein Discoverer software. Proteins and peptides were matched using the PATRIC *V. cholerae* database. ANOVA for individual proteins was applied across three replicates for WT and Δ*lon* strains and an adjusted p-value was calculated using Benjamini Hochberg analysis. A FDR of 15% was then applied to identify differentially enriched proteins.

3.3.5 RNA-seq Analysis

For RNA-seq analysis, biofilms of WT and *lon* strains were grown in a separate DFR experiment. The experiment proceeded as indicated above; however, the entire biofilm was harvested and resuspended in 2.5mLs of TRIzol reagent (ThermoFisher). RNA isolation was performed using the TRIzol reagent protocol. RNA quality was assessed by NanoDrop and agarose gel analysis. The samples were flash frozen at stored at -80°C and then shipped to the Microbial Genome Sequencing Center (MiGS) for RNA-seq. The 12M paired end read analysis was performed and rRNA reads were filtered and non rRNA reads were mapped to *V. cholerae* O1 biovar El Tor str. N16961

(assembly GCA_000006745.1) reference genome. Significantly regulated genes were determined using EdgeR and a FDR of 0.5% was applied to identify differentially expressed transcripts.

3.3.6 Protein Abundance and Stability Assays

Overnight cultures of *V. cholerae* were diluted 1:200 in 10mL of LB medium. Cells were grown until an OD600 = 0.1 was reached, 0.1mM IPTG was added to induce overexpression of *purH*, *ndk*, and *cspD*. Induction proceeded overnight; 2mL aliquots were taken immediately prior, and then at the time points indicated after the addition of 100x the minimum inhibitory concentration of chloramphenicol (100μg/mL). Detection of epitope tagged proteins was performed using polyclonal αFLAG antibody (Invitrogen) at a final concentration of 2μg/mL. RbmA and RbmC detection was performed as previously described [90,91]. TcpA levels were analyzed using TcpA antiserum diluted 1:1000. RNAP antibody was used at a concentration of 0.625μg/mL.

3.3.7 Interbacterial Killing Assays

V. cholerae WT and mutant strains and the *E. coli* strain MC4100 were grown overnight on high salt (340mM NaCl) LB agar plates at 30°C and 37°C, respectively. Single colonies were harvested and resuspended in 1mL of high salt LB broth. Approximately 109 *V. cholerae* and 108 *E. coli* cells were mixed and 25μL of this mixture was spotted in technical duplicate onto nitrocellulose membrane that had been placed on high salt LB agar plates or on high salt plates containing 0.1mM IPTG. The strains

were then incubated for 4-hours at 37°C. The filter membranes were then resuspended in 1mL of 1x PBS. Cells were resuspended, and serial dilutions were generated and spotted onto LB plates containing 100μg/mL of streptomycin, grown overnight, and the surviving *E. coli* was enumerated. Statistical analysis of T6SS killing was performed using an unpaired Student's t-test.

3.3.8 Motility Assays

Flagellar motility was determined by inoculating a single overnight colony into the center of LB soft agar plates (0.3% wt/vol). The plates were moved to 30°C and the swimming diameter was recorded at the time indicated in the figure legend. The motility phenotype of each mutant was assessed using at least three independent biological replicates. Statistical analysis of motility was performed using an unpaired Student's t-test.

3.3.9 Nucleotide Extraction Procedures

For quantification of c-di-GMP from WT and Δ*lon* biofilms, strains were grown in drip flow reactors or tube biofilms using the procedures outlined above. For drip flow reactor biofilms, the entire biofilm was harvested and resuspended thoroughly in 2.5mLs of 1xPBS buffer. Then, 1mL of resuspended culture was spun down and c-di-GMP extraction was performed as previously described [88]. For tube biofilms, the entire biofilm was harvested and resuspended in 1.5mLs of 1xPBS. For both drip flow reactor and tube biofilms, 250μL of bacterial culture was spun down, resuspended in 2% SDS,

boiled, and used for BCA. Quantification of c-di-GMP in each sample was determined by evaluating values to a standard curve generated with pure c-di-GMP (Sigma) that had been resuspended in 184mM NaCl. At least three biological replicates were analyzed. Statistical analysis of c-di-GMP was performed using an unpaired Student's t-test.

3.3.10 Streptonigrin and Mitomycin C Sensitivtiy Assays

Overnight cultures of *V. cholerae* WT and mutant strains were diluted 1:200 in 200uL of LB containing 1μg/mL of streptonigrin or 0.025μg/mL of mitomycin C as indicated. The bacterial antibiotic mixture was grown statically, overnight at 30C in a 96-well plate. The next day the cultures were serial diluted and the CFU/mL of surviving bacteria were enumerated. A non antibiotic control was included to ensure equal loading of bacterial culture.

Bibliography

[1] H.-C. Flemming, J. Wingender, U. Szewzyk, P. Steinberg, S.A. Rice, and S. Kjelleberg. Biofilms: an emergent form of bacterial life. *Nat Rev Microbiol*, 14:563–575.

[2] J.K. Teschler, D. Zamorano-Sánchez, A.S. Utada, C.J.A. Warner, G.C.L. Wong, and R.G. Linington. Living in the matrix: assembly and control of *Vibrio cholerae* biofilms. *Nat Rev Microbiol*, 13:255–268.

[3] C. Matz, D. McDougald, A.M. Moreno, P.Y. Yung, F.H. Yildiz, and S. Kjelleberg.

Biofilm formation and phenotypic variation enhance predation-driven persistence of *Vibrio cholerae*. *Proc Natl Acad Sci*, 102:16819–16824.

[4] S. Beyhan and F.H. Yildiz. Smooth to rugose phase variation in *Vibrio cholerae* can be mediated by a single nucleotide change that targets c-di-gmp signalling pathway. *Mol Microbiol*, 63:995–1007.

[5] A.L. Gallego-Hernandez, W.H. DePas, J.H. Park, J.K. Teschler, R. Hartmann, and H. Jeckel. Upregulation of virulence genes promotes *Vibrio cholerae* biofilm hyperinfectivity. *Proc Natl Acad Sci*, 117:11010–11017.

[6] S.M. Faruque, K. Biswas, S.M.N. Udden, Q.S. Ahmad, D.A. Sack, and G.B. Nair. Transmissibility of cholera: in vivo-formed biofilms and their relationship to infectivity and persistence in the environment. *Proc Natl Acad Sci U S A*, 103:6350–6355.

[7] A.T. Nielsen, N.A. Dolganov, G. Otto, M.C. Miller, C.Y. Wu, and G.K. Schoolnik. Rpos controls the *Vibrio cholerae* mucosal escape response. *PLoS Pathog*, 2:109.

[8] S.A. Mahmoud and P. Chien. Regulated proteolysis in bacteria. *Annu Rev Biochem*, 87:677–696.

[9] A.O. Olivares, T.A. Baker, and R.T. Sauer. Mechanistic insights into bacterial AAA+ proteases and protein-remodelling machines. *Nat Rev Microbiol*, 14:33–44.

[10] E. Gur, D. Biran, and E.Z. Ron. Regulated proteolysis in gram-negative bacteria — how and when? *Nat Rev Microbiol*, 9:839–848.

[11] K. Jonas, J. Liu, P. Chien, and M.T. Laub. Proteotoxic stress induces a cell-cycle arrest by stimulating Lon to degrade the replication initiator dnaa. *Cell*, 154:623–636.

[12] R.D. Zeinert, H. Baniasadi, B.P. Tu, and P. Chien. The Lon protease links nucleotide metabolism with proteotoxic stress. *Mol Cell*, 79:758–767 6.

[13] A. Rogers, L. Townsley, A.L. Gallego-Hernandez, S. Beyhan, L. Kwuan, and F.H. Yildiz. The LonA protease regulates biofilm formation, motility, virulence, and the type vi secretion system in *Vibrio cholerae*. *J Bacteriol*, 198:973–985.

[14] L. He, M.K.M. Nair, Y. Chen, X. Liu, M. Zhang, and K.R.O. Hazlett. The protease locus of *francisella tularensis* lvs is required for stress tolerance and infection in the mammalian host. *Infect Immun*, 84:1387–1402.

[15] K. Pressler, D. Vorkapic, S. Lichtenegger, G. Malli, B.P. Barilich, and F. Cakar. AAA+ proteases and their role in distinct stages along the *Vibrio cholerae* lifecycle. *Int J Med Microbiol*, 306:452–462.

[16] the Lon protease homologue LonA, not LonC, contributes to the stress tolerance and biofilm formation of *Actinobacillus pleuropneumoniae*.

[17] Elena BM Breidenstein, Laure Janot, Janine Strehmel, Lucia Fernandez, Patrick K Taylor, Irena Kukavica-Ibrulj, Shaan L Gellatly, Roger C Levesque, Joerg Overhage, and Robert EW Hancock. The Lon protease is essential for full virulence in *Pseudomonas aeruginosa*. *PloS one*, 7(11):e49123, 2012.

[18] Avatar Joshi, Benjamin Kostiuk, Andrew Rogers, Jennifer Teschler, Stefan Pukatzki, and Fitnat H Yildiz. Rules of engagement: the type vi secretion system in *Vibrio cholerae*. *Trends in microbiology*, 25(4):267–279, 2017.

[19] S. Pukatzki, A.T. Ma, D. Sturtevant, B. Krastins, D. Sarracino, and W.C. Nelson. Identification of a conserved bacterial protein secretion system in *Vibrio cholerae* using the *Dictyostelium* host model system. *Proc Natl Acad Sci*, 103:1528–1533.

[20] K.-J. Lee, Y.-C. Jung, S.-J. Park, and K.-H. Lee. Role of heat shock proteases in quorum-sensing-mediated regulation of biofilm formation by vibrio species. *mBio*, 9:02086–17.

[21] A. Joshi, S.A. Mahmoud, S.-K. Kim, J.L. Ogdahl, V.T. Lee, and P. Chien. c-di-gmp inhibits LonA-dependent proteolysis of TfoY in *Vibrio cholerae*. *PLOS Genet*, 16:1008897.

[22] N. Puri and A.W. Karzai. Hspq functions as a unique specificity-enhancing factor for the AAA+ Lon protease. *Mol Cell*, 66:672–683 4.

[23] X. Zhou, D. Teper, M.O. Andrade, T. Zhang, S. Chen, and W.-Y. Song. A phosphorylation switch on Lon protease regulates bacterial type iii secretion system in host. *mBio*, 9:02146–17.

[24] A. Joshi, B. Kostiuk, A. Rogers, J. Teschler, S. Pukatzki, and F.H. Yildiz. Rules of engagement: The type vi secretion system in *Vibrio cholerae*. *Trends Microbiol*, 25:267–279.

[25] D. Zamorano-Sánchez, J.C.N. Fong, S. Kilic, I. Erill, and F.H. Yildiz. Identification and characterization of vpsr and vpst binding sites in *Vibrio cholerae*. *J Bacteriol*, 197:1221–1235.

[26] Mu Ya Liu, Honghui Yang, and Tony Romeo. The product of the pleiotropic *Escherichia coli* gene csrA modulates glycogen biosynthesis via effects on mRNA stability. *Journal of bacteriology*, 177(10):2663–2672, 1995.

[27] Nara Figueroa-Bossi, Annie Schwartz, Benoit Guillemardet, François D'Heygère, Lionello Bossi, and Marc Boudvillain. Rna remodeling by bacterial global regulator csrA promotes rho-dependent transcription termination. *Genes & development*, 28(11):1239–1251, 2014.

[28] Archana Pannuri, Helen Yakhnin, Christopher A Vakulskas, Adrianne N Edwards, Paul Babitzke, and Tony Romeo. Translational repression of nhar, a novel pathway for multi-tier regulation of biofilm circuitry by csrA. *Journal of bacteriology*, 194(1):79–89, 2012.

[29] Laura M Patterson-Fortin, Christopher A Vakulskas, Helen Yakhnin, Paul Babitzke, and Tony Romeo. Dual posttranscriptional regulation via a cofactor-responsive mRNA leader. *Journal of molecular biology*, 425(19):3662–3677, 2013.

[30] H.A. Butz, A.R. Mey, A.L. Ciosek, A.A. Crofts, B.W. Davies, and S.M. Payne. Regulatory effects of csrA in *Vibrio cholerae*. *mBio*, 12:03380–20.

[31] K.A. Syed, S. Beyhan, N. Correa, J. Queen, J. Liu, and F. Peng. The *Vibrio*

cholerae flagellar regulatory hierarchy controls expression of virulence factors. *J Bacteriol*, 191:6555–6570.

[32] S. Chakraborty, M. Biswas, S. Dey, S. Agarwal, T. Chakrabortty, and B. Ghosh. The heptameric structure of the flagellar regulatory protein flrc is indispensable for atpase activity and disassembled by cyclic-di-GMP. *J Biol Chem*, 295:16960–16974.

[33] D. Srivastava, M.-L. Hsieh, A. Khataokar, M.B. Neiditch, and C.M. Waters. Cyclic di-GMP inhibits *Vibrio cholerae* motility by repressing induction of transcription and inducing extracellular polysaccharide production. *Mol Microbiol*, 90:1262–1276.

[34] T. Ramamurthy, R.K. Nandy, A.K. Mukhopadhyay, S. Dutta, A. Mutreja, and K. Okamoto. Virulence regulation and innate host response in the pathogenicity of *Vibrio cholerae*. *Front Cell Infect Microbiol*, 10:520.

[35] K.D. Everiss, K.J. Hughes, M.E. Kovach, and K.M. Peterson. The *Vibrio cholerae* acfB colonization determinant encodes an inner membrane protein that is related to a family of signal-transducing proteins. *Infect Immun*, 62:3289–3298.

[36] R.L. Szabady, J.H. Yanta, D.K. Halladin, M.J. Schofield, and R.A. Welch. Taga is a secreted protease of *Vibrio cholerae* that specifically cleaves mucin glycoproteins. *Microbiology*, 157:516–525.

[37] A. Kumar, B. Das, and N. Kumar. Vibrio pathogenicity island-1: The master determinant of cholera pathogenesis. *Front Cell Infect Microbiol*, 10:561296.

[38] D.K.R. Karaolis, J.A. Johnson, C.C. Bailey, E.C. Boedeker, J.B. Kaper, and P.R.

Reeves. A *Vibrio cholerae* pathogenicity island associated with epidemic and pandemic strains. *Proc Natl Acad Sci U S A*, 95:3134–3139.

[39] E.S. Krukonis, R.R. Yu, and V.J. DiRita. The *Vibrio cholerae* ToxR/TcpP/ToxT virulence cascade: distinct roles for two membrane-localized transcriptional activators on a single promoter. *Mol Microbiol*, 38:67–84.

[40] V.J. DiRita, C. Parsot, G. Jander, and J.J. Mekalanos. Regulatory cascade controls virulence in *Vibrio cholerae*. *Proc Natl Acad Sci U S A*, 88:5403–5407.

[41] A. Hsiao and J. Zhu. Pathogenicity and virulence regulation of *Vibrio cholerae* at the interface of host-gut microbiome interactions. *Virulence*, 11:1582–1599.

[42] G.G. Weber, K.E. Klose, and Klose. The complexity of ToxT-dependent transcription in *Vibrio cholerae*. *Indian J Med Res*, 133:201–206.

[43] Wei Lin, Gabriela Kovacikova, and Karen Skorupski. The quorum sensing regulator hapr downregulates the expression of the virulence gene transcription factor apha in *Vibrio cholerae* by antagonizing lrp-and vpsr-mediated activation. *Molecular microbiology*, 64(4):953–967, 2007.

[44] Zhi Liu, Tim Miyashiro, Amy Tsou, Ansel Hsiao, Mark Goulian, and Jun Zhu. Mucosal penetration primes *Vibrio cholerae* for host colonization by repressing quorum sensing. *Proceedings of the National Academy of Sciences*, 105(28):9769–9774, 2008.

[45] M.J. Lowden, K. Skorupski, M. Pellegrini, M.G. Chiorazzo, R.K. Taylor, and F.J.

Kull. Structure of *Vibrio cholerae* toxt reveals a mechanism for fatty acid regulation of virulence genes. *Proc Natl Acad Sci U S A*, 107:2860–2865.

[46] G. Kovacikova, W. Lin, R.K. Taylor, and K. Skorupski. The fatty acid regulator fadr influences the expression of the virulence cascade in the el tor biotype of *Vibrio cholerae* by modulating the levels of ToxT via two different mechanisms. *DiRita VJ, editor. J Bacteriol*, 199:00762–16, 00762–16.

[47] Y. Fujita, H. Matsuoka, and K. Hirooka. Regulation of fatty acid metabolism in bacteria. *Mol Microbiol*, 66:829–839.

[48] Cronan JE, Jr and Subrahmanyam S. Fadr, transcriptional co-ordination of metabolic expediency. *Mol Microbiol*, 29:937–943.

[49] G.B. Severin, M.S. Ramliden, L.A. Hawver, K. Wang, M.E. Pell, and A.-K. Kieninger. Direct activation of a phospholipase by cyclic GMP-AMP in el tor *Vibrio cholerae*. *Proc Natl Acad Sci*, 115:6048– 6055.

[50] B.W. Davies, R.W. Bogard, T.S. Young, and J.J. Mekalanos. Coordinated regulation of accessory genetic elements produces cyclic di-nucleotides for *V. cholerae* virulence. *Cell*, 149:358–370.

[51] T.P.A. Devasagayam, S. Steenken, M.S.W. Obendorf, W.A. Schulz, and H. Sies. Formation of 8-hydroxy(deoxy)guanosine and generation of strand breaks at guanine residues in dna by singlet oxygen. *Biochemistry*, 30:6283–6289.

[52] S. Steenken and S.V. Jovanovic. How easily oxidizable is dna? one-electron reduction potentials of adenosine and guanosine radicals in aqueous solution. *J Am Chem Soc*, 119:617–618.

[53] E. Cabiscol, J. Tamarit, and J. Ros. Oxidative stress in bacteria and protein damage by reactive oxygen species. *Int Microbiol Off J Span Soc Microbiol*, 3:3–8.

[54] M. Zhu and X. Dai. Maintenance of translational elongation rate underlies the survival of *Escherichia coli* during oxidative stress. *Nucleic Acids Res*, 47:7592–7604.

[55] D. Reichmann, W. Voth, and U. Jakob. Maintaining a healthy proteome during oxidative stress. *Mol Cell*, 69:203–213.

[56] J.-U. Dahl, M.J. Gray, and U. Jakob. Protein quality control under oxidative stress conditions. *J Mol Biol*, 427:1549–1563.

[57] P. Kirthika, A. Senevirathne, V. Jawalagatti, S. Park, and J.H. Lee. Deletion of the lon gene augments expression of *Salmonella* pathogenicity island (spi)-1 and metal ion uptake genes leading to the accumulation of bactericidal hydroxyl radicals and host pro-inflammatory cytokine-mediated rapid intracellular clearance. *Gut Microbes*, 11:1695–1712.

[58] Hui Wang, Nawar Naseer, Yaran Chen, Anthony Y Zhu, Xuewen Kuai, Nirupa Galagedera, Zhi Liu, and Jun Zhu. Oxyr2 modulates OxyR1 activity and *Vibrio cholerae* oxidative stress response. *Infection and immunity*, 85(4):e00929–16, 2017.

[59] Xiaoyun Xia, Jessie Larios-Valencia, Zhi Liu, Fu Xiang, Biao Kan, Hui Wang,

and Jun Zhu. Oxyr-activated expression of dps is important for *Vibrio cholerae* oxidative stress resistance and pathogenesis. *PloS one*, 12(2):e0171201, 2017.

[60] Soisig Steunou Anne, Babot Marion, Bourbon Marie-Line, Tambosi Reem, Durand Anne, Liotenberg Sylviane, Krieger-Liszkay Anja, Yamaichi Yoshiharu, and Ouchane Soufian. Additive effects of metal excess and superoxide, a highly toxic mixture in bacteria. *Microbial biotechnology*.

[61] Cheolju Lee, Soon Mi Lee, Partha Mukhopadhyay, Seung Jun Kim, Sang Chul Lee, Woo-Sung Ahn, Myeong-Hee Yu, Gisela Storz, and Seong Eon Ryu. Redox regulation of OxyR requires specific disulfide bond formation involving a rapid kinetic reaction path. *Nature structural & molecular biology*, 11(12):1179–1185, 2004.

[62] Haike Antelmann and John D Helmann. Thiol-based redox switches and gene regulation. *Antioxidants & redox signaling*, 14(6):1049–1063, 2011.

[63] Bruce Demple. Redox signaling and gene control in the *Escherichia coli* soxrs oxidative stress regulon—a review. *Gene*, 179(1):53–57, 1996.

[64] Hui Wang, Shusu Chen, Juan Zhang, Francesca P Rothenbacher, Tiantian Jiang, Biao Kan, Zengtao Zhong, and Jun Zhu. Catalases promote resistance of oxidative stress in *Vibrio cholerae*. *PloS one*, 7(12):e53383, 2012.

[65] Jacquin C Niles, John S Wishnok, and Steven R Tannenbaum. A novel nitroimidazole compound formed during the reaction of peroxynitrite with 2 ‘, 3 ‘, 5 ‘-tri-o-

acetyl-guanosine. *Journal of the American Chemical Society*, 123(49):12147–12151, 2001.

[66] Jacquin C Niles, John S Wishnok, and Steven R Tannenbaum. Peroxynitrite-induced oxidation and nitration products of guanine and 8-oxoguanine: structures and mechanisms of product formation. *Nitric Oxide*, 14(2):109–121, 2006.

[67] Andrew M Stern, Amanda J Hay, Zhi Liu, Fiona A Desland, Juan Zhang, Zengtao Zhong, and Jun Zhu. The norr regulon is critical for *Vibrio cholerae* resistance to nitric oxide and sustained colonization of the intestines. *MBio*, 3(2):e00013–12, 2012.

[68] NP Tucker, B D'autreaux, S Spiro, and R Dixon. Mechanism of transcriptional regulation by the *Escherichia coli* nitric oxide sensor NorR. *Biochemical Society Transactions*, 34(1):191–194, 2006.

[69] Patrícia N da Costa, Miguel Teixeira, and Lígia M Saraiva. Regulation of the flavorubredoxin nitric oxide reductase gene in *Escherichia coli*: nitrate repression, nitrite induction, and possible post-transcription control. *FEMS microbiology letters*, 218(2):385–393, 2003.

[70] Matthew I Hutchings, Neeraj Mandhana, and Stephen Spiro. The norr protein of *Escherichia coli* activates expression of the flavorubredoxin gene *norV* in response to reactive nitrogen species. *Journal of Bacteriology*, 184(16):4640–4643, 2002.

[71] Seung-Joo Lee, Rou-Jia Sung, and Gregory L Verdine. Mechanism of dna lesion

homing and recognition by the uvr nucleotide excision repair system. *Research*, 2019, 2019.

[72] Christian J Rudolph, Amy L Upton, and Robert G Lloyd. Replication fork stalling and cell cycle arrest in uv-irradiated *Escherichia coli*. *Genes & development*, 21(6):668–681, 2007.

[73] Saeko Mizusawa and Susan Gottesman. Protein degradation in *Escherichia coli*: the *lon* gene controls the stability of sula protein. *Proceedings of the National Academy of Sciences*, 80(2):358–362, 1983.

[74] Mark Itsko and Roel M Schaaper. dGTP starvation in *Escherichia coli* provides new insights into the thymineless-death phenomenon. *PLoS genetics*, 10(5):e1004310, 2014.

[75] A. Aiba and K. Mizobuchi. Nucleotide sequence analysis of genes *purH* and *purD* involved in the de novo purine nucleotide biosynthesis of *Escherichia coli**. *J Biol Chem*, 264:21239–21246.

[76] NANCY B RAY and CHRISTOPHER K MATHEWS. Nucleoside diphosphokinase: a functional link between intermediary metabolism and nucleic acid synthesis. *Current topics in cellular regulation*, 33:343–357, 1992.

[77] Ioan Lascu and Philippe Gonin. The catalytic mechanism of nucleoside diphosphate kinases. *Journal of bioenergetics and biomembranes*, 32(3):237–246, 2000.

[78] P. Agnihotri, A.K. Shakya, A.K. Mishra, and J.V. Pratap. Crystal structure and

characterization of nucleoside diphosphate kinase from *Vibrio cholerae*. *Biochimie*, 190:57–69.

[79] Ioan Lascu, Solange Moréra, Mohammed Chiadmi, Jacqueline Cherfils, Joël Janin, and Michel Véron. Mechanism of the nucleoside diphosphate kinase reaction: X-ray structure of the phosphohistidine intermediate. In *Techniques in Protein Chemistry*, volume 7, pages 209–217. Elsevier, 1996.

[80] S. Langklotz and F. Narberhaus. The *Escherichia coli* replication inhibitor cspd is subject to growth-regulated degradation by the Lon protease. *Mol Microbiol*, 80:1313–1325.

[81] Milena Jaskólska and Kenn Gerdes. CRP-dependent positive autoregulation and proteolytic degradation regulate competence activator Sxy of *Escherichia coli*. *Molecular Microbiology*, 95(5):833–845, 2015.

[82] C. Barembruch and R. Hengge. Cellular levels and activity of the flagellar sigma factor flia of *Escherichia coli* are controlled by flgm-modulated proteolysis. *Mol Microbiol*, 65:76–89.

[83] M.L. Wohlever, A.R. Nager, T.A. Baker, and R.T. Sauer. Engineering fluorescent protein substrates for the AAA+ Lon protease. *Protein Eng Des Sel PEDS*, 26:299–305.

[84] Alexandra R Mey, Elizabeth E Wyckoff, Vanamala Kanukurthy, Carolyn R Fisher,

and Shelley M Payne. Iron and fur regulation in *Vibrio cholerae* and the role of fur in virulence. *Infection and immunity*, 73(12):8167–8178, 2005.

[85] HEATHER N Yeowell and JAMES R White. Iron requirement in the bactericidal mechanism of streptonigrin. *Antimicrobial agents and chemotherapy*, 22(6):961–968, 1982.

[86] Evelyne Krin, Sebastian Aguilar Pierlé, Odile Sismeiro, Bernd Jagla, Marie-Agnès Dillies, Hugo Varet, Oihane Irazoki, Susana Campoy, Zoé Rouy, Stéphane Cruveiller, et al. Expansion of the sos regulon of *Vibrio cholerae* through extensive transcriptome analysis and experimental validation. *BMC genomics*, 19(1):1–18, 2018.

[87] Hideshi Ihara, Tomohiro Sawa, Yusaku Nakabeppu, and Takaaki Akaike. Nucleotides function as endogenous chemical sensors for oxidative stress signaling. *Journal of clinical biochemistry and nutrition*, 48(1):33–39, 2010.

Chapter 4

Future Perspectives

4.1 Introduction

Lon was first identified in the 1960s as a regulator of capsule biosynthesis (cps) in *E. coli* [1]. Due to Lon's ability to bind DNA and its function as a repressor of *cps* operon transcription, it was thought that Lon acted as a DNA binding transcriptional repressor [2, 3]. It wasn't until the 1980s when it was finally recognized that Lon was, in fact, an ATP-dependent protease [2, 4, 5]. Since then, Lon has been identified as a key regulator of protein quality control and diverse cellular processes in archaea, bacteria, as well as in the mitochondria of eukaryotic cells. Lon's conservation across all domains of life alludes to its biological importance. Despite nearly 60 years of research, the substrates of Lon and the mechanisms that dictate Lon proteolysis remain poorly understood. For example, it is known that Lon proteolysis is highly regulated and is influenced by accessory factors or small signaling molecules that alter substrate acquisition

or proteolytic rate, however, only two known Lon adaptors have been identified [6, 7]. Furthermore, while Lon has been shown to respond to diverse signaling molecules *in vitro*, little is known regarding their relevance *in vivo* [8]. Finally, most work performed on prokaryotic Lon has been confined to *E. coli* and thus, relatively little is known regarding the mechanisms and consequences of Lon proteolysis in bacterial pathogens. The focus of my research was to address key knowledge gaps regarding Lon proteolysis in the bacterial pathogen *Vibrio cholerae*.

Previous work performed by the Yildiz lab identified Lon as a regulator of processes important for *V. cholerae*'s infectious cycle [9]. This work found that deletion of *lon* results in a severe colonization defect in the infant mouse model [10]. In addition, Lon regulates virulence factor production, biofilm formation, T6SS-dependent killing, cell division, and c-di-GMP pools [10, 11]. It was later determined that Lon targets the alternative sigma factor FliA as well as the transcriptonal regulator HapR [12, 13]. Lon proteolysis of FliA regulates flagellar assembly and virulence factor gene expression [12]. In addition, Lon proteolysis of HapR was found to induce biofilm formation [13]. However, proteolysis of both substrates is highly condition dependent. Lon only proteolyzes FliA during flagellar breakage; a condition that permits the secretion of the Lon anti-adaptor, FlgM, out of the cell [12, 14]. Furthermore, Lon only proteolyzes HapR during heat shock [15]. Since proteolysis is irreversible, condition dependent proteolysis of FliA and HapR is consistent with idea that proteolysis must be tightly regulated. However, since Lon is capable of regulating motility, virulence factor production, and biofilm formation in the absence of flagellar breakage and heat shock, it suggests that

Lon regulates other targets as well [9, 12, 15].

To better understand Lon-dependent regulation in *V. cholerae*, we used whole proteome analysis to identify potential Lon targets that might explain Δ*lon*'s associated phenotypes (Chapter 2). We identified TfoY as a Lon substrate and showed that Lon-dependent proteolysis of TfoY represses T6SS-dependent killing and motility. In addition, we used a combination of genetic and biochemical approaches to demonstrate that Lon binds to c-di-GMP and that c-di-GMP inhibits Lon-dependent proteolysis of TfoY. This work identified a new substrate of the *V. cholerae* Lon protease and also provided the first *in vivo* evidence that Lon activity is regulated by c-di-GMP [16].

Since most analyses on Lon have focused on Lon-dependent regulation in planktonic grown cells, relatively little is known regarding how Lon regulates processes important for biofilm formation. We performed whole proteome and whole transcriptome analyses on WT and Δ*lon* biofilms to identify potential Lon substrates and Lon-regulated pathways in biofilms (Chapter 3). Our analyses indicates that Lon is an important regulator of biofilm matrix production, virulence factor production, nucleotide pool homeostasis, iron homeostasis, and DNA repair pathways during the biofilm growth mode. In addition, we provide evidence that PurH and CspD are Lon targets and that PurH, NDK, and CspD function in mitigating genotoxic stress in Lon-deficient mutants. The work outlined here provides valuable insights into how regulated proteolysis functions to regulate processes important for *V. cholerae* environmental and host fitness. It also identifies proteins that may be targeted by Lon.

4.1.1 Future Directions

While the work documented here identifies important aspects of Lon-dependent regulation in *V. cholerae* there are still many questions that remain unanswered. For example, we demonstrated that c-di-GMP inhibits Lon-dependent proteolysis of TfoY *in vivo* and also limits Lon proteolysis of casein *in vitro*, however, it remains unclear exactly how c-di-GMP inhibits Lon activity. Lon is a member of the AAA+ superfamily of ATPases and many of these enzymes have been found to be c-di-GMP receptors. Existing work suggests that the c-di-GMP binding motifs of these proteins are diverse, however, a common trend is that c-di-GMP binds to the ATPase domain and influences protein functionality without directly interfering with ATPase activity. Consistent with this, c-di-GMP inhibited Lon proteolysis of casein *in vitro* without altering Lon's ATPase activity. It is also interesting to mention that Lon's ATPase domain was found to be important in its DNA binding ability. DNA binding also influences Lon activity. Thus, it's interesting to speculate that c-di-GMP and DNA may compete for the same motif and that this binding influences substrate selectivity.

In addition, it is unclear if c-di-GMP functions to inhibit proteolysis of other Lon targets or if c-di-GMP might instead regulate Lon substrate selectivity. We identified TfoY, PurH, and CspD as Lon targets in *V. cholerae*, though *in vitro* studies are required to determine if this occurs directly or is influenced by adaptors, anti-adaptors, or signaling molecules. Future studies should use a combination of *in vivo* and *in vitro* approaches to determine whether or not c-di-GMP influences Lon proteolysis of these

proteins, as well as HapR and FliA. To begin addressing this question, we took an unbiased approach to identify putative Lon targets that are regulated by c-di-GMP levels. We used whole proteome analysis to determine how protein steady state levels change in strains that overproduce c-di-GMP relative to those that don't in WT and Δlon strains. This work, however, was too preliminary to be included in this document. However, it does lay a foundation for future identification of Lon substrates and those that may be regulated by c-di-GMP.

Additional analysis is also needed to establish the role of PurH, NDK, and CspD on Lon biofilm phenotypes. Since a role for these proteins in biofilm formation has not been explored in *V. cholerae*, an assessment of their impact at different stages of biofilm development would be informative. Furthermore, it is unclear if they influence *V. cholerae* virulence factor production or what role they may play in *V. cholerae* host colonization. PurH, NDK, and CspD appear to protect Lon-deficient mutants from genotoxic stress caused by streptonigrin. Many enzymes involved in stress response pathways have been shown to enhance *V. cholerae* host fitness, thus it is possible that these proteins may also be important. Finally, future studies can address what types of stressors these proteins respond to and the mechanisms that govern these protective phenotypes.

Bibliography

[1] Alvin Markovitz. Regulatory mechanisms for synthesis of capsular polysaccharide in mucoid mutants of escherichia coli k12. *Proceedings of the National Academy of Sciences of the United States of America*, 51(2):239, 1964.

[2] KH Sreedhara Swamy and Alfred L Goldberg. E. coli contains eight soluble proteolytic activities, one being atp dependent. *Nature*, 292(5824):652–654, 1981.

[3] Barbara A Zehnbauer, Edward C Foley, Gordon W Henderson, and Alvin Markovitz. Identification and purification of the lon+ (capr+) gene product, a dna-binding protein. *Proceedings of the National Academy of Sciences*, 78(4):2043–2047, 1981.

[4] Chin Ha Chung and Alfred L Goldberg. The product of the lon (capr) gene in escherichia coli is the atp-dependent protease, protease la. *Proceedings of the National Academy of Sciences*, 78(8):4931–4935, 1981.

[5] Chin Ha Chung and Alfred L Goldberg. DNA stimulates ATP-dependent proteolysis and protein-dependent ATPase activity of protease La from *Escherichia coli*. *Proceedings of the National Academy of Sciences*, 79(3):795–799, 1982.

[6] Sampriti Mukherjee, Anna C Bree, Jing Liu, Joyce E Patrick, Peter Chien, and Daniel B Kearns. Adaptor-mediated Lon proteolysis restricts *Bacillus subtilis* hyperflagellation. *Proceedings of the National Academy of Sciences*, 112(1):250–255, 2015.

[7] Neha Puri and A Wali Karzai. Hspq functions as a unique specificity-enhancing factor for the AAA+ Lon protease. *Molecular cell*, 66(5):672–683, 2017.

[8] Devon O Osbourne, Valerie WC Soo, Igor Konieczny, and Thomas K Wood. Polyphosphate, cyclic AMP, guanosine tetraphosphate, and c-di-GMP reduce *in vitro* Lon activity. *Bioengineered*, 5(4):264–268, 2014.

[9] A. Rogers, L. Townsley, A.L. Gallego-Hernandez, S. Beyhan, L. Kwuan, and F.H. Yildiz. The LonA protease regulates biofilm formation, motility, virulence, and the type vi secretion system in *Vibrio cholerae*. *J Bacteriol*, 198:973–985.

[10] Andrew Rogers, Loni Townsley, Ana L Gallego-Hernandez, Sinem Beyhan, Laura Kwuan, and Fitnat H Yildiz. The LonA protease regulates biofilm formation, motility, virulence, and the type vi secretion system in *Vibrio cholerae*. *Journal of bacteriology*, 198(6):973–985, 2016.

[11] Katharina Pressler, Dina Vorkapic, Sabine Lichtenegger, Gerald Malli, Benjamin P Barilich, Fatih Cakar, Franz G Zingl, Joachim Reidl, and Stefan Schild. AAA+ proteases and their role in distinct stages along the *Vibrio cholerae* lifecycle. *International Journal of Medical Microbiology*, 306(6):452–462, 2016.

[12] K. Pressler, D. Vorkapic, S. Lichtenegger, G. Malli, B.P. Barilich, and F. Cakar. AAA+ proteases and their role in distinct stages along the *Vibrio cholerae* lifecycle. *Int J Med Microbiol*, 306:452–462.

[13] Kyung-Jo Lee, You-Chul Jung, Soon-Jung Park, and Kyu-Ho Lee. Role of heat

shock proteases in quorum-sensing-mediated regulation of biofilm formation by Vibrio species. *Mbio*, 9(1), 2018.

[14] C. Barembruch and R. Hengge. Cellular levels and activity of the flagellar sigma factor flia of *Escherichia coli* are controlled by flgm-modulated proteolysis. *Mol Microbiol*, 65:76–89.

[15] K.-J. Lee, Y.-C. Jung, S.-J. Park, and K.-H. Lee. Role of heat shock proteases in quorum-sensing-mediated regulation of biofilm formation by vibrio species. *mBio*, 9:02086–17.

[16] A. Joshi, S.A. Mahmoud, S.-K. Kim, J.L. Ogdahl, V.T. Lee, and P. Chien. c-di-gmp inhibits LonA-dependent proteolysis of TfoY in *Vibrio cholerae*. *PLOS Genet*, 16:1008897.

Appendix A

Chapter 2 Supporting Material

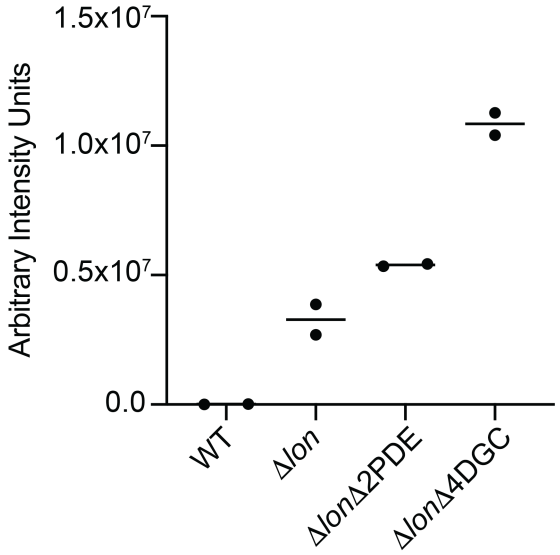

Figure A.1: Levels of TfoY are elevated in the Δ*lonA*Δ2PDE and lonAΔ4DGC strains relative to Δ*lonA*. Semiquantitative densitometric analysis from western blots shown in Fig 5B. Levels of TfoY from WT, Δ*lonA*, Δ*lonA*Δ2PDE, and Δ*lonA*Δ4DGC mutants were analyzed using Image Lab. Shown are the arbitrary intensity values from two independent biological replicates.

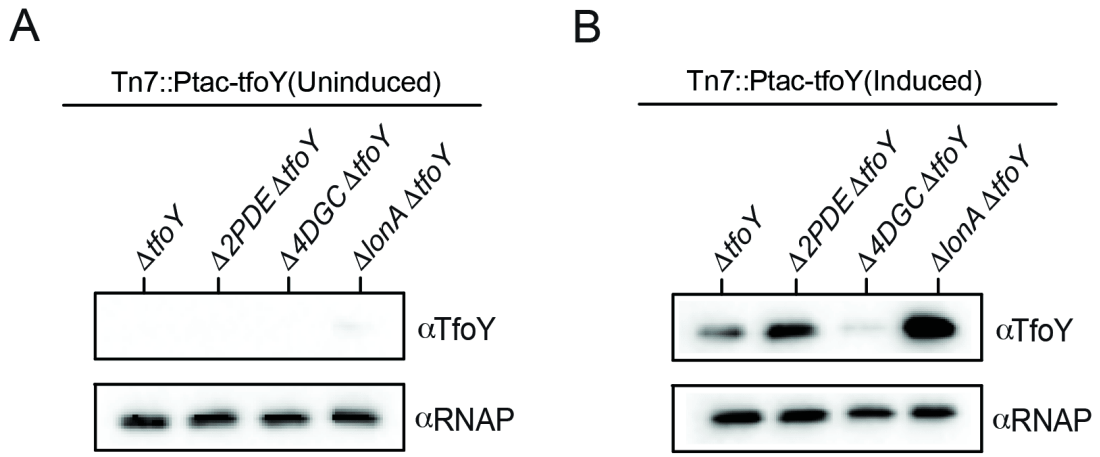

Figure A.2: *In vivo* abundance of TfoY was analyzed in Δ*tfoY*, Δ*tfoY*Δ2PDE, and Δ*tfoY*Δ4DGC mutant strains before mixing V. cholerae with E. coli in the T6SS-dependent killing experiment described in Fig 5H. (A) Cells were either grown in the absence of IPTG (-) or (B) in the presence of IPTG (+) to overexpress *tfoY* from the Ptac promoter. Levels of TfoY were analyzed by western blot using the TfoY antibody. RNAP was used as a control for sample loading in all western blots.

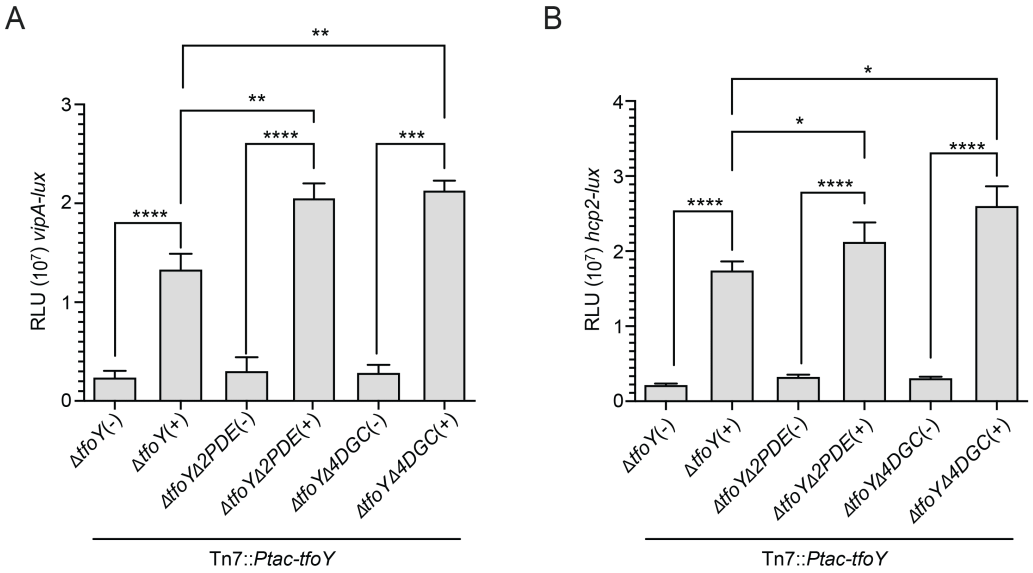

Figure A.3: The impact of TfoY on T6SS gene expression phenotypes was assessed in Δ*tfoY*, Δ*tfoY*Δ2PDE, and Δ*tfoY*Δ4DGC strains harboring T6SS gene transcriptional reporters for either the (A) regulatory region upstream of vipA or (B) the regulatory region upstream of *hcp*2. Cells were either grown in the absence of IPTG (-) or in the presence of IPTG (+) to overexpress *tfoY* from the Ptac promoter. Bioluminescence was assessed at late exponential phase. Statistical analysis was performed using an unpaired Student's t-test. Statistical values indicated are (*p<0.05, **p<0.01, and ****p<0.0001).

Table A.1: Proteins enriched in $\Delta lonA$ relative to WT. A Student's t-test using a Benjamini-Hochberg FDR cutoff of 5% was used to identify proteins that were differentially expressed.

Gene	Description	Fold Change (log2)
VC1722	T6SS and motility regulator; TfoY	4.289727879
VC0049	hypothetical protein	1.289696121
VCA0422	hypothetical protein	0.922209424
VCA1069	methyl-accepting chemotaxis protein	0.783467412
VCA0540	formate transporter 1, putative	0.693574789
VCA0349;VCA0504	relB protein	0.688476652
VC0018	16 kDa heat shock protein A	0.66216644
VCA0107	T6SS outer tube; vipA	0.646651164
VC2240	decarboxylase	0.641421098
VCA0271	hypothetical protein	0.607169032
VCA0933	cold shock domain-contain protein; cspV	0.580625454
VC0715	nitroreductase A	0.570175745
VCA0281	integrase, putative	0.568173608
VCA0248	putative L-ascorbate 6-phosphate lactonase	0.544823691
VC2296	bolA protein	0.509163114
VC0092	LexA repressor	0.508418256
VC2735	hypothetical protein	0.500998747
VC2664	chaperonin GroEL	0.455176759
VC2675	ATP-dependent protease peptidase subunit; HslV	0.443346247
VC0945	hypothetical protein	0.437054759
VCA0752	thioredoxin 2	0.410689113
VCA0020	T6SS pore forming cargo effector; vasX	0.385393411
VC2674	ATP-dependent protease ATP-binding subunit; HslU	0.382376111
VC1585	catalase	0.378509766
VC0985	heat shock protein 90	0.372646378
VC1373	DnaK-related protein	0.368682857
VCA1060	3,4-dihydroxy-2-butanone 4-phosphate synthase ribB	0.362447606
VCA0386;VCA0312	parD3 and parD1 antitoxin hypothetical protein	0.362062904
VCA0116	T6SS recycling protease; clpV	0.361890930
VCA0291	site-specific recombinase IntI4	0.358570534
VCA0112	T6SS hypothetical protein; predicted membrane complex; vasC	0.356863976
VC0856	dnaJ protein	0.328421535
VC2197	flagellar hook protein; FlgE	0.326331303
VC0711	clpB protein	0.309919798
VC0276	bifunctional phosphoribosylaminoimidazolecarboxamide formyltransferase/IMP cyclohydrolase purH	0.307131082
VCA0197	guanosine 5'-monophosphate oxidoreductase	0.305691639
VCA0114	T6SS membrane complex protein; vasD	0.304550272
VCA0110	T6SS baseplate protein; vasA	0.294662915
VC0188	oligopeptidase A	0.285309334
VC0854	heat shock protein; GrpE	0.273338759
VC0424	hypothetical protein	0.261236140
VC0556	glutamate--cysteine ligase	0.259535497

Table A.1 Continued: Proteins enriched in $\Delta lonA$ relative to WT.

VC0052	phosphoribosylaminoimidazole carboxylase catalytic subunit	0.258014281
VC0855	molecular chaperone DnaK	0.253726052
VC0342	iron-sulfur cluster-binding protein	0.232818107
VC0477	phosphoglycerate kinase pgk	0.232540797
VC2044	hypothetical protein	0.215146647
VC2389	carbamoyl phosphate synthase large subunit carB	0.209713917
VCA0005	hypothetical protein	0.208643919
VC1077	hypothetical protein	0.207402191
VC0275	phosphoribosylamine--glycine ligase	0.203069308
VCA0120	T6SS membrane complex protein; vasK	0.202494032
VC0051	phosphoribosylaminoimidazole carboxylase ATPase subunit	0.194501306
VC0543	recombinase A	0.193190268
VCA0637	dihydropteridine reductase	0.188420276
VC1483	3-hydroxydecanoyl-(acyl carrier protein) dehydratase	0.185845292
VC0186	glutathione reductase	0.177990329
VC0374	glucose-6-phosphate isomerase; pgi	0.177020508
VC2751	adenosine deaminase	0.176349793
VC2670	triosephosphate isomerase; tpiA	0.171415676
VC2394	preprotein translocase subunit; SecA	0.144433991
VC2775	tRNA uridine 5-carboxymethylaminomethyl modification enzyme; GidA	0.140049843
VC2764	F0F1 ATP synthase subunit beta	0.137417904
VC2720	putative DNA uptake protein	0.137019093
VCA0013	maltodextrin phosphorylase	0.133502567
glyA	serine hydroxymethyltransferase	0.130214809
ispH	4-hydroxy-3-methylbut-2-enyl diphosphate reductase	0.129959770
VC0394	excinuclease ABC subunit A ; uvrA	0.123902710
VC0521	O-sialoglycoprotein endopeptidase; gcp	0.117857361
VC0223	ADP-heptose--LPS heptosyltransferase II, putative	0.117303348
VC2766	F0F1 ATP synthase subunit alpha	0.112933807
VC2716	hypothetical protein	0.108732759
VC2660	elongation factor P	0.104389852
VC1000	acetyl-CoA carboxylase subunit beta	0.099589657
VC0695	phospho-2-dehydro-3-deoxyheptonate aldolase	0.098998883
VC2623	tryptophanyl-tRNA synthetase	0.098328265
VC0108	DNA polymerase I	0.096278320
VC0451	hypothetical protein	0.093923081
VC0190	DNA-dependent helicase II; uvrD	0.088613892
VC2765	F0F1 ATP synthase subunit gamma	0.080352199

Table A.2: Proteins enriched in WT relative to Δ*lonA*. A Student's t-test using a Benjamini-Hochberg FDR cutoff of 5% was used to identify proteins that were differentially expressed.

Gene	Description	Fold Change (log2)
VC1920	ATP-dependent protease LA; LonA	2.621082664
VC0620	peptide ABC transporter, periplasmic peptide-binding protein	0.77313396
VC1403	methyl-accepting chemotaxis protein	0.616571678
VC1523	hypothetical protein	0.588189086
VC1622	outer membrane protein, putative	0.580670401
VCA0697	sensory box/GGDEF family protein; cdgD	0.542207244
VC1621	agglutination protein	0.498378366
VC1441	cytochrome c oxidase, subunit CcoO	0.478708832
VC1424	spermidine/putrescine ABC transporter, periplasmic spermidine/putrescine-binding protein	0.409029135
VCA0849	hypothetical protein	0.400282145
VCA0405	hypothetical protein	0.397481483
VC1692	trimethylamine-N-oxide reductase	0.37527705
VCA0205	anaerobic C4-dicarboxylate transporter	0.365745926
VC2217	beta-N-acetylhexosaminidase	0.362460785
VC0490	hypothetical protein	0.342823848
VC1425	spermidine/putrescine ABC transporter, periplasmic spermidine/putrescine-binding protein	0.340334343
VC0538	thiosulfate ABC transporter, periplasmic thiosulfate-binding protein	0.300140437
VC0907	DL-methionine transporter ATP-binding subunit	0.291273999
VCA0807	ABC transporter, periplasmic substrate-binding protein	0.283885768
VC1844	cytochrome d ubiquinol oxidase, subunit I	0.266298023
VCA1043	tagE protein	0.260448366
VC2051	thiol:disulfide interchange protein DsbE	0.249364711
VC0156	vitamin B12 receptor	0.248729424
VC2259	sulfate adenylyltransferase subunit 1	0.22870666
VC2213	outer membrane protein OmpA	0.213343266
VCA0585	glutathione S-transferase, putative	0.212515607
VC1170	tryptophan synthase subunit beta	0.208670749

Table A.2 Continued: Proteins enriched in $\Delta lonA$ relative to WT. Continued.

VC1680	peptide ABC transporter, periplasmic peptide-binding protein	0.201142681
VC0927	UDP-N-acetyl-D-mannosamine transferase	0.188408013
VC1414	thermostable carboxypeptidase 1	0.171369224
VCA0998	Oye family NADH-dependent flavin oxidoreductase	0.16395781
VC0918	UDP-N-acetyl-D-mannosamine dehydrogenase	0.145839381
VC1769	DNA methylase HsdM, putative	0.137020074
VC1021	LuxO repressor protein	0.121211053
VC1834	hypothetical protein	0.119616623
VC2510	aspartate carbamoyltransferase catalytic subunit	0.110111106
VC1503	hypothetical protein	0.109697749
VC1839	tolQ protein	0.089846289

Table A.3: COMSTAT2 analysis of WT, $\Delta tfoY$, $\Delta lonA$, and $\Delta lonA\Delta tfoY$ biofilms grown for 24 hrs. Quantitative analysis of biofilm formation by CLSM was performed using COMSTAT2. Statistcal analysis was performed with a One-way ANOVA with Tukey's post-hoc analysis (*p<0.05, **p<0.01, ***P<0.005 ****p<0.0001).

		Mean Thickness (SD) (μm)			
Strain	Biomass ($\mu m^3/\mu m^2$)	Avg.	Maximum	Substrate Coverage	Roughness Coeffecient
WT	12.21 (2.52)	12.46 (2.97)	16.45 (3.30)	0.76 (0.14)	0.15 (0.13)
Δ*tfoY*	12.08 (1.76)	12.61 (2.21)	17.12 (2.71)	0.82 (0.12)	0.12 (0.01)
Δ*lonA*	8.40 (4.40) *	11.26 (3.07)	21.29 (4.21) *	0.28 (0.12) ****	0.39 (0.19) ***
Δ*lonA* Δ*tfoY*	8.36 (2.74) *	11.34 (3.82)	20.72 (4.39) *	0.30 (0.10) ****	0.41 (0.11) **

Table A.4: Strains and plasmids used in this study.

FY#	***V. cholerae* Strains**	**Resistance**	**Reference**
FY_1	*Vibrio cholerae* O1 El Tor, Smooth A1552 (Wild Type)	Rif	Yildiz FH, Dolganov NA, Schoolnik GK. 2001
FY_1053	Δ*ctxAB*	Rif	This study
FY_11013	Δ*ctxAB* Δ*lonA*	Rif	This study
FY_4507	Δ*lonA*	Rif	Rogers
FY_12974	*lonA*(S678A)	Rif	This study
FY_9789	Δ*lonA* Tn7::*lonA*	Rif, Gm	Rogers
FY_12953	Δ*tfoY*	Rif	This study
FY_7150	ΔcdgJ ΔrocS ΔlacZ (Δ2PDE)	Rif, Gm	This study
FY_6347	ΔcdgD ΔcdgH ΔcdgK ΔcdgL (Δ4DGC)	Rif, Gm	This study
FY_13650	Δ*tfoY* Tn7::*tfoY*	Rif, Gm	This study
FY_12956	ΔlonA Δ*tfoY*	Rif	This study
FY_13652	ΔlonA Δ*tfoY* Tn7::*tfoY*	Rif, Gm	This study
FY_13971	ΔlonA Δ*tfoY* Tn7::*lonA*	Rif, Gm	This study
FY_237	Wild Type Tn7::gfp	Rif, Gm	Lim B, Beyhan S, Meir J, Yildiz FH. 2006.
FY_13017	Δ*tfoY* Tn7::gfp	Rif, Gm	This study
FY_4512	Δ*lonA* Tn7::gfp	Rif, Gm	This study
FY_13016	ΔlonA Δ*tfoY* Tn7::gfp	Rif, Gm	This study
FY_14002	Wild Type Tn7::*ptac-tfoY*	Rif, Gm	This study
FY_14006	ΔlonA Tn7::*ptac-tfoY*	Rif, Gm	This study
FY_14208	Δ2PDE Tn7::*ptac-tfoY*	Rif, Gm	This study
FY_14209	Δ4DGC Tn7::*ptac-tfoY*	Rif, Gm	This study
FY_15961	ΔlonA Tn7::*ptac-tfoY*	Rif, Gm	This study
FY_15962	ΔlonA Δ2PDE Tn7::*ptac-tfoY*	Rif, Gm	This study
FY_15963	ΔlonA Δ4DGC Tn7::*ptac-tfoY*	Rif, Gm	This study
FY_15964	Δ*tfoY* Tn7::*ptac-tfoY*	Rif, Gm	This study
FY_15965	Δ*tfoY* ΔlonA Tn7::*ptac-tfoY*	Rif, Gm	This study
FY_15966	Δ*tfoY* Δ2PDE Tn7::*ptac-tfoY*	Rif, Gm	This study
FY_15967	Δ*tfoY* Δ4DGC Tn7::*ptac-tfoY*	Rif, Gm	This study
FY_15968	Δ*tfoY* Tn7::*ptac-tfoY* pBBR-*vipA-lux*	Rif, Gm, Cm	This study
FY_15969	Δ*tfoY* Δ2PDE Tn7::*ptac-tfoY* pBBR-*vipA-lux*	Rif, Gm, Cm	This study
FY_15970	Δ*tfoY* Δ4DGC Tn7::*ptac-tfoY* pBBR-*vipA-lux*	Rif, Gm, Cm	This study
FY_15971	Δ*tfoY* Tn7::*ptac-tfoY* pBBR-*hcp2-lux*	Rif, Gm, Cm	This study
FY_15972	Δ*tfoY* Δ2PDE Tn7::*ptac-tfoY* pBBR-*hcp2-lux*	Rif, Gm, Cm	This study
FY_15973	Δ*tfoY* Δ4DGC Tn7::*ptac-tfoY* pBBR-*hcp2-lux*	Rif, Gm, Cm	This study

Table A.4 Continued: Strains and plasmids used in this study.

FY#	Plasmid Harboring Strains	Resistance	Reference
pGP704SacB	pGP704 derivative; mob/oriT sacB	Amp	G. Schoolnik
pFY_5867	pGP704SacB-Δ*ctxAB*	Amp	This study
pFY_596	pGP704SacB-Δ*lonA*	Amp	Rogers et al. 2016
pFY_5532	pGP704SacB-Δ*tfoY*	Amp	This study
pFY_5523	pGP704SacB-*lonA* Full Length (For Site Directed Mutagenesis)	Amp	This study
pFY_5517	pGP704SacB-*lonA*(S678A)	Amp	This study
pFY_720	pGP704-Tn7	Amp, Gm	Lim B, Beyhan S, Meir J, Yildiz FH. 2006.
pUX-BF13	oriR6K helper plasmid, mobl oriT, provides the Tn7 transposition function in trans	Amp	Lim B, Beyhan S, Meir J, Yildiz FH. 2006.
pFY_117	pGP704-Tn7::*gfp*	Amp, Gm	Lim B, Beyhan S, Meir J, Yildiz FH. 2006.
pFY_3488	pGP704-Tn7::*lonA*	Amp, Gm	Rogers et al. 2016
pFY_5665	pGP704-Tn7::*tfoY* (Contains *tfoY* open reading frame and 500bp upstream)	Amp, Gm	This study
pFY_5833	pGP704-Tn7::*Ptac-tfoY*	Amp, Gm	This study
pFY_4431	pBBR-*hcp2-lux* (Contains 300bp upstream of VCA0017 open reading frame as well as 100bp into the gene)	Amp, Cm	This study
pFY_4434	pBBR-*vipA-lux* (Contains 400bp upstream of VCA0107 open reading frame as well as 100bp into the gene)	Amp, Cm	This study

Appendix B

Chapter 3 Supporting Material

Table B.1: Proteins enriched in Δ*lon* biofilms relative to WT. A ANOVA using a Benjamini-Hochberg FDR cutoff of 15% was used to identify proteins that were differentially expressed. Select proteins with at least a 1.5-fold change are shown.

VC Number	Gene Name	Log_2 Fold Change (Δlon/wt)	GO Biological Processes and Functions
VC0276	*purH*	2.648	de novo' IMP biosynthetic process [GO:0006189]; purine ribonucleotide biosynthetic process [GO:0009152]; IMP cyclohydrolase activity [GO:0003937]; phosphoribosylaminoimidazolecarboxamide formyltransferase activity [GO:0004643]
VC0756	*ndk*	2.202	CTP biosynthetic process [GO:0006241]; GTP biosynthetic process [GO:0006183]; nucleobase-containing small molecule interconversion [GO:0015949]; purine nucleotide metabolic process [GO:0006163]; pyrimidine nucleotide metabolic process [GO:0006220]; UTP biosynthetic process [GO:0006228];ATP binding [GO:0005524]; metal ion binding [GO:0046872]; nucleoside diphosphate kinase activity [GO:0004550]
VC2759	*fadA*	2.111	fatty acid beta-oxidation [GO:0006635]; fatty acid catabolic process [GO:0009062]; phenylacetate catabolic process [GO:0010124];acetyl-CoA C-acyltransferase activity [GO:0003988]
VC0178A		2.022	
VC1142	*cspD*	2.008	regulation of transcription, DNA-templated [GO:0006355]; response to cold [GO:0009409];DNA binding [GO:0003677]
VCA0685		1.963	iron ion transport [GO:0006826]; ATPase-coupled transmembrane transporter activity [GO:0042626]; iron ion transmembrane transporter activity [GO:0005381]
VC2635	*mrcA*	1.589	cell wall organization [GO:0071555]; peptidoglycan biosynthetic process [GO:0009252]; regulation of cell shape [GO:0008360]; response to antibiotic [GO:0046677]; catalytic activity [GO:0003824]; drug binding [GO:0008144]; penicillin binding [GO:0008658]; peptidoglycan glycosyltransferase activity [GO:0008955]; serine-type D-Ala-D-Ala carboxypeptidase activity [GO:0009002]
VCA1031		1.567	
VC2424	*pilB*	1.416	pilus assembly [GO:0009297]; protein secretion by the type II secretion system [GO:0015628]; ATPase activity [GO:0016887]
VC0840	*acfB mlp8*	1.297	pathogenesis [GO:0009405]; signal transduction [GO:0007165];
VC0178	*capV*	1.198	lipid catabolic process [GO:0016042];1-acyl-2-lysophosphatidylserine acylhydrolase activity [GO:0052740]; phosphatidylserine 1-acylhydrolase activity [GO:0052739]; phospholipase A1 activity [GO:0008970]

Table B.1 Continued: Proteins enriched in Δ*lon* biofilms relative to WT.

VCA0749	*glpC*	1.195	anaerobic respiration [GO:0009061]; glycerol-3-phosphate dehydrogenase (quinone) activity [GO:0004368]; iron-sulfur cluster binding [GO:0051536]
VC0417	*mreD*	1.191	regulation of cell shape [GO:0008360];
VC0543	*recA*	1.166	DNA recombination [GO:0006310]; DNA repair [GO:0006281]; SOS response [GO:0009432]; ATP binding [GO:0005524]; damaged DNA binding [GO:0003684]; DNA-dependent ATPase activity [GO:0008094]; single-stranded DNA binding [GO:0003697]
VC0021	*glyQ*	1.146	glycyl-tRNA aminoacylation [GO:0006426]; ATP binding [GO:0005524]; glycine-tRNA ligase activity [GO:0004820]
VC2765	*atpG*	1.131	ATP biosynthetic process [GO:0006754]; ATP synthesis coupled proton transport [GO:0015986]; plasma membrane ATP synthesis coupled proton transport [GO:0042777]; ATP binding [GO:0005524]; proton-transporting ATP synthase activity, rotational mechanism [GO:0046933]
VCA0183	*hmpA*	1.124	cellular iron ion homeostasis [GO:0006879]; cellular response to nitrosative stress [GO:0071500]; nitric oxide catabolic process [GO:0046210]; response to toxic substance [GO:0009636];6,7-dihydropteridine reductase activity [GO:0004155]; FAD binding [GO:0071949]; heme binding [GO:0020037]; metal ion binding [GO:0046872]; nitric oxide dioxygenase activity [GO:0008941]; oxygen binding [GO:0019825]; oxygen carrier activity [GO:0005344]
VC1046	*fadI*	1.116	fatty acid beta-oxidation [GO:0006635]; fatty acid catabolic process [GO:0009062]; acetyl-CoA C-acetyltransferase activity [GO:0003985]; acetyl-CoA C-acyltransferase activity [GO:0003988]
VCA0511	*nrdD*	1.114	2'-deoxyribonucleotide biosynthetic process [GO:0009265]; DNA replication [GO:0006260]; ATP binding [GO:0005524]; ribonucleoside-triphosphate reductase activity [GO:0008998]
VC0696	*tyrA*	1.110	chorismate metabolic process [GO:0046417]; oxidation-reduction process [GO:0055114]; tyrosine biosynthetic process [GO:0006571]; chorismate mutase activity [GO:0004106]; NAD+ binding [GO:0070403]; prephenate dehydrogenase (NAD+) activity [GO:0008977]; prephenate dehydrogenase (NADP+) activity [GO:0004665]
VC2767	*atpH*	1.102	ATP synthesis coupled proton transport [GO:0015986]; proton-transporting ATP synthase activity, rotational mechanism [GO:0046933]
VC2763	*atpC*	1.082	ATP synthesis coupled proton transport [GO:0015986]; ATP binding [GO:0005524]; proton-transporting ATP synthase activity, rotational mechanism [GO:0046933]
VC2758	*fadB*	1.069	fatty acid beta-oxidation [GO:0006635]; fatty acid catabolic process [GO:0009062];3-hydroxyacyl-CoA dehydrogenase activity [GO:0003857]; 3-hydroxybutyryl-CoA epimerase activity [GO:0008692]; dodecenoyl-CoA delta-isomerase activity [GO:0004165]; enoyl-CoA hydratase activity [GO:0004300]; long-chain-3-hydroxyacyl-CoA dehydrogenase activity [GO:0016509]

Table B.1 Continued: Proteins enriched in Δ*lon* biofilms relative to WT.

VCA0984	*lldD*	1.025	glycolytic process [GO:0006096]; lactate oxidation [GO:0019516];FMN binding [GO:0010181]; L-lactate dehydrogenase (cytochrome) activity [GO:0004460]; L-lactate dehydrogenase activity [GO:0004459]
VC0428		1.002	
VC2764	*atpD*	0.970	ATP synthesis coupled proton transport [GO:0015986];ATP binding [GO:0005524]; proton-transporting ATP synthase activity, rotational mechanism [GO:0046933]
VCA0004		0.955	
VCA0280	*gcvT*	0.951	
VC2436	*tolC*	0.924	pathogenesis [GO:0009405]; protein secretion [GO:0009306]; response to antibiotic [GO:0046677]; efflux transmembrane transporter activity [GO:0015562]; porin activity [GO:0015288]
VC2766	*atpA*	0.922	ATP synthesis coupled proton transport [GO:0015986]; ADP binding [GO:0043531]; ATP binding [GO:0005524]; proton-transporting ATP synthase activity, rotational mechanism [GO:0046933]
VC0736	*aceA*	0.922	carboxylic acid metabolic process [GO:0019752]; tricarboxylic acid cycle [GO:0006099]; isocitrate lyase activity [GO:0004451]; metal ion binding [GO:0046872]
VC1359		0.921	amino acid transport [GO:0006865]; ATPase activity [GO:0016887]; ATPase-coupled amino acid transmembrane transporter activity [GO:0015424]; ATP binding [GO:0005524]
VC0118		0.919	methylation [GO:0032259]; porphyrin-containing compound biosynthetic process [GO:0006779];uroporphyrin-III C-methyltransferase activity [GO:0004851]
VC1356		0.918	sulfur compound metabolic process [GO:0006790]; tRNA wobble position uridine thiolation [GO:0002143]; hydrogensulfite reductase activity [GO:0018551]; sulfur carrier activity [GO:0097163]; transferase activity [GO:0016740]
VCA0946	*malK*	0.903	maltose transport [GO:0015768]; ATPase activity [GO:0016887]; ATPase-coupled maltose transmembrane transporter activity [GO:0015423]; ATP binding [GO:0005524]
VC0573	*petA*	0.875	mitochondrial electron transport, ubiquinol to cytochrome c [GO:0006122];2 iron, 2 sulfur cluster binding [GO:0051537]; oxidoreductase activity [GO:0016491]; ubiquinol-cytochrome-c reductase activity [GO:0008121]
VC2657	*frdB*	0.864	anaerobic respiration [GO:0009061]; tricarboxylic acid cycle [GO:0006099];2 iron, 2 sulfur cluster binding [GO:0051537]; 3 iron, 4 sulfur cluster binding [GO:0051538]; 4 iron, 4 sulfur cluster binding [GO:0051539]; electron transfer activity [GO:0009055]; metal ion binding [GO:0046872]; succinate dehydrogenase (ubiquinone) activity [GO:0008177]; succinate dehydrogenase activity [GO:0000104]
VC0165	*vexA*	0.816	efflux transmembrane transporter activity [GO:0015562]; xenobiotic transmembrane transporter activity [GO:0042910]

Table B.1 Continued: Proteins enriched in Δ*lon* biofilms relative to WT.

VC0139	*dps*	0.814	cellular iron ion homeostasis [GO:0006879]; ferric iron binding [GO:0008199]; oxidoreductase activity, oxidizing metal ions [GO:0016722]
VCA0582		0.811	RNA binding [GO:0003723]
VC1082		0.806	phosphorelay signal transduction system [GO:0000160];phosphorelay response regulator activity [GO:0000156]
VC0168	*cycB*	0.781	electron transfer activity [GO:0009055]; heme binding [GO:0020037]; iron ion binding [GO:0005506]
VC2665	*groS1*	0.778	chaperone cofactor-dependent protein refolding [GO:0051085]; protein folding [GO:0006457]; ATP binding [GO:0005524]; chaperone binding [GO:0051087]; metal ion binding [GO:0046872]; unfolded protein binding [GO:0051082]
VC0349	*hflK*	0.750	proteolysis [GO:0006508]; peptidase activity [GO:0008233]
VC0394	*uvrA*	0.736	DNA repair [GO:0006281]; nucleotide-excision repair [GO:0006289]; SOS response [GO:0009432]; ATPase activity [GO:0016887]; ATP binding [GO:0005524]; DNA binding [GO:0003677]; excinuclease ABC activity [GO:0009381]; zinc ion binding [GO:0008270]
VCA0514		0.731	
VC1129	*gsk-1*	0.727	nucleobase-containing small molecule interconversion [GO:0015949]; carbohydrate kinase activity [GO:0019200]; inosine kinase activity [GO:0008906]
VCA0981		0.713	
VCA0108	*vipB*	0.701	
VC0973		0.683	
VC0829	*tcpB*	0.680	pathogenesis [GO:0009405]; pilus assembly [GO:0009297];
VC0180		0.661	cyclic threonylcarbamoyladenosine biosynthetic process [GO:0061504]; tRNA threonylcarbamoyladenosine dehydratase [GO:0061503]; ubiquitin-like modifier activating enzyme activity [GO:0008641]
VC2197	*flgE*	0.654	bacterial-type flagellum-dependent swarming motility [GO:0071978]; structural molecule activity [GO:0005198]
VC0560	*ffh*	0.634	SRP-dependent cotranslational protein targeting to membrane [GO:0006614];7S RNA binding [GO:0008312]; GTPase activity [GO:0003924]; GTP binding [GO:0005525]
VC2277	*gpt*	0.626	GMP salvage [GO:0032263]; IMP salvage [GO:0032264]; purine ribonucleoside salvage [GO:0006166]; XMP salvage [GO:0032265]; hypoxanthine phosphoribosyltransferase activity [GO:0004422]; magnesium ion binding [GO:0000287]; xanthine phosphoribosyltransferase activity [GO:0000310]
VC0339	*psd*	0.614	phosphatidylethanolamine biosynthetic process [GO:0006646]; phospholipid biosynthetic process [GO:0008654]; phosphatidylserine decarboxylase activity [GO:0004609]
VC1589	*aldC*	0.614	acetoin biosynthetic process [GO:0045151]; acetolactate decarboxylase activity [GO:0047605]

Table B.1 Continued: Proteins enriched in Δ*lon* biofilms relative to WT.

VC2590	*rpsC*	0.607	translation [GO:0006412]; mRNA binding [GO:0003729]; rRNA binding [GO:0019843]; structural constituent of ribosome [GO:0003735]
VC0767	*guaB*	0.596	GMP biosynthetic process [GO:0006177]; GTP biosynthetic process [GO:0006183]; purine ribonucleotide biosynthetic process [GO:0009152]; IMP dehydrogenase activity [GO:0003938]; metal ion binding [GO:0046872]; nucleotide binding [GO:0000166]
VC0604	*acnB*	0.590	propionate catabolic process, 2-methylcitrate cycle [GO:0019629]; tricarboxylic acid cycle [GO:0006099];2-methylisocitrate dehydratase activity [GO:0047456]; 4 iron, 4 sulfur cluster binding [GO:0051539]; aconitate hydratase activity [GO:0003994]; citrate dehydratase activity [GO:0047780]; metal ion binding [GO:0046872]
VC0828	*tcpA*	0.589	cell projection organization [GO:0030030]; pathogenesis [GO:0009405]; protein secretion by the type II secretion system [GO:0015628]; structural molecule activity [GO:0005198]
VCA0748	*glpB*	0.581	anaerobic respiration [GO:0009061]; glycerol-3-phosphate metabolic process [GO:0006072]; glycerol catabolic process [GO:0019563]; glycerol-3-phosphate dehydrogenase (quinone) activity [GO:0004368]; sn-glycerol-3-phosphate:ubiquinone-8 oxidoreductase activity [GO:0052591]
VC0548	*csrA*	0.564	mRNA catabolic process [GO:0006402]; mRNA metabolic process [GO:0016071]; negative regulation of translational initiation [GO:0045947]; positive regulation of translational initiation [GO:0045948]; regulation of carbohydrate metabolic process [GO:0006109]; mRNA 5'-UTR binding [GO:0048027]; RNA binding [GO:0003723]
VCA1063	*speF*	0.561	cellular amino acid metabolic process [GO:0006520]; spermidine biosynthetic process [GO:0008295]; carboxy-lyase activity [GO:0016831]; ornithine decarboxylase activity [GO:0004586]; pyridoxal phosphate binding [GO:0030170]
VC2656	*frdA*	0.549	anaerobic respiration [GO:0009061]; fermentation [GO:0006113]; electron transfer activity [GO:0009055]; flavin adenine dinucleotide binding [GO:0050660]; fumarate reductase (menaquinone) [GO:0102040]; oxidoreductase activity [GO:0016491]; succinate dehydrogenase activity [GO:0000104]
Located between VC2390 and VC2391		0.547	
VC1256	*nrdA*	0.542	2'-deoxyribonucleotide biosynthetic process [GO:0009265]; deoxyribonucleotide biosynthetic process [GO:0009263]; DNA replication [GO:0006260]; ATP binding [GO:0005524]; ribonucleoside-diphosphate reductase activity, thioredoxin disulfide as acceptor [GO:0004748]
VC2550		0.537	

Table B.1 Continued: Proteins enriched in Δ*lon* biofilms relative to WT.

VC1428	*potA*	0.521	putrescine transport [GO:0015847]; spermidine transport [GO:0015848]; ATPase activity [GO:0016887]; ATPase-coupled polyamine transmembrane transporter activity [GO:0015417]; ATPase-coupled putrescine transmembrane transporter activity [GO:0015594]; ATPase-coupled spermidine transmembrane transporter activity [GO:0015595]; ATP binding [GO:0005524]
VCA1079	*pdxH*	0.519	pyridoxal phosphate biosynthetic process [GO:0042823]; pyridoxine biosynthetic process [GO:0008615]; FMN binding [GO:0010181]; pyridoxamine-phosphate oxidase activity [GO:0004733]
VCA0774	*galE-2*	0.513	galactose catabolic process [GO:0019388]; galactose catabolic process via UDP-galactose [GO:0033499]; galactose metabolic process [GO:0006012]; UDP-glucose 4-epimerase activity [GO:0003978]
VC2087	*sucA*	0.501	tricarboxylic acid cycle [GO:0006099]; oxoglutarate dehydrogenase (succinyl-transferring) activity [GO:0004591]; thiamine pyrophosphate binding [GO:0030976]
VC2295	*nqrA*	0.498	sodium ion transport [GO:0006814]; NADH dehydrogenase (ubiquinone) activity [GO:0008137]
VC0991	*asnB*	0.496	asparagine biosynthetic process [GO:0006529]; glutamine metabolic process [GO:0006541]; asparagine synthase (glutamine-hydrolyzing) activity [GO:0004066]; ATP binding [GO:0005524]
VC0371	*dnaB*	0.479	DNA replication, synthesis of RNA primer [GO:0006269]; DNA replication initiation [GO:0006270]; DNA strand elongation involved in DNA replication [GO:0006271]; DNA unwinding involved in DNA replication [GO:0006268]; ATP binding [GO:0005524]; DNA binding [GO:0003677]; DNA-dependent ATPase activity [GO:0008094]; DNA helicase activity [GO:0003678]
VC0350	*hflC*	0.465	proteolysis [GO:0006508]; regulation of peptidase activity [GO:0052547]; peptidase activity [GO:0008233]
VC2296	*bolA*	0.465	regulation of cell shape [GO:0008360]; transcription, DNA-templated [GO:0006351]; DNA binding [GO:0003677]
VC0179	*dncV*	0.460	cyclic nucleotide biosynthetic process [GO:0009190]; negative regulation of chemotaxis [GO:0050922]; pathogenesis [GO:0009405]; ATP binding [GO:0005524]; cyclic-GMP-AMP synthase activity [GO:0061501]; diguanylate cyclase activity [GO:0052621]; GTP binding [GO:0005525]; metal ion binding [GO:0046872]
VC1255	*nrdB*	0.458	2'-deoxyribonucleotide biosynthetic process [GO:0009265]; ribonucleoside-diphosphate reductase activity, thioredoxin disulfide as acceptor [GO:0004748]
VC0175	*dcdV*	0.443	catalytic activity [GO:0003824]; zinc ion binding [GO:0008270]
VC2675	*hslV*	0.439	proteolysis [GO:0006508]; proteolysis involved in cellular protein catabolic process [GO:0051603];metal ion binding [GO:0046872]; peptidase activity [GO:0008233]; threonine-type endopeptidase activity [GO:0004298]
VCA1115		0.434	

Table B.1 Continued: Proteins enriched in Δ*lon* biofilms relative to WT.

VC1249		0.425	regulation of transcription, DNA-templated [GO:0006355]; transcription, DNA-templated [GO:0006351]
VC0761		0.402	
VC0163		0.376	
VCA0800	*creA*	0.376	
VC0856	*dnaJ*	0.346	chaperone cofactor-dependent protein refolding [GO:0051085]; DNA replication [GO:0006260]; protein folding [GO:0006457]; protein refolding [GO:0042026]; response to heat [GO:0009408]; ATP binding [GO:0005524]; heat shock protein binding [GO:0031072]; unfolded protein binding [GO:0051082]; zinc ion binding [GO:0008270]
VC0453	*trmB*	0.336	RNA (guanine-N7)-methylation [GO:0036265]; tRNA methylation [GO:0030488]; tRNA (guanine-N7-)-methyltransferase activity [GO:0008176]
VCA0112	*vasC*	0.328	
VC1304		0.314	tricarboxylic acid cycle [GO:0006099];4 iron, 4 sulfur cluster binding [GO:0051539]; fumarate hydratase activity [GO:0004333]; metal ion binding [GO:0046872]
VC1364		0.305	dephosphorylation [GO:0016311]; magnesium ion binding [GO:0000287]; phosphatase activity [GO:0016791]
VC0487	*glmS*	0.273	amino sugar metabolic process [GO:0006040]; carbohydrate metabolic process [GO:0005975]; fructose 6-phosphate metabolic process [GO:0006002]; glutamine metabolic process [GO:0006541]; protein N-linked glycosylation [GO:0006487]; UDP-N-acetylglucosamine metabolic process [GO:0006047]; carbohydrate derivative binding [GO:0097367]; glutamine-fructose-6-phosphate transaminase (isomerizing) activity [GO:0004360]

Table B.2: Proteins enriched in Δlon biofilms relative to WT. An ANOVA using a Benjamini-Hochberg FDR cutoff of 15% was used to identify proteins that were differentially expressed. Select proteins with at least a 1.5-fold change are shown.

VC Number	Gene Name	Log_2 Fold Change (Δlon/wt)	GO Biologocal Processes and Functions
VC1920	*lon*	-3.796	cellular response to heat [GO:0034605]; protein quality control for misfolded or incompletely synthesized proteins [GO:0006515]; proteolysis [GO:0006508]; ATP binding [GO:0005524]; ATP-dependent peptidase activity [GO:0004176]; peptidase activity [GO:0008233]; sequence-specific DNA binding [GO:0043565]; serine-type endopeptidase activity [GO:0004252]
VC0930	*rbmC*	-1.727	
VCA0227	*vctP*	-1.713	iron ion transport [GO:0006826];
VCA0908	*hutX*	-1.458	metal ion binding [GO:0046872]
VC2358		-1.308	
VC1146	*grxA*	-1.255	cell redox homeostasis [GO:0045454]; electron transfer activity [GO:0009055]; protein disulfide oxidoreductase activity [GO:0015035]
VC1264		-1.201	cellular iron ion homeostasis [GO:0006879];
VC1337	*prpC*	-1.111	carbohydrate metabolic process [GO:0005975]; fermentation [GO:0006113]; propionate metabolic process, methylcitrate cycle [GO:0019679]; tricarboxylic acid cycle [GO:0006099];2-methylcitrate synthase activity [GO:0050440]; citrate (Si)-synthase activity [GO:0004108]; oxo-acid-lyase activity [GO:0016833]
VC0330	*rsd*	-1.056	regulation of transcription, DNA-templated [GO:0006355];DNA-binding transcription factor activity [GO:0003700]
VC0475	*irgA*	-1.029	enterobactin transport [GO:0042930]; ferric-enterobactin import into cell [GO:0015685]; pathogenesis [GO:0009405]; siderophore-dependent iron import into cell [GO:0033214];enterobactin transmembrane transporter activity [GO:0042931]; siderophore uptake transmembrane transporter activity [GO:0015344]
VC0646	*rpsO*	-1.023	translation [GO:0006412]; rRNA binding [GO:0019843]; structural constituent of ribosome [GO:0003735]
VC0797	*citD*	-1.009	fermentation [GO:0006113]; citrate (pro-3S)-lyase activity [GO:0008815]
VC2022	*fabD*	-0.963	fatty acid biosynthetic process [GO:0006633]; [acyl-carrier-protein] S-malonyltransferase activity [GO:0004314]
VC2349	*deoA*	-0.963	nucleobase-containing compound metabolic process [GO:0006139]; pyrimidine nucleobase metabolic process [GO:0006206]; thymidine metabolic process [GO:0046104];phosphorylase activity [GO:0004645]; pyrimidine-nucleoside phosphorylase activity [GO:0016154]; thymidine phosphorylase activity [GO:0009032]
VC0928	*rbmA*	-0.960	

Table B.2 Continued: Proteins reduced in Δ*lon* biofilms relative to WT.

VC2211	*viuA*	-0.894	enterobactin transport [GO:0042930]; ferric-enterobactin import into cell [GO:0015685]; siderophore-dependent iron import into cell [GO:0033214]; enterobactin transmembrane transporter activity [GO:0042931]; siderophore uptake transmembrane transporter activity [GO:0015344]; signaling receptor activity [GO:0038023]
VC0608	*fbpA*	-0.881	iron ion transport [GO:0006826]; ATPase-coupled transmembrane transporter activity [GO:0042626]; iron ion transmembrane transporter activity [GO:0005381]; metal ion binding [GO:0046872]
VC1547	*exbB*	-0.834	protein import [GO:0017038]; proton transmembrane transport [GO:1902600]; proton transmembrane transporter activity [GO:0015078]
VC0368	*rpsR*	-0.824	translation [GO:0006412]; small ribosomal subunit rRNA binding [GO:0070181]; structural constituent of ribosome [GO:0003735]
VC2587	*rpsQ*	-0.821	translation [GO:0006412]; rRNA binding [GO:0019843]; structural constituent of ribosome [GO:0003735]
VCA1028	*ompS*	-0.769	ion transport [GO:0006811]; maltose transport [GO:0015768]; polysaccharide transport [GO:0015774]; carbohydrate transmembrane transporter activity [GO:0015144]; maltodextrin transmembrane transporter activity [GO:0042958]; maltose transporting porin activity [GO:0015481]; porin activity [GO:0015288]
VC1919	*hupB*	-0.751	chromosome condensation [GO:0030261]; DNA packaging [GO:0006323]; DNA binding [GO:0003677]
VC0692	*nagZ*	-0.723	carbohydrate metabolic process [GO:0005975]; cell cycle [GO:0007049]; cell division [GO:0051301]; cell wall organization [GO:0071555]; peptidoglycan-based cell wall biogenesis [GO:0009273]; peptidoglycan biosynthetic process [GO:0009252]; peptidoglycan turnover [GO:0009254]; regulation of cell shape [GO:0008360]; response to antibiotic [GO:0046677]; beta-N-acetylhexosaminidase activity [GO:0004563]; N-acetyl-beta-D-galactosaminidase activity [GO:0102148]
VCA0576	*hutA*	-0.713	heme transport [GO:0015886]; siderophore-dependent iron import into cell [GO:0033214]; heme transporter activity [GO:0015232]; siderophore uptake transmembrane transporter activity [GO:0015344]
VCA0805	*rnb*	-0.683	mRNA catabolic process [GO:0006402]; RNA catabolic process [GO:0006401]; exoribonuclease II activity [GO:0008859]; RNA binding [GO:0003723]
VC1220	*pheT*	-0.655	phenylalanyl-tRNA aminoacylation [GO:0006432]; ATP binding [GO:0005524]; magnesium ion binding [GO:0000287]; phenylalanine-tRNA ligase activity [GO:0004826]; tRNA binding [GO:0000049]
VCA0591		-0.639	microcin transport [GO:0042884]; peptide transport [GO:0015833]; ATPase-coupled transmembrane transporter activity [GO:0042626]; peptide transmembrane transporter activity [GO:1904680]

Table B.2 Continued: Proteins reduced in Δ*lon* biofilms relative to WT.

VC2020	*acpP*	-0.628	fatty acid biosynthetic process [GO:0006633]; lipid A biosynthetic process [GO:0009245]; acyl binding [GO:0000035]; acyl carrier activity [GO:0000036]
VC0695	*aroF*	-0.628	aromatic amino acid family biosynthetic process [GO:0009073]; chorismate biosynthetic process [GO:0009423];3-deoxy-7-phosphoheptulonate synthase activity [GO:0003849]
VC2261	*map*	-0.606	cellular protein modification process [GO:0006464]; protein initiator methionine removal [GO:0070084];metal ion binding [GO:0046872]; metalloaminopeptidase activity [GO:0070006]
VC0483		-0.604	
VC2480	*rpiA*	-0.602	D-ribose metabolic process [GO:0006014]; pentose-phosphate shunt [GO:0006098]; pentose-phosphate shunt, non-oxidative branch [GO:0009052];ribose-5-phosphate isomerase activity [GO:0004751]
VC0911	*treA*	-0.589	oligosaccharide catabolic process [GO:0009313]; trehalose catabolic process [GO:0005993];alpha,alpha-phosphotrehalase activity [GO:0008788]; alpha-amylase activity [GO:0004556]
VC2019	*fabF*	-0.586	fatty acid biosynthetic process [GO:0006633];3-oxoacyl-[acyl-carrier-protein] synthase activity [GO:0004315]; beta-ketoacyl-acyl-carrier-protein synthase II activity [GO:0033817]